Continuous Esterification of Crude Palm Oil with Ethanol

Thanet Waisuwan

A Thesis Submitted in Fulfillment of the Requirements for the Degree of
Doctor of Philosophy in Chemical Engineering
Prince of Songkla University
2012

Thesis Title Continuous Esterification of Crude Palm Oil with Ethanol

Author Mr.Thanet Waisuwan

Major Program Chemical Engineering

Major Advisor:

……..…

(Assoc.Prof.Dr.Chakrit Tongurai)

Co-advisor:

…….…….

(Dr.Sutham Sukmanee)

Examining Committee:

……Chairperson

(Assoc.Prof.Dr.Galaya Srisuwan)

…….....

(Assoc.Prof.Dr.Chakrit Tongurai)

……...

(Dr.Sutham Sukmanee)

……...

(Asst.Prof.Dr.Sukritthira Ratanawilai)

…….……..

(Dr.Sininart Chongkhong)

The Graduate School, Prince of Songkla University, has approved this thesis as fulfillment of the requirements for the Degree of Doctor of Philosophy in Chemical Engineering

..……

(Prof.Dr.Amornrat Phongdara)

Dean of Graduate School

ชื่อวิทยานิพนธ์ การทำปฏิกิริยาเอสเตอริฟิเคชันแบบต่อเนื่องของน้ำมันปาล์มดิบด้วยเอทานอล
ผู้เขียน นายธเนศ วัยสุวรรณ
สาขาวิชา วิศวกรรมเคมี
ปีการศึกษา 2554

บทคัดย่อ

ไบโอดีเซลเป็นพลังงานหมุนเวียนที่โดดเด่นมาก ซึ่งสามารถผลิตจากน้ำมันหรือไขมันได้หลายชนิด ด้วยปฏิกิริยาทรานส์เอสเตอริฟิเคชันกับแอลกอฮอล์โดยใช้ด่างเป็นตัวเร่งปฏิกิริยา ถ้าใช้เอทานอลทำปฏิกิริยาจะได้เอทิลเอสเตอร์เป็นผลิตภัณฑ์ ซึ่งถือว่าเป็นไบโอดีเซลจากธรรมชาติอย่างบริบูรณ์ ส่วนน้ำมันปาล์มดิบก็เป็นวัตถุดิบที่มีศักยภาพในการผลิตไบโอดีเซลสำหรับประเทศไทย แต่เนื่องจากมีกรดไขมันอิสระอยู่มาก จึงจำเป็นต้องลดกรดก่อนที่จะเข้าสู่การทรานส์เอสเตอริฟิเคชัน งานวิจัยนี้มีจุดมุ่งหมายที่จะลดกรดไขมันอิสระและฟอสฟอรัสในน้ำมันปาล์มดิบโดยการเอสเตอริฟิเคชันด้วยเอทานอล ซึ่งเป็นวิธีที่เหมาะสม เพราะได้เอทิลเอสเตอร์เป็นผลิตภัณฑ์และสามารถกำจัดฟอสฟาไทด์ไปพร้อมกัน การศึกษานี้ได้ตรวจสอบหาสภาวะที่เหมาะสมของเอสเตอริฟิเคชัน 3 แบบคือ การใช้คลื่นอัลตราโซนิคแบบกะ (ขนาด 300 กรัมต่อกะ) และแบบต่อเนื่อง (ขนาด 1.47 ลิตร) และแบบถังกวนต่อเนื่อง (ขนาด 87 ลิตร) โดยออกแบบการทดลองด้วยวิธีของ Taguchi ผลการศึกษาพบว่า ในการใช้คลื่นอัลตราโซนิค สำหรับแบบกะและแบบต่อเนื่อง สภาวะที่เหมาะสมเรียงตามลำดับความสำคัญ คือ ปริมาณตัวเร่งปฏิกิริยาร้อยละ 60 โดยน้ำหนักของกรดไขมันอิสระ อัตราส่วนโดยโมลของเอทานอลต่อกรดไขมันอิสระ เป็น 30 ต่อ 1 อุณหภูมิ 60 องศาเซลเซียส (เป็นค่าคงที่สำหรับแบบต่อเนื่อง) เวลาในการทำปฏิกิริยา 1 ชั่วโมง และแอมปลิจูดของกำลังอะคูสติกร้อยละ 75 (สำหรับแบบกะ) สามารถลดกรดไขมันอิสระลงจากร้อยละ 6 เหลือร้อยละ 0.50 และ 0.35 โดยน้ำหนักตามลำดับ หากกำจัดน้ำออกจากปฏิกิริยาด้วยการเอสเตอริฟิเคชันแบบสองขั้นตอน สมดุลก็จะเลื่อนไปทางด้านผลิตภัณฑ์ และสามารถลดกรดไขมันอิสระลงได้เหลือร้อยละ 0.22 โดยน้ำหนัก สำหรับแบบถังกวนต่อเนื่อง สภาวะที่เหมาะสมเรียงตามลำดับความสำคัญในการทำปฏิกิริยาที่อุณหภูมิ 60 องศาเซลเซียส คือ เวลาในการทำปฏิกิริยา 1 ชั่วโมง อัตราส่วนโดยโมลของ เอทานอลต่อกรดไขมันอิสระ เป็น 30 ต่อ 1 ปริมาณตัวเร่งปฏิกิริยาร้อยละ 60 โดยน้ำหนักของกรดไขมันอิสระ สามารถลดกรดไขมันอิสระลงจากร้อยละ 7.5 เหลือร้อยละ 0.81 โดยน้ำหนัก จากการเปรียบเทียบการใช้พลังงานพบว่าประสิทธิภาพเชิงพลังงาน ของการใช้คลื่นอัลตราโซนิคแบบกะและแบบต่อเนื่องและแบบถังกวนต่อเนื่องมีค่าเป็นร้อยละ 8.23 6.85 และ 79.70 ตามลำดับ การเอสเตอริฟิเคชันแบบต่อเนื่องโดยใช้คลื่นอัลตราโซนิคมีข้อดี คือไม่จำเป็นต้องพึ่งแหล่งความร้อนจากภายนอก ทำให้ประหยัดหน่วยให้ความร้อน และใช้เวลาเพียง 1 ชั่วโมง ก็สามารถลดกรดไขมันอิสระจากร้อยละ 6.26 เหลือเพียง 0.35 และกำจัดฟอสฟอรัสจาก 11.24 เหลือเพียง 1.46 มก./กก. ปริมาณฟอสฟอรัสผ่านมาตรฐาน EN 14214: 2008

Thesis Title	Continuous Esterification of Crude Palm Oil with Ethanol
Author	Mr.Thanet Waisuwan
Major Program	Chemical Engineering
Academic Year	2011

ABSTRACT

Biodiesel is the most outstanding renewable energy, produced from several oils and fats through base catalyzed transesterification with an alcohol. If ethanol is used, ethyl ester, completely natural biodiesel, will be obtained. Crude palm oil (CPO) is the most potential raw material for biodiesel production in Thailand, but unfortunately it contains a high level of free fatty acid (FFA) content which should be reduced before conducting the transesterification. This research aimed to reduce FFA and phosphorus content of CPO using acid catalyzed esterification with ethanol; it is the optimized pretreatment process for CPO because the product is ethyl ester and degumming of phosphatide can be concurrent. This study investigated optimized conditions of the esterification using 3 experimental types i.e. batch (300 g/batch) and continuous (1.47 L) assisted by ultrasonic irradiation and also a continuous stirred-tank reactor (87 L), exploiting Taguchi method to design the experiments. The optimum conditions in descending order for batch and continuous ultrasonic methods are catalyst amount 60 wt% of FFA, molar ratio of ethanol to FFA at 30:1, temperature at 60ºC (fixed for continuous experiments), reaction time of one hour and amplitude of acoustic power at 75% (for batch method only), consequently reduce FFA content (from 6 wt%) to 0.50 and 0.35 wt%, respectively. If water, by product of the reaction, can be abolished, the equilibrium will shift to the product side that be shown by FFA reduction to 0.22 wt% with 2 steps esterification. The optimum conditions in descending order of CSTR method (reacted at 60ºC) are retention time of one hour, molar ratio of ethanol: FFA at 30: 1 and catalyst amount 60 wt% of FFA, obtaining final FFA content (from 7.5 wt%) of 0.81 wt%. As for energy consumption comparison shows that batch ultrasonic, continuous ultrasonic and CSTR experiments have an energy efficiency of 8.23, 6.85 and 79.70%, respectively. The obvious advantages of ultrasonic irradiation over the conventional method are that no external heating source is required for the reaction, resulting in saving the heating unit and a shorter time to achieve a lower FFA content and it can reduces FFA and phosphorus content from 6.26 to 0.35 wt% and from 11.24 to 1.46 mg/kg, respectively. This phosphorus content also meets the EN 14214: 2008.

Acknowledgement

I would like to put a special thank to my advisor, Assoc.Prof.Dr.Chakrit Tongurai for his advisory and financial support on this research and also to my co-advisor Dr.Sutham Sukmanee for many useful advisory.

I am very grateful to my examination committees for their useful suggestion.

I appreciate the help from the staff members of Department of Chemical Engineering, and Specialized R&D Center for Alternative Energy from Palm Oil and Oil Crops, Faculty of Engineering, Prince of Songkla University for their helpful coordinate.

I appreciate the scholarships subsidized by The National Research Council of Thailand (NRCT) and Prince of Songkla University Graduate Studies Grant Contract (2010 Academic Year).

Finally, I would like to thank Mrs.Niramon Waisuwan and my family for their help, encouragement and support my study thoroughly.

Thanet Waisuwan

Contents

Contents (Continued)

Contents (Continued)

List of Tables

List of Tables (Continued)

List of Figures

List of Figures (Continued)

List of Abbreviations and Symbols

amp	Amplitude
cal	Calculated
cat	Catalyst
conc.	Concentrated
conf.	Confirmation
Cont.	Continue
CPO	Crude Palm Oil
CSTR	Continuous Stirred-Tank Reactor
expt.	Experiment
FFA	Free Fatty Acid
ID	Inner Diameter
MR	Molar Ratio
N_{Re}	Reynolds Number
Q	Heat in kJ
Q′	Heat in Wh
RT	Retention Time
T	Overall experiment average
Temp	Temperature
y	Mean response characteristic
μ	Prediction equation
ΔT	Delta of Temperature

CHAPTER 1

Introduction

1.1 Rationale/Problem Statement

According to energy crisis and global warming expanding over the world are crucial factors which have prompted many countries to concentrate on development of substituted energy, especially, biodiesel. The main advantages of using biodiesel are renewability, better quality exhaust gas emissions, biodegradability and all the organic carbon present is photosynthetic in origin, it does not contribute to a rise in the level of carbon dioxide in the atmosphere and consequently to the greenhouse effect (Srivastava and Prasad, 2000). The biodiesel can be substituted petroleum diesel in every concentration and produced by various sources of oil and fat of plants and animals which mainly contain triglyceride. So nowadays each country uses his potential sources for industrial scale of biodiesel manufacturing such as rape seed oil in United State, etc.

In Thailand, crude palm oil (CPO) is the most potential source for biodiesel production because there are huge oil palm plantations in southern Thailand and it has the highest oil yield (5,000 kg/ha/a) (Addison, 2009 and Vanichseni et al., 2002) compared to others oil plants. The industrial scale of biodiesel production should be processed by utilizing continuous streams of alkali catalyzed transesterification to convert most of glyceride to ester or biodiesel and thus it would be obtained a good yield when the raw material is refined oil or has low free fatty acid (FFA) content. If the oil contains higher amounts of FFA (> 1 wt%), it will form soap by reacting with the base catalyst and the ester conversion is decreased due to this soap formation which can also prevent the glycerine phase separation of the biodiesel, if ethanol is used as a reactant (Hanh et al., 2009b). Therefore, raw material pretreatment becomes an important role, especially FFA reduction is described as the de-acid step. Unfortunately, commercial CPO has high phosphorus and FFA (~5 wt%) content and if it is used as the raw material for alkali catalyzed transesterification, it does need to be pretreated by degumming and de-acidification to

reduce respectively the phosphorus and FFA content. Due to phosphorus content in CPO is higher than the limitation of national biodiesel standards; therefore it must be reduced to meet the standards. In order to maximize the final yield of ester from transesterification, the FFA content of the raw material feedstock should be lowered than 0.5 wt% (Freedman et al., 1984 and Kusdiana and Saka, 2003). There are three chemical methods to reduce FFA content; the first method available is saponification or neutralization of the FFA with an alkali solution (sodium or potassium hydroxide) which also called FFA stripping, the second is glycerolysis and another one is esterification by using an acid catalyst. The main product of the first method is soap which is troublesome in further processing since it is difficult to separate the soap and this can result in a loss of biodiesel yield. The second method transforms FFA to glycerides and the latter method will yield fatty acid alkyl ester as the main product and water as a byproduct. Overall, this method will increase the ester yield and obviates the need to separate the pretreatment product before feeding it into the subsequent transesterification step. Clearly, the esterification is considered as an optimum method for reducing the FFA content of this kind of feedstock before conducting base-catalyzed transesterification particularly since acid degumming can be carried out simultaneously.

Ultrasound can also be efficiently utilized to optimize the conversion of triglyceride to biodiesel. For instance, the influence of low-frequency ultrasound (28 and 40 kHz) on biodiesel production from triglyceride, free fatty acids and fatty acid cut (C8–C10) was tested using either methanol or ethanol in the presence of different catalysts, such as sodium hydroxide (NaOH), potassium hydroxide (KOH) and sulfuric acid (H_2SO_4) and compared to a conventional transesterification process. These experiments demonstrated that the use of ultrasound significantly reduced the amount of required catalyst, whilst eliminating saponification and dramatically shortening the reaction time from 2 h to 30 minutes. Moreover, the molar ratio of methanol to fatty acids was found to be capable of reduction by as much as three times, which resulted in high biodiesel yields of 95–97 wt%, regardless of the initial material used. In addition to accelerating biodiesel production, ultrasound can be used to monitor the biodiesel production process (Rokhina et al., 2009).

Nowadays, typical processing of biodiesel uses oil and alcohol as main

reactants. Normal short chain alcohol used is methanol because it promotes the highest activity and it is low cost product. On the other hand, the disadvantages of methanol are its lower solubility with oil and toxicity as well as the fact that it is not produced locally in Thailand so has to be imported. This study focused on substituting ethanol for methanol because of its nontoxic nature, good solubility and local availability. Not only would the wider use of ethanol reduce the need to import methanol, but ethyl ester is also a completely natural and recyclable source of energy.

This research aimed to determine the optimal conditions for batch and continuous acid catalyzed esterification of CPO with ethanol assisted by high intensity ultrasonic irradiation including acid catalyzed esterification with a continuous stirred-tank reactor. These pretreatments encompassed both the degumming and acid catalysis steps in the esterification process reducing the phosphorus and FFA content, respectively.

1.2 Research Background

1.2.1 Oil Palm (*Elaeis guineensis*)

Palm oil is derived from the fleshy part or the mesocarp of the palm fruit species *Elaeis guineensis*. However in Thailand, *Tenera* (hybrid of *Dura* x *Psifera*) palm fruit is widely cultivated due to commercial and processing viability as harvesting becomes easier since the palm trees are relatively shorter, producing good fruit bunch and higher fruit oil content (Kulavanich et al., 1988). Figure 1.1 shows the cross-section of palm oil fruits indicating the mesocarp and kernel of the fruit.

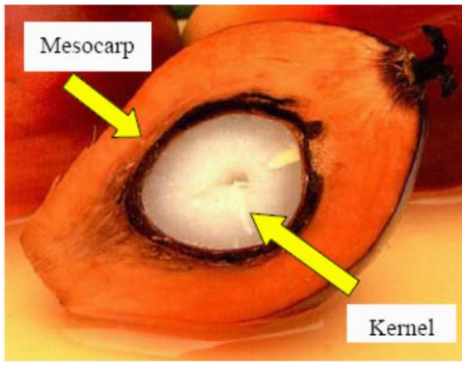

Figure 1.1 Cross-section of palm oil fruit (Noor Azian, et al., 2006)

Table 1.1 Some oil yields per area per annum

Crop	kg oil/ha	liters oil/ha	lbs oil/acre	US gal/acre
Corn (maize)	145	172	129	18
Cashew nut	148	176	132	19
Cotton	273	325	244	35
Soybean	375	446	335	48
Coffee	386	459	345	49
Linseed (flax)	402	478	359	51
Sesame	585	696	522	74
Safflower	655	779	585	83
Rice	696	828	622	88
Tung oil tree	790	940	705	100
Sunflowers	800	952	714	102
Cocoa (cacao)	863	1026	771	110
Peanuts	890	1059	795	113
Rapeseed	1000	1190	893	127
Olives	1019	1212	910	129
Castor beans	1188	1413	1061	151
Pecan nuts	1505	1791	1344	191
Jojoba	1528	1818	1365	194
Jatropha	1590	1892	1420	202
Macadamia nuts	1887	2246	1685	240
Brazil nuts	2010	2392	1795	255
Avocado	2217	2638	1980	282
Coconut	2260	2689	2018	287
Oil palm	5000	5950	4465	635

(Addison, 2009)

Remark

- 1 ha is equivalent to 6.25 Rai,
- 1 acre is equivalent to 2.53 Rai,

The compositions of crude palm oil can be classified as a mixture of 5 main chemical groups shown in Table 1.2 below.

Table 1.2 General compositions of crude palm oil.

Group	Components in the group
Oil	- Triglyceride, Diglyceride , Monoglyceride
	- Phospholipids, Glycolipid and Lipoprotein
	- Free fatty acids
Oxidized products	- Peroxides, Aldehydes, Ketones, Furfurals
Non-oil (but oil solubles)	- Carotene
	- Tocopherols
	- Squalene
	- Sterols
Impurities	- Metal particles
	- Metal ions
	- Metal complexes
Water soluble	- Water (moisture)
	- Glycerol
	- Chlorophyll pigments
	- Phenols
	- Sugars (soluble carbohydrates)

(Morad et al., 2006)

Some of these chemical groups need to be removed partially or completely through the refining process in order to produce good edible oil that has better stability and keepability. Thus, in palm oil refineries the CPO produced undergoes degumming, bleaching and deodorization obtaining refined, bleached and deodorized oil (RBDPO). Table 1.3 shows the typical composition of the main constituents of crude palm oil (Morad et al., 2006).

Table 1.3 Typical compositions of the main components of CPO

Constituent	Crude Palm Oil
Triglyceride, wt%	95
Free Fatty Acids, FFA, wt%	2 - 5
Red Colour (5 ¼ " Lovibond Cell)	Orange red
Moisture & Impurities, wt%	0.15 – 3.0
Peroxide Value, PV (meq/kg)	1 -5.0
Anisidine Value, AV	2 – 6
β-carotene content, ppm	500-700
Phosphorus, P, ppm	10-20
Iron (Fe), ppm	4-10
Tocopherols, ppm	600-1000
Diglyceride, wt%	2-6

(Morad et al., 2006)

Palm oil consists mainly of glyceride made up of a range of fatty acids. Triglyceride constitutes the major component, with small proportions of diglyceride and monoglyceride. Palm oil also contains other minor constituents, such as free fatty acids and non-glyceride components. This composition determines the oil's chemical and physical characteristics (Morad et al., 2006).

The fatty acid composition of crude palm oil is given in Table 1.4. About 50 wt% of them are saturated, 40 wt% of mono-unsaturated, and 10 wt% of polyunsaturated fatty acids. In its content of monounsaturated 18:1 acid, palm oil is similar to olive oil, which is as effective as the more polyunsaturated oils in reducing blood cholesterol and the risk of coronary heart disease. Crude palm oil contains approximately 1 wt% of minor components: carotenoid, vitamin E (tocopherol and tocotrienol), sterols, phospholipids, glycolipid, terpenic and aliphatic hydrocarbons, and other trace impurities (Table 1.5). The most important components are carotenoid and vitamin E, both of which possess important physiological properties. The iodine value is between 50 and 56 (May, 1994).

Table 1.4 Fatty acid composition of crude palm oil

	wt% of total acids	
Acid	Range	Mean
12:0	0.1-1.0	0.2
14:0	0.9-1.5	1.1
16:0	41.8-46.8	44.0
16:1	0.1-0.3	0.1
18:0	4.2-5.1	4.5
18:1	37.3-40.8	39.2
18:2	9.1-11.0	10.1
18:3	0.0-0.6	0.4

(May, 1994)

Table 1.5 Minor components of crude palm oil

Minor components	ppm
Carotenoids	500-700
Tocopherol and tocotrienols	600-1,000
Sterols	326-527
Phospholipids	5-130[a]
Triterpene alcohol	40-80[a]
Methyl sterols	40-80
Squalene	200-500
Aliphatic alcohols	100-200
Aliphatic hydrocarbon	50

a. Estimated

(May, 1994)

1.2.2 Degumming (Morad et al., 2006)

Technically, degumming is referred to an operation of purification of seed oils, which normally contain impurities in colloidal state or dissolved in them. Fats and oils contain complex organo-phosphorus compounds referred to as phospholipids (phosphatide) or more usually, as gums. Phospholipids should be removed because of their strong emulsifying action and if they are not removed, the oils will be gone through undue darkening during deodorization at high temperature. The phospholipids are removed during processing by a variety of treatments collectively referred to as degumming. The treatment usually involves hydration with water, orthophosphoric acid, and polybasic organic acids either single or in combination, followed by centrifuging the precipitated material or by adsorption on bleaching earth or filler.

In more simple words, degumming is a process of removing the unwanted gums, which the stability of the oil products will be interfered in later stages. The objective is achieved by treating the crude palm oil with the specified quantity of food grade acid normally phosphoric or citric acid of certain concentration.

1.2.2.1 Type of degumming

There are 6 types of degumming in vegetable oil industry. The difference between all these types are based on methods of processing, chemical used and degumming phosphatides content in the crude vegetable oil. The types of degumming process are following;

(a) Dry degumming

Dry degumming process involved removal of gums through precipitation by acid conditioning and via filtration during the bleaching process, not via centrifugal separation. This process is used for low-phosphatide oil such as palm oil, lauric oils, and edible tallow which suitable to be used for preparing oils before subsequently physical refining. This type of process eliminates bleaching, as separate processing step thus, it is cost-advantage and it is a well-proven process.

(b) Water degumming

Water degumming is a process of removing gums through precipitation by pure water hydration of crude oil via centrifugal separation. This method is used when

extracting gums for production of lecithin in soybean oil and crude oil in which containing 200 ppm of phosphorus content. In this process, water is the main agent used to remove the hydratable phosphatide from vegetable oils and it can be carried out in batch or continuous procedure depending on the type of the oil to be degummed and amount of oil to be processed.

(c) Acid degumming

In this acid degumming process, gums are precipitated by some form of acid conditioning process and subsequently removed by centrifugal separation. In this process method, the gums can be hydrated at temperature higher than 40°C and the process may lead to some dewaxing which usually associated with processing of sunflower and rice bran oils. In organic refining process, dilute organic (citric) acid is normally used and the residual phosphatide is removed by bleaching with silica hydrogel.

(d) Enzymatic degumming

Enzymatic degumming is a special degumming that enhanced by using some food-grade enzymes. Types of oil that uses this process method are soybean and rapeseed oil. The advantage of the enzymatic degumming is no soap stock produced during the process; therefore it is no any oil losses due to soap stock separation.

(e) EDTA- degumming

EDTA degumming is a physico-chemical degumming process. It involves a complete elimination of phospholipids by a chelating agent, Ethylene Diamine Tetraacetic Acid (EDTA), in the presence of an emulsifying additive.

(f) Membrane degumming

Membrane degumming is usually used in extraction plant. Membrane separation is primarily a size-exclusion-based pressure-driven process. It separates different components according to molecular weights or particle sizes, shapes of individual components which are dependent on their interactions with membrane surfaces and other components of the mixture. During oil processing, micelle containing 25-30 wt% of crude oil and 70-75 wt% of hexane are obtained from extraction prior to solvent removal. Phospholipids can be separated from triglyceride

in the micelle stage using appropriate membrane. The membrane-based crude oil degumming produces permeate and retentate containing triglyceride and phospholipids, respectively. The majority of coloring materials, some of the FFA and other impurities are included in phospholipids micelles and removed as well.

1.2.2.2 Process theory of degumming

Theoretically, phospholipids, protein and carbohydrate, vegetable gum and colloidal components have negative influence towards the keepability of oil. They are considered as undesirable substances in refining process because they increase the oil loss and hamper other operations. Therefore, oils that have certain amount of these substances should be degummed in order to remove all those substances.

There are 2 kinds of phospholipids exist, hydratable and non-hydratable phosphatides. Hydratable phospholipids can be removed easily by the addition of water where the process can be conducted rapidly at elevated temperature or slowly at low temperature. However the temperature should stay below the temperature at which the phospholipids hydrate starts to become liquid crystals (usually ~ 40ºC). By taking up water, phospholipids lose their lipophilic character and become lipophobic and thus precipitate from oil.

When the non-hydratable phospholipids have to be converted to hydratable ones, the conversion of them is usually performed through acidulation followed by neutralization. Traditionally, acids used are usually sufficiently strong to hydrate phospholipids without hydrolyzing the triglyceride. At present, citric or phosphoric acid is normally being used for any type of vegetable oil. However, phosphoric acid is more preferred by the palm oil refiners because of a lower unit cost and easier handling. The main component of phospholipids is phosphatides. Figure 1.2 shows the chemical structure of phosphatides.

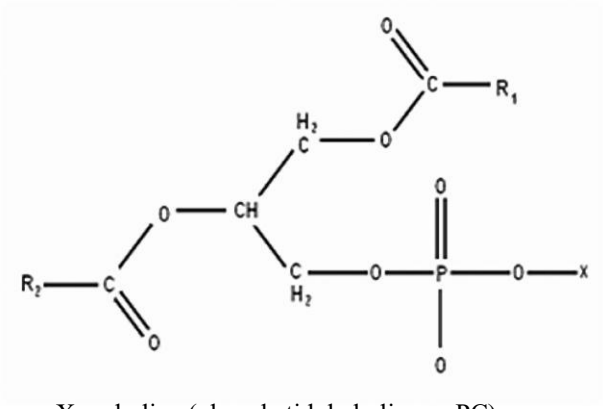

X = choline (phosphatidyl choline or PC)

X = ethanolamine (phosphatidylethanolamine or PE)

X = inositol (phosphatidylinositol or PI)

X = hydrogen (phosphatidyl acid or PA)

Figure 1.2 Chemical structures of phosphatides (Morad et al., 2006)

Phospholipids are present in relatively small quantities of about 5–130 ppm in palm oil as compared with other vegetables oils. The solvent extracted mesocarp oil usually contained 100-200 ppm phospholipids, however it only presents at level of 20-80 ppm in commercial crude palm oil.

Phospholipids have been reported to show antioxidant affects. Their antioxidant-synergistic effects can be attributed to the sequestering of soluble pro-oxidant metal ions to form inactive species. There is also a synergism between phospholipids and naturally occurring antioxidants such as α-tocopherol and quercetin. Hydratable insoluble metal ions could also dispersed by phospholipids through miscellar action. Since phospholipids and glycolipids cause reverse micelle, vesicle or emulsion droplet formation, phospholipids can remove metal ions and their hydrophilic salts from the lipid phase to reduce oxidation.

1.2.2.3 Degumming agents

There are two types of degumming agents that are usually being used in palm oil refining industry, are phosphoric and citric acid.

Phosphoric acid (H_3PO_4), is a colorless and odorless liquid. A food grade phosphoric acid with concentration of 85 wt% is normally used in palm oil refining process.

Citric acid or 2-hydroxy-1,2,3-propanetricarboxylic acid, an organic carboxylic acid containing three carboxyl groups; it is a solid at room temperature, melted at 153ºC and decomposed at a higher temperature.

1.2.3 Esterification (Clark, 2004)

Esterification is the general name for a chemical reaction in which two reactants (typically an alcohol and an acid) form an ester as the reaction product. Esters are common in organic chemistry and biological materials, and often have a characteristic pleasant, fruity odor. This leads to their extensive use in the fragrance and flavor industry. Esterification is a reversible reaction. Hydrolysis- literally "water splitting" involves adding water and a catalyst (commonly NaOH) to an ester to get the sodium salt of the carboxylic acid and alcohol. As a result of this reversibility, many esterification reactions are equilibrium reactions.

1.2.3.1 The mechanism for the esterification reaction

This example looks in detail at the mechanism for the formation of esters from carboxylic acids and alcohols in the presence of concentrated sulfuric acid acting as the catalyst. It uses the formation of ethyl ethanoate from ethanoic acid and ethanol as a typical example (Eq 1.1). The reaction is slow and reversible. To reduce the chances of the reverse reaction happening, the ester is distilled off as soon as it is formed.

$$CH_3COOH + CH_3CH_2OH \xleftrightarrow{\text{Conc. } H_2SO_4} CH_3COOCH_2CH_3 + H_2O \quad \text{(Eq 1.1)}$$

All the steps in the mechanism below are shown as one-way reactions because it makes the mechanism look less confusing. The reverse reaction is actually done sufficiently and differently that it affects the way the mechanism is written.

Step 1

In the first step, the ethanoic acid takes a proton (a hydrogen ion) from the concentrated sulfuric acid. The proton becomes attached to one of the lone pairs on the oxygen atom which is double-bonded to the carbon atom.

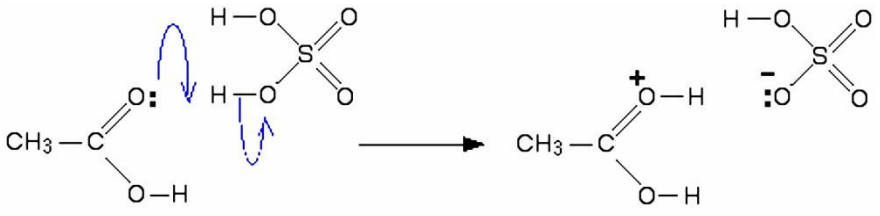

(Eq 1.2)

The proton transferring to the oxygen gives it a positive charge, but it is actually misleading to draw the structure in this way. The positive charge is delocalised over the whole of the right-hand end of the ion, with a fair amount of positiveness on the carbon atom. In other words, an electron pair shifting gives this structure:

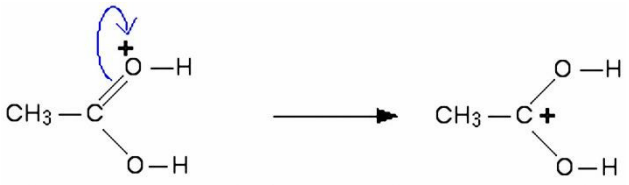

(Eq 1.3)

It can also imagine another electron pair shift producing a third structure:

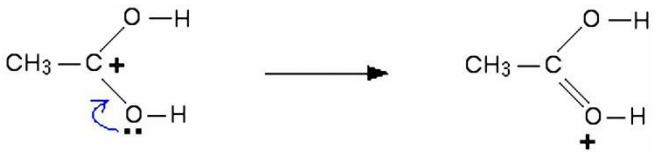

(Eq 1.4)

But none of these is the correct structure of the ion formed. The truth lies somewhere in between all of them. One way of writing the delocalized structure of the ion is like this:

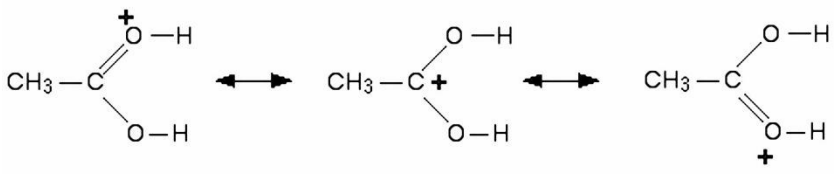

(Eq 1.5)

The double headed arrows are shown that each of the individual structures makes a contribution to the real structure of the ion. They don't mean that the bonds are flipping back and forth between one structure and another. The various structures are known as **resonance structures** or **canonical forms**. There will be some degree of positive charge on both of the oxygen atoms, and also on the carbon atom. Each of the bonds between the carbon and the two oxygen atoms will be the same - somewhere between a single bond and a double bond.

For the purposes of the rest of this discussion, it should use the structure where the positive charge is on the carbon atom.

Step 2

The positive charge on the carbon atom is attacked by one of the lone pairs on the oxygen atom of the ethanol molecule.

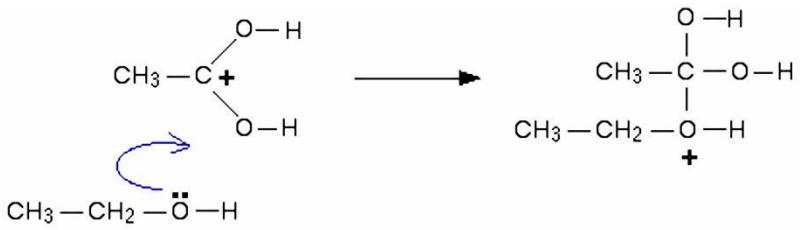

(Eq 1.6)

Step 3

What happens next is that a proton (a hydrogen ion) gets transferred from the bottom oxygen atom to one of the others. It gets picked off by one of the other substances in the mixture (for example, by attaching to a lone pair on an unreacted ethanol molecule), and then dumped back onto one of the oxygen atom more or less at random. The net effect is:

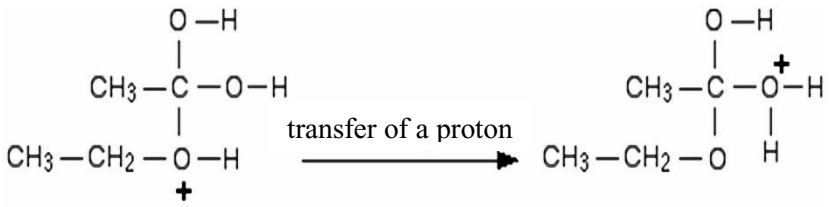

(Eq 1.7)

Step 4

Now a molecule of water is lost from the ion.

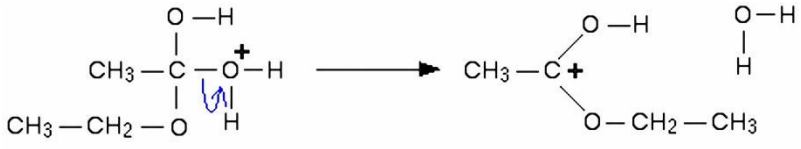

(Eq 1.8)

The product ion has been drawn in a shape to closely reflect the final product. The structure for the latest ion is just like the one discussed in step 1. The positive charge is actually delocalized all over that end of the ion, and there will also be contributions from structures where the charge is on the either of the oxygen atoms.

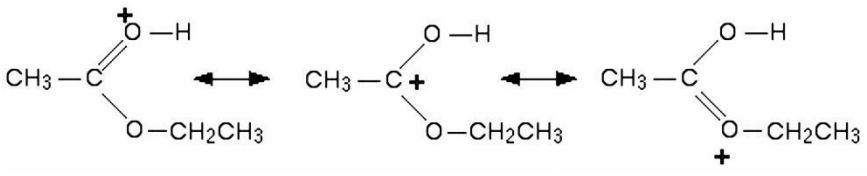

(Eq 1.9)

It is easier to follow what is happening if we keep going with the structure with the charge on the carbon atom.

Step 5

The hydrogen is removed from the oxygen atom by reaction with the hydrogen sulfate ion which was formed way back in the first step.

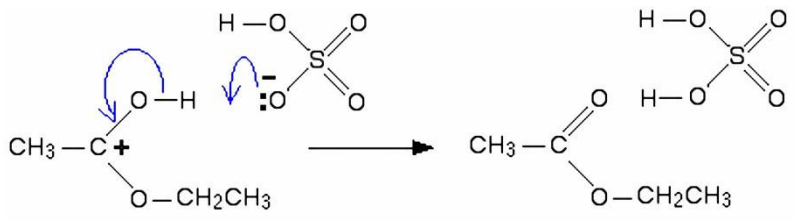

(Eq 1.10)

The ester has been formed and the sulfuric acid catalyst has been regenerated.

1.2.4 Transesterification

Transesterification also called alcoholysis is the displacement of alcohol from an ester by another alcohol in a process similar to hydrolysis, except than an alcohol is used instead of water. This process has been widely used to reduce the viscosity of triglyceride. The transesterification reaction is represented by the general equation:

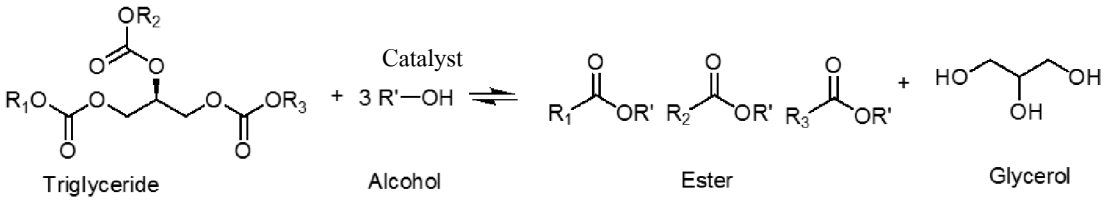

(Eq 1.11)

1.2.5 Biodiesel (University of Strathelyde, 2008)

Biodiesel is an alternative fuel similar to conventional or 'fossil' diesel. Biodiesel can be produced from straight vegetable oil, animal oil/fats, tallow and waste cooking oil. The process used to convert these oils to biodiesel is called transesterification. The largest possible source of suitable oil comes from oil crops

such as rapeseed, palm or soybean. Waste vegetable oil can often be sourced for a small price. (The waste oil must be treated before conversion to biodiesel by removing impurities). The result is biodiesel produced from waste vegetable oil can compete with fossil diesel.

Biodiesel has many environmentally beneficial properties. The main benefit of biodiesel is that it can be described as 'carbon neutral'. This means that the fuel produces no net output of carbon in the form of carbon dioxide (CO_2). This effect occurs because when the oil crop grows it absorbs the same amount of CO_2 as is released when the fuel is combusted. In fact this is not completely accurate as CO_2 is released during the production of the fertilizer required to fertilize the fields in which the oil crops are grown. Fertilizer production is not the only source of pollution associated with the production of biodiesel, other sources include the esterification process, the solvent extraction of the oil, refining, drying and transporting. All these processes require an energy input either in the form of electricity or from fuel, both of which will generally result in the release of green house gases. To properly assess the impact of all these sources requires use of a technique called life cycle analysis. Biodiesel is rapidly biodegradable and completely non-toxic, meaning spillages represent far less of a risk than fossil diesel spillages. Biodiesel has a higher flash point than fossil diesel and so is safer in the event of a crash.

1.2.5.1 Biodiesel productions

There are three basic routes to biodiesel production from oils and fats:

- Base catalyzed transesterification of the oil.
- Direct acid catalyzed transesterification of the oil.
- Conversion of the oil to its fatty acids and then to biodiesel.

Almost all biodiesel is produced using base catalyzed transesterification as it is the most economical process requiring only low temperatures and pressures and producing a 98 wt% conversion yield. The transesterification process is the reaction of a triglyceride with an alcohol to form esters and glycerol. A triglyceride has a glycerine molecule as its base with three long chain fatty acids attached. The characteristics of the fat are determined by the nature of the fatty acids attached to the

glycerine. The nature of the fatty acids can in turn affect the characteristics of the biodiesel. During the transesterification process, the triglyceride is reacted with alcohol in the presence of a catalyst, usually a strong alkaline like sodium hydroxide. The alcohol reacts with the fatty acids to form the mono-alkyl ester, or biodiesel and crude glycerol. In most production methanol or ethanol is the alcohol used (methanol produces methyl esters, ethanol produces ethyl esters) and is base catalyzed by either potassium or sodium hydroxide. Potassium hydroxide has been found to be more suitable for the ethyl ester production; either base can be used for the methyl ester. A common product of the transesterification process is Rape Methyl Ester (RME) produced from raw rapeseed oil reacted with methanol. The reaction between the fat or oil and the alcohol is a reversible reaction and so the alcohol must be added in excess to drive the reaction towards the product side and ensure complete conversion.

A successful transesterification reaction is signified by the separation of the ester and glycerol phases after the reaction time. The heavier, co-product, glycerol settles out and may be sold as it is or it may be purified for use in other industries, e.g. the pharmaceutical, cosmetics etc.

1.2.6 Sonochemistry (Thompson and Doraiswamy, 1999 and Suslick, 1989)

Sonochemistry is the use of ultrasound to enhance or alter chemical reactions. Sonochemistry in the true sense of the term occurs when ultrasound induces “true” chemical effects on the reaction system, such as forming free radicals which accelerate the reaction. However, ultrasound may have other mechanical effects on the reaction, such as increasing the surface area between the reactants, accelerating dissolution, and/or renewing the surface of a solid reactant or catalyst.

Ultrasound has proven to be a very useful tool in enhancing the reaction rates in a variety of reacting systems. It has successfully increased the conversion, improved the yield, changed the reaction pathway, and/or initiated the reaction in biological, chemical, and electrochemical systems. This nonclassical method of rate enhancement, a field termed *sonochemistry*, is becoming a widely used laboratory technique. However, its use in industry is limited because the process of producing ultrasound is very inefficient and burdened with high operating costs. It is starting to attract attention because the operating costs may be off-set by reducing or eliminating

other process costs. The use of ultrasound may enable operation at milder operating conditions (e.g. lower temperatures and pressures), eliminate the need for extra costly solvents, and reduce the number of synthesis steps while simultaneously increasing end yields, permit the use of lower purity reagents and solvents, and/or increase the activity of existing catalysts. For these reasons, use of ultrasound appears to be a promising alternative for high-value chemicals and pharmaceuticals. In addition, research is continually underway to make it a feasible option in the ongoing effort to intensify large-scale processes.

Much of the pioneering work in the field has been done by chemists and physicists who have found that **the chemical, and some mechanical, effects of ultrasound are a result of the implosive collapse of cavitation bubbles.**

Ultrasound occurs at a frequency above 16 kHz, higher than the audible frequency of the human ear, and is typically associated with the frequency range of 20 kHz to 500 MHz. The frequency level is inversely proportional to the power output. Low-intensity, high frequency ultrasound (in the megahertz range) does not alter the state of the medium through which it travels and is commonly used for nondestructive evaluation and medical diagnosis. However, high-intensity, low-frequency ultrasound does alter the state of the medium and is the type of ultrasound typically used for sonochemical applications. Many of these applications are briefly explained in the Kirk-Othmer Encyclopedia of Chemical Technology (1983).

1.2.6.1 Theory

The chemical and mechanical effects of ultrasound are caused by cavitation bubbles which are generated during the rarefaction, or negative pressure, period of sound waves. During the negative-pressure cycle, the liquid is pulled apart at sites containing some gaseous impurity (nucleation sites), forming a void. Nucleation sites are also known as “weak spots” in the fluid. Nucleation in the absence of ultrasound can be seen every day when drinking a carbonated beverage. The bubbles of carbon dioxide form at scratches in the glass where gaseous impurities, such as air, are harbored and act as nucleation sites. When using ultrasound, the cavitational activity is directly proportional to the number density of particles present in the medium. Chemical effects due to ultrasound are not observed

when there are no dissolved gases in the system, when the sound intensity is not greater than the cavitation threshold of the system or when the reactant is not volatile enough to enter the cavitation bubble during its formation. As ultrasound passes through a liquid, the expansion cycles exert negative pressure on the liquid, pulling the molecules away from one another. If the ultrasound is sufficiently intense, the expansion cycle can create cavities in the liquid. This will occur when the negative pressure exceeds the local tensile strength of the liquid, which varies according to the type and purity of liquid. (Tensile strength is the maximum stress that a material can withstand from a stretching load without tearing.) Normally, cavitation is a nucleated process; that is, it occurs at pre-existing weak points in the liquid, such as gas-filled crevices in suspended particulate matter or transient microbubbles from prior cavitation events. Most liquids are sufficiently contaminated by small particles that cavitation can be readily initiated at moderate negative pressures.

Once formed, small gas bubbles irradiated with ultrasound will absorb energy from the sound waves and grow. Cavity growth depends on the intensity of the sound. At high intensities, a small cavity may grow rapidly through inertial effects. If cavity expansion is sufficiently rapid during the expansion half of a single cycle, it will not have time to recompress during the compression half of the acoustic cycle.

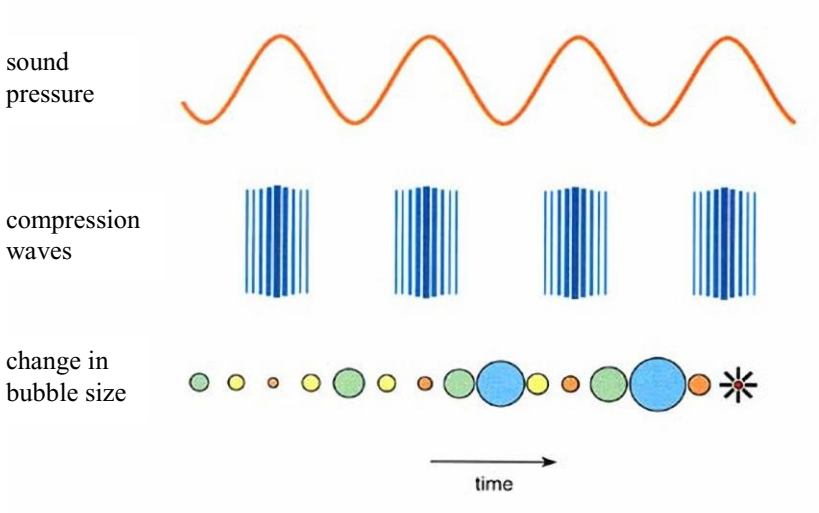

Figure 1.3 Cavitation by ultrasound irradiation (Suslick, 1989)

The physical and chemical effects of ultrasound are a result of both stable and transient cavitational events, which are described in the following sections. Two competing theories exist to explain the chemical effects due to cavitation: the *hot-spot theory* and *the electrical theory*. The hot-spot theory postulates that when the bubbles cavitate, localized hot spots are formed which reach temperatures and pressures in excess of 5000 K and 500 atm. The electrical theory postulates that an electrical charge is created on the surface of a cavitation bubble, forming enormous electrical field gradients across the bubble which is capable of bond breakage upon collapse. The hot-spot theory is generally more accepted, although Margulis (1992, 1994) reports many phenomena which contradict this theory but are supported by the electrical theory. A Letter to the Editor published in 1996 completely discounted the electrical theory as a valid mechanism behind sonoluminescence and sonochemistry.

1.2.6.2 Bubble dynamics.

The chemical effects of ultrasound have been attributed to the collapse of both stable and transient cavitational events. Stable cavities oscillate for several acoustic cycles before collapsing, or never collapse at all. Transient cavities, conversely, exist for only a few acoustic cycles. The following sections provide a brief explanation of bubble dynamics and its modeling.

(a) Stable cavities.

Stable cavities are bubbles which form and oscillate around a mean radius in a sound field and exist for many acoustic cycles. For this occurrence their growth rate during the rarefaction must be equivalent to their rate of contraction during the compression phase. This specifies that rectified diffusion, or the unequal transfer of mass into the bubble during the acoustic wave cycle, is not occurring. Because many ultrasonic transducers are designed with a set frequency, operating under resonance conditions is achieved by changing the system parameters in order to alter the bubble resonant frequency to match that of the transducer. This can be done by varying the hydrostatic pressure and the system temperature. Other factors which affect the resonating frequency of the bubble include the characteristics of the liquid, such as its density and surface tension. Conversely, varying the ultrasonic frequency

in order to drive the bubble dynamics toward transient cavitation was also investigated.

(b) Rectified diffusion.

At lower acoustic intensities cavity growth can also occur by a slower process called rectified diffusion. Rectified diffusion is the event where cavitation bubbles grow more during expansion than they shrink during contraction due to the unequal diffusion of gases and vapor from the bulk liquid phase into the bubble. Cavity growth during each expansion is, therefore, slightly larger than shrinkage during the compression. Thus, over many acoustic cycles, the cavity will grow. The growing cavity can eventually reach a critical size where it can efficiently absorb energy from the ultrasonic irradiation. Called the resonant size, this critical size depends on the liquid and the frequency of sound; at 20 kHz, for example, it is roughly 170 micrometers. At this point the cavity can grow rapidly during a single cycle of sound.

(c) Transient cavitation.

A transient cavity is one which exists for only a few acoustic cycles. During its existence it grows several times larger than its initial size and, upon implosion, creates extreme temperatures and pressures within its cavity.

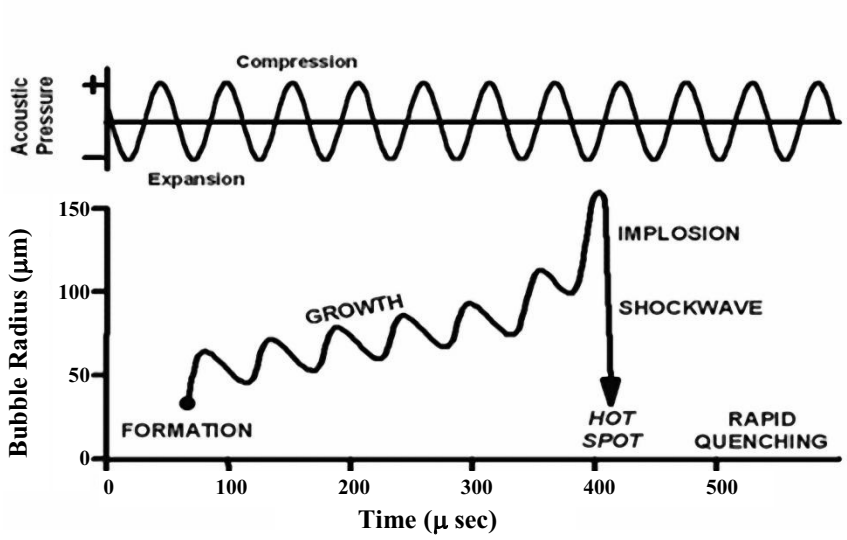

Figure 1.4 Transient cavitation process (Suslick, 1989)

1.2.6.3 Factors affecting cavitation

The ambient conditions of the reaction system can greatly influence the intensity of cavitation, which directly affects the reaction rate and/or yield. These conditions include the reaction temperature, hydrostatic pressure, irradiation frequency, acoustic power, and ultrasonic intensity. Other factors which significantly affect the cavitational intensity are the presence and nature of dissolved gases, choice of solvent, sample preparation, and choice of buffer. Each of these factors is described in detail below.

(a) Presence and nature of dissolved gases

Dissolved gases act as nucleation sites for cavitation. As gases are removed from the reaction mixture because of the implosion of the cavitation bubbles, initiation of new cavitational events becomes increasingly difficult. Bubbling gases through the mixture facilitates the production of cavitation bubbles, but the type of gas used is important. As a general rule, a gas with a high specific heat ratio gives a greater cavitational effect than one with a low specific heat ratio. Because the collapse of the bubble occurs in such a small amount of time (~ 3.5 μs), it can be assumed to occur diabatically. Monatomic gases, such as argon and helium, convert more energy upon cavitation than diatomic gases, such as nitrogen and oxygen, because of the larger ratio of specific heats. Gases which are extremely soluble in the reaction mixture may reduce the cavitational effect because the bubbles formed may redissolve before collapse occurs. The bubbles which do not dissolve often become so large (because of facile penetration of gas into the bubble) that they float to the surface and explode. The thermal conductivity of the gas is also important because, although the collapse is modeled as adiabatic, there is a small amount of heat which is transferred to the bulk liquid mixture during collapse. As the thermal conductivity of the gas increases, the amount of heat loss due to thermal dissipation also increases.

(b) Ambient temperature

Contrary to chemical reactions in general, an increase in the ambient reaction temperature results in an overall decrease in the sonochemical effect. The

decrease is a result of a sequence of events. First, as the reaction temperature is raised, the equilibrium vapor pressure of the system is also increased. This leads to easier bubble formation (due to the decrease of the cavitation threshold); however, the cavitation bubbles which are formed contain more vapor. As discussed above, vapor reduces the ultrasonic energy produced upon cavitation because it cushions the implosion in addition to using enthalpy generated in the implosion for the purposes of condensation. In general, the largest sonochemical effects are observed at lower temperatures when a majority of the bubble contents is gas.

In certain reaction systems, an optimum reaction temperature may lead to more favorable results. In such systems, an increase in temperature will increase the kinetic reaction to a point at which the cushioning effect of the vapor in the bubble begins to dominate the system. When this occurs, the rate of the reaction decreases upon further increase in ambient reaction temperature. The rate may even reach a plateau with temperature and then decrease as the temperature increases. The observed temperature effect was dominated by the reaction kinetics in and around the cavitating bubble. However, increasing the temperature was also simultaneously decreasing the intensity of cavitation, thus reducing the amount of free radicals produced within the bubble. It was speculated that these free radicals were required for the degradation reaction to occur and that they diffuse from the vapor cavity to the gas-liquid film where reaction ensues. As the rates of the counter diffusing reactants became comparable, a further increase in temperature had little or no effect on the reaction (i.e. the percent change in thymine concentration reached a plateau as a function of temperature). However, as the temperature continued to be increased, the declining production of free radicals began to have a negative effect on the rate of degradation.

(c) Ambient pressure

An increase in the ambient reaction pressure generally results in an overall increase in the sonochemical effect because of the decrease in the vapor pressure of the mixture. Decreasing the vapor pressure increases the intensity of the implosion, thus increasing the ultrasonic energy produced upon cavitation.

However, there is a limitation to this, as found by Moulton et al. (1983, 1987) when investigating the ultrasonic hydrogenation of soybean oil. When they operated at an ambient pressure of 200 psig and greater, they found ultrasound to have little effect on the catalyst activity. When the pressure was decreased to 115 psig, the effects of ultrasound were significantly increased. It appeared that operating at pressures of 200 psig and above increased the cavitation threshold in the system to a level at which the cavitation bubbles could no longer be produced or were produced in such small quantities that they did not significantly effect the overall reaction. For any given system an optimum operating pressure will most likely exist.

Cum et al. (1988) found that operating the system under resonance conditions increased the rate and yield of the reaction.

(d) Choice of solvent

Cavities are more readily formed when using a solvent with a high vapor pressure, low viscosity, and low surface tension. However, the intensity of cavitation is benefited by using solvents with opposing characteristics (i.e. low vapor pressure, high viscosity, and high surface tension). Other researchers found that cavitation was inhibited when using the extremely volatile solvent diethyl ether, which has a vapor pressure of ~ 0.73 atm at 25°C. When choosing a solvent for a particular reaction system, the appropriate "family" of solvents to use is frequently dictated by the type of chemistry involved (i.e. due to temperature, solubility and/or other issues). Once a family of solvents is identified, then the effects of the various solvents within that family on cavitation can be investigated.

(e) Ultrasonic frequency

The frequency of the ultrasound has a significant effect on the cavitation process because it alters the critical size of the cavitation bubble. At very high frequencies, the cavitational effect is reduced because either (1) the rarefaction cycle of the sound wave produces a negative pressure which is insufficient in its duration and/or intensity to initiate cavitation or (2) the compression cycle occurs faster than the time required for the microbubble to collapse.

In summary, lower frequency ultrasound produces more violent cavitation, leading to higher localized temperatures and pressures at the cavitation site. However, higher frequencies may actually increase the number of free radicals in the system because, although cavitation is less violent, there are more cavitational events and thus more opportunities for free radicals to be produced. In addition, the shortened bubble lifetime may increase the amount of free radicals which are able to escape from the cavitation site to the bulk mixture, where they facilitate the bulk reaction. It is contended that the optimum frequency is system specific and depends on whether intense temperatures and pressures are required (thus enhanced by lower frequencies) or if the rate of single electron transfer is more important (enhanced by higher frequencies).

(f) Acoustic power

Many authors have found that as the power delivered to the reaction mixture increases, the rate of the reaction increases to a maximum and then decreases with a continued increase in power. A possible explanation for the observed decrease at high powers is the formation of a dense cloud of cavitation bubbles near the probe tip which acts to block the energy transmitted from the probe to the fluid.

1.2.6.4 Methods of producing cavitation

Cavitation can be generated within fluid using transducers (devices which convert one form of energy to another). Gas-driven transducers, such as dog whistles, use high-velocity gas flow to generate ultrasound. Liquid-driven transducers, such as submarine propellers, force liquid across a vibrating plate or through an orifice, creating a cavitation zone. Electromechanical transducers, the most commonly used transducers in sonochemical research, convert electrical energy to sound energy.

When using gas- or liquid-driven transducers, cavitation is generated in situ; i.e., cavities are formed within the fluid by forcing the fluid through a physical object which generates shearing forces great enough to tear the fluid apart. Direct sonication occurs when a device which generates sound waves, such as a probe or horn, is place directly in a fluid system. Indirect sonication occurs when the sound waves propagate through some other medium before they come into contact with the vessel containing the reaction mixture, which is often the case when using an ultrasonic cleaning bath. As is evident by the nature of sonication, probe systems

produce higher intensities in reaction mixtures as compared to ultrasonic cleaning baths. Cavitation generated in situ can reach intensities comparable to direct sonication where hydrodynamically induced cavitation with a throttling valve to increase the hydrolysis of fatty oils. The yields and reaction conditions obtained using a hydrodynamic system, were similar to those of a probe system. Cavitation can also be induced in situ using a focused electromagnetic acoustic transducer (EMAT) which produces a high-intensity lithotripter shock wave in the fluid concerned. Once the shock wave is induced, cavitational bubbles are formed in the negative pressure region of the wave, causing rupturing of the fluid. Secondary cavitational transients, created by the collapse of the primary bubbles, may also occur.

(a) Piezoelectric vs Magnetostrictive transducers.

The two main types of electrochemical transducers used in industrial applications are piezoelectric and magnetostrictive. Piezoelectric transducers are constructed using a piezoelectric material, such as quartz, which expands and contracts in an alternating *electric* field, thus producing sound waves from the electric signal. Magnetostrictive transducers are constructed from materials, such as nickel alloys, which expand and contract in an alternating *magnetic* field. Each transducer has its own advantages and disadvantages, as outlined in Table 1.6.

Table 1. 6 Comparison of piezoelectric and magnetostrictive transducers

Piezoelectric transducers	Magnetostrictive transducers
- relatively inexpensive - relatively small and light - damaged at temperatures > ~150 °C - will age considerably, i.e., have a reduced power output, with continuous operation at high temperatures and/or over long periods of time - may be damaged by large impact - structure will be damaged if operated “dry”	- more expensive than piezoelectric for similar power ratings - heavier and bulkier than piezoelectric - with special precautions, can be operated at temperatures >250 °C - will not degrade or fail over time by their very nature; some have been used successfully for over 20 years of commercial operation - extremely resistant to mechanical damage, such as large impacts - no damage when operated “dry”

(Thomson and Doraiswamy, 1999)

As is evident from the table, piezoelectric transducers are normally used with small-volume processes. When large volumes and/or long, continuous reaction times are required, the more robust magnetostrictive transducer may be the preferred option.

1.2.6.5 Ultrasonic system types

(a) Ultrasonic bath

Ultrasonic baths were originally manufactured for cleaning purposes. Typical baths have the transducers attached to the bottom, although the transducers can be submersed in a conventional tank to obtain similar effects. Bath systems are widely used in sonochemical research because they are readily available and relatively inexpensive. The reaction vessel is typically immersed in the coupling fluid contained in the bath (indirect sonication). However, the bath itself can be used as the reaction vessel but would require additional mechanical agitation. In addition, the bath walls would be exposed to the reaction mixture and/or irradiation, making them susceptible to corrosion or erosion.

When indirect sonication is used, the ultrasonic power which reaches the reaction vessel is relatively low as compared to other ultrasonic systems, such as a probe. In addition, obtaining reproducible results may be difficult because the amount of power reaching the reaction mixture is highly dependent upon the placement of the sample in the bath. The results can also vary with time as the bath warms during operation. Because every bath has different characteristics, it is important to determine the optimum conditions for each bath and to place the reaction vessel in the same location for each experiment. In addition, it is important to use the same type of reaction vessel for each reaction because the shape of the bottom of the reaction vessel significantly influences the wave pattern, even when placed in the same position in the bath. Another disadvantage to using a bath system is that the coupling fluid surrounding the reaction vessel(s) will eventually increase in temperature, making the maintenance of isothermal conditions difficult. Cooling coils can be placed within the bath, but they will have an effect on the sound field and may reduce the amount of power reaching the vessel.

(b) Probe (horn) systems

Probe systems, also called horn systems, are being more frequently used for sonochemical research in the laboratory. This may be because manufacturers are aware that this type of research is increasing and are providing equipment to meet the demand. In addition, probe systems are capable of delivering large amounts of power directly to the reaction mixture which can be regulated by varying the amplitude delivered to the transducer. Disadvantages in using a probe system include erosion and pitting of the probe tip, which may contaminate the reaction solution. Fortunately several probes are available with removable tips, making replacement relatively inexpensive. The localized areas of ultrasonic intensity in a fluid are highly dependent on the power delivered to the transducer. However, as the power delivered increases, the ultrasonic intensity increases at the center of the reactor and dissipates in the radial direction. At an input power of 200 W, the active region in the radial direction is equal to that of the horn (the remaining radial direction had negligible activity).

(c) Planar Transducers.

This type of setup is typically made in the laboratory and consists of a planar transducer (Figure 1.5) connected to a vessel which contains either the reaction mixture (a. Direct sonication) or a coupling fluid (b. Indirect sonication) into which the reaction vessel is immersed. “Cup-horn” designs are very similar to planar transducer designs, with the exception that the horn is designed to allow for cooling capabilities, facilitating the maintenance of isothermal conditions. Both planar transducer and cup-horn systems are capable of delivering higher powers than ultrasonic bath systems. However, they are both difficult to scale-up.

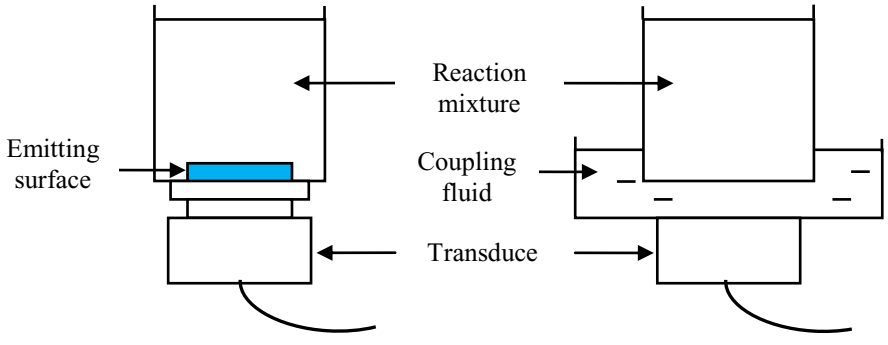

a. Direct sonication b. Indirect sonication

Figure 1.5 Planar transducer systems (Thomson and Doraiswamy, 1999)

1.2.6.6 Conclusions

The advances in the field of ultrasound in the last 20 years have been plentiful, but there is still a lot of new frontier to be covered. Researchers have found that ultrasound chemically enhances reactions which depend on a SET (single electron transfer) process as a key step. Reaction systems which follow an ionic mechanism are enhanced by the mechanical effects of ultrasound. These enhancements are a result of increases in the intrinsic mass-transfer coefficient, increases in surface area resulting from particle degradation, and, in some cases, increases in the driving force for dissolution. In some reaction systems, ultrasound changes the reaction pathway from ionic to one which involves a SET step.

Several other aspects of sonochemical behavior are unclear. The manner by which free radicals are produced within the cavitation bubble remains elusive, although several researchers have concluded that they are formed during the adiabatic implosion of the cavitation bubble. Ultrasound has been found to enhance the effective diffusivity in a solid-liquid system, increase the intrinsic mass-transfer coefficient, induce supersaturation, and increase the activation energy and frequency factor of various reaction systems. However, the actual mechanisms behind these enhancements have not been discerned. In addition, the amount of available engineering data in the areas of ultrasonic reactor design and scale-up are lacking. It will take the combined work of scientists from all fields to resolve the role of ultrasound in reacting systems and to make it a viable rate enhancement technique for commercial industrial processes.

1.3 Literature Review

Wright et al. (1944) noted that the starting materials used for alkali-catalyzed transesterification of glyceride must meet certain specifications. The glyceride should have an acid value less than 1 mgKOH/g and all materials should be substantially anhydrous. If the acid value was greater than 1 mgKOH/g, more NaOH was required to neutralize the free fatty acids. Water also caused soap formation, which consumed the catalyst and reduce catalyst efficiency. The resulting soaps caused an increase in viscosity, formation of gels and made the separation of glycerol difficult.

Bradshaw and Meuly (1944) and Feuge and Grose (1949) also stressed the importance of oils being dry and containing less than 0.5 wt% of free fatty acid.

Freedman et al. (1984) stated that ester yields were significantly reduced if the reactants were not dry and containing free fatty acids less than 0.5 wt%.

Ma et al. (1998) investigated the effects of free fatty acids and water on transesterification of beef tallow with methanol. Their results showed that the water and free fatty acid content of beef tallow should be kept below 0.06 and 0.5 wt%, respectively in order to get the best conversion. Water content was a more critical variable in the transesterification process than was free fatty acid.

Crabble et al. (2001) stated that the presence of free fatty acid in vegetable oils makes the oil more acidic. In the alkali-catalyzed method, the amount of catalyst used depends very much on the acidity of the vegetable oil. More catalyst is necessary to eliminate fatty acids in crude and used frying/waste vegetable oil since they usually contain more fatty acids than do the refined ones. The presence of fatty acid in high content in vegetable oil deactivates alkali catalysts, and the addition of an excessive amount of alkali as compensation give rise to the formation of emulsions, which increase viscosity, thus leading to the formation of gel and the problems associated with glycerol separation and the loss in yield of methyl ester.

Kusdiana and Saka (2004) studied the effect of free fatty acid on the yield of methyl ester in the supercritical methanol method. They chose oleic acid as a model of free fatty acid because oleic acid is most abundant in rapeseed oil. They showed that both acid- and alkali- catalyzed transesterification resulted in a lower conversion when free fatty acid content increased in the reaction system. In the acid-

catalyzed method, a reaction system with 20 wt% of free fatty acid reduced the conversion to about a half, while in the alkali-catalyzed method only 35 wt% methyl esters were obtained.

Stavarache et al. (2005) studied the transesterification of vegetable oil with short-chain alcohols, in the presence of base-catalyst, by means of low frequency ultrasound (Honda Electronics Ultrasonic Cleaners WS1200-28 and WS1200-40 of 28 and 40 kHz, respectively) with a total power of 1200 W, working power being set at 60%) in order to obtain biodiesel fuel. By using ultrasounds the reaction time is much shorter (10–40 minutes) than for mechanical stirring. The quantity of required catalyst is 2 or 3 times lower. The molar ratio of alcohol: oil used is only 6:1. Normal chain alcohols react fast, while secondary and tertiary alcohols show some or no conversion after 60 min of reaction. Surprisingly, 40 kHz ultrasounds are much more effective in the reduction of the reaction time (10–20 minutes). Twenty eight kilohertz give slightly better yields (98–99 wt%), but longer reaction time, while higher frequencies are not useful at all for the transesterification of fatty acids.

Stavarache, et al. (2007) studied the batch transesterification of vegetable oil with methanol, in the presence of potassium hydroxide as catalyst, by means of low frequency ultrasound (40 kHz) with the aim of gaining more knowledge on intimate reaction mechanism. The ester preparation involved a batch transesterification reaction, followed by washing and drying. The one step reaction utilized a 100 wt% excess methanol, or a total molar ratio of methanol to oil of 6:1. The quantity of catalyst was 0.5 wt% of the oil, determined as optimum in a previous study. All experiments were performed in an Erlenmeyer type flask, having 100 ml total volume, immersed into the cleaning bath in the optimum position towards the transducer in order to ensure maximum ultrasound entering the reaction mixture. The ultrasonic reactions were performed using Honda Electronics Ultrasonic Cleaner WS 1200–40, with a total power of 1200 W, working power being set at 70%. The reaction temperature was 36 ± 2°C for all experiments and was maintained constant by circulating water through the bath. They can suppose that in the first two steps of the ultrasonically driven transesterification (TG→DG and DG →MG) the fatty acids in positions 1 and 3 are esterified. The saturated fatty acids have a natural preference for these positions and therefore they should be esterified at the very beginning of the

reaction, fact plentifully demonstrated by the behavior of palm oil. After 20 min of ultrasonic irradiation the reaction is almost complete or in the last stage of completion for all types of fatty acids. The presence of MG in high amount, even after 60 minutes of ultrasonic irradiation, proves that the fatty acids in position 2 are not easily esterified. The major part of the ultrasonically driven transesterification of vegetable oils under base catalysis took place in the first 3–10 minutes of reaction if not faster, making from this technique a unique one for FAME synthesis. Diglyceride were found in small amounts during the ultrasonically driven transesterification process, while monoglycerides were detected in high amount, indicating that the last step of transesterification – MG + ROH → Gly + ME – is slower. The conversion of FAME at the end of 60 minutes of sonication was almost same regardless the type of oil, meaning that the reaction mixture was in steady state (i.e. equilibrium concentration was reached). They can conclude that the ultrasonically driven transesterification is a tool applicable to almost all types of vegetable oils. The saturated fatty acids were transesterified mostly at the beginning of the reaction, while the amount of unsaturated fatty acids esters increased as the reaction progressed.

Marchetti and Errazu (2008) studied direct esterification of triglyceride to biodiesel and effects of the main variables involved in the process, reaction temperature, amount of catalyst, initial amount of free fatty acid and molar ratio alcohol to oil. They used concentrated sulfuric acid (98 wt%) as the catalyst and used anhydrous ethanol as the reactant. A mixture of refined sunflower oil with pure oleic acid was used to make an acid oil model. The lab scale reactor of 500 ml with mechanic agitation was used and also accompanied with a warmer jacket. Ethanol was used in the experiments instead of methanol since it is less toxic and safer to handle. They also studied modifications in initial amount of free fatty acids. The result showed that the amount of FFA was reduced from 10.684 to 0.54 wt%.

Kelkar et al. (2008) illustrated the use of cavitation for intensification of biodiesel synthesis (esterification) reaction, which is mass transfer limited reaction considering the immiscible nature of the reactants, i.e., fatty acids and alcohol. Esterification of fatty acid cut (C8–C10) with methanol in the presence of concentrated H_2SO_4 as a catalyst has been studied in hydrodynamic cavitation reactor as well as in the sonochemical reactor. It has been observed that ambient operating

conditions of temperature and pressure and reaction times of <3 hours, for all the different combinations of acid and methanol studied in the present work, was sufficient for giving > 90 mol% conversion. This clearly establishes the efficacy of cavitation as an excellent way to achieve process intensification of the biodiesel synthesis process. Optimization in terms of the operating molar ratio of the fatty acid to alcohol (1:10 ratio is the optimum in the present case) and catalyst loading (2 wt% of conc. H_2SO_4 catalyst) results in > 95 mol% conversion in about 90 minutes of processing time.

Hanh et al. (2009a) described that if oil contains higher amounts of FFA (>1 wt%), FFA form soap with the base catalysts. Consequently, it is considered that the ester conversion is decreased by the formation of soap that can prevent separation of the biodiesel from the glycerin. At present, there were little data about the esterification of free fatty acid with alcohol under ultrasonic irradiation condition as well as the effects of molar ratio (ethanol to free fatty acid), acid catalyst concentration (H_2SO_4 and CH_3COOH), and temperature. They investigated production of fatty acid ethyl ester (FAEE) from oleic acid with short-chain alcohols (ethanol, propanol, and butanol) under ultrasonic irradiation. The ultrasonic experiments were carried out using a Honda Electronics Ultrasonic Cleaner (WS 1200-40, 40 kHz with a maximum power of 1200 W). Batch esterification of oleic acid was carried out to study the effect of test temperatures of 10–60°C, molar ratios of alcohol to oleic acid of 1:1–10:1, quantity of catalysts of 0.5–10 wt% of oleic acid and irradiation times of 10 hours. The optimum condition for the esterification process was molar ratio of alcohol to oleic acid at 3:1 with 5 wt% of H_2SO_4 at 60°C with an irradiation time of 2 h.

Hanh et al. (2009b) investigated the biodiesel production through transesterification of triolein with various alcohols such as methanol, ethanol, propanol, butanol, hexanol, octanol and decanol was at molar ratio 6:1 (alcohol: triolein) and 25°C in the presence of base catalysts (NaOH and KOH) under ultrasonic irradiation (Honda Electronics Ultrasonic Cleaner WS 1200-40; 40 kHz) and mechanical stirring (1800 rpm) conditions. It was found that the rate of the alkyl ester formation under the ultrasonic irradiation condition was higher than that under the stirring condition. The relationships between ester conversion (wt%) and

irradiation time for various alcohols at molar ratio 6:1 (alcohol: triolein) and 1 wt% KOH under the ultrasonic irradiation condition was shown that ester conversions for all alcohols increase rapidly just after the irradiation and then reach maximum around 15 minutes. The highest ester conversion is obtained at the transesterification of triolein with methanol and ethanol. In addition, it was confirmed that the rate depended upon the kind of alcohols; as the number of carbon in alcohol increased, the rate of the ester formation tended to decrease. On the other hand, the secondary alcohols such as 2-propanol, 2-butanol, 2-hexanol, and 2-octanol showed little ester conversion, suggesting that steric hindrance strongly affected the transesterification of triolein.

1.4 Research Objectives

1.4.1 To design and construct equipment used for the batch acid degumming and acid catalyzed esterification of CPO.

1.4.2 To perform batch acid degumming and acid catalyzed esterification of CPO with ethanol assisted by ultrasonic irradiation.

1.4.3 To design and construct equipment used for the continuous acid degumming and acid catalyzed esterification of CPO.

1.4.4 To perform continuous acid degumming and acid catalyzed esterification of CPO with ethanol assisted by ultrasonic irradiation.

1.4.5 To design and construct CSTR used for the continuous acid degumming and acid catalyzed esterification of CPO.

1.4.6 To perform continuous acid degumming and acid catalyzed esterification of CPO with ethanol by CSTR.

1.4.7 To investigate the optimum conditions for the batch and continuous acid degumming and acid catalyzed esterification of CPO with ethanol assisted by ultrasonic irradiation and for conducting by CSTR.

1.5 Scopes of Research Work

1.5.1 To reduce phosphorus content of CPO less than 10 ppm using continuous acid degumming process.

1.5.2 To reduce FFA content of CPO lower than 0.5 wt% using continuous acid catalyzed esterification of CPO with ethanol assisted by ultrasonic irradiation.

1.5.3 To fabricate the lab scale equipment (capacity of 1 L) for continuous acid degumming and acid catalyzed esterification of CPO with ethanol assisted by ultrasonic irradiation.

1.5.4 To fabricate the lab scale equipment (capacity of 50 L) for acid degumming and continuous acid catalyzed esterification of CPO with ethanol using CSTR.

1.6 Expected Benefits

1.6.1 Phosphorus content of CPO is reduced to meet the EN 14214: 2008, biodiesel standard (ME standard).

1.6.2 The CPO as the raw material for biodiesel production is treated by lowering FFA content to the optimized level of 0.5 wt% before conducting the alkali catalyzed transesterification.

1.6.3 The optimal conditions for the batch and continuous acid catalyzed esterification of CPO with ethanol assisted by ultrasonic irradiation and conducting by CSTR are investigated.

CHAPTER 2

Experimentation

2.1 Materials

2.1.1 **Raw material**

2.1.1.1 Commercial CPO (~5 wt% of FFA) purchased from a local palm oil mill was used as feedstock for the experimentation.

2.1.2 **Chemicals**

2.1.2.1 Ethanol (C_2H_5OH) 99.5 wt% commercial grade

2.1.2.2 Sulfuric acid (H_2SO_4) 98 wt% commercial grade

2.2 Equipment and instrument

2.2.1 Ultrasonic processor, model UP400S, 24 kHz, 400 W. produced by Hielscher, Germany fitted with a 22 mm diameter sonotrode was used as the ultrasound generator. It can be adjusted to produce varying amplitude across a full range up to a maximum of 100 micrometers and has an acoustic power density of 85 W/cm^2 and a maximum submerged depth of 45 mm. This ultrasonic processor was used for batch ultrasonic experiments.

2.2.2 Ultrasonic processor: model YPSH1020204, 20 kHz, 1000 W (including transducer with cover, booster, titanium horn and generator) produced by Hangzhou Success Ultrasonic Equipment Co., Ltd., China. This ultrasonic processor was used for continuous ultrasonic experiments.

2.2.3 A 400-mL glass reactor, (ID: 60 mm, height: 155 mm) with a plastic sealed lid was used as the esterification reactor for the batch ultrasonic experiments. The attachment between the sonotrode and the glass reactor lid was sealed with a synthetic rubber o-ring in order to prevent any gas leakage.

2.2.4 A 4.60 L stainless steel reactor, 97 mm ID, 700 mm in length was used for continuous ultrasonic experiments.

2.2.5 A 1.47 L stainless steel reactor, 61 mm ID, 700 mm in length was used for continuous ultrasonic experiments.

2.2.6 A 87.4 L continuous stirred-tank reactor (CSTR), 310 mm ID and 1200 mm in length, a baffle tank equipped with 3-levels blade (6 blades), (details of the reactor were shown in appendix D) was used for CSTR experiments.

2.2.7 A water chiller controlled by a thermostat was provided by the Scientific Equipment Center, PSU, Songkhla, Thailand.

2.2.8 A cooling bath, a plastic container, inner diameter of 100 mm, height of 140 mm.

2.2.9 A water circulating pump was used as the temperature controlling system and assembled in the cooling bath.

2.2.10 Digital dosing pumps, model DMS and DME, Grundfos, Germany used for feeding CPO and ethanol-acid mixture.

2.2.11 A 17 L stainless steel heater tank equipped with 3 kW coiled heater used for heating CPO, as external heating source before feeding to CSTR.

2.2.12 A temperature monitoring was carried out using a Templog Temperature Data Logger version 1.0 digital thermometer with 8 channels purchased from the Scientific Equipment Center, PSU, Songkhla, Thailand. The thermometer probe was dipped into the reaction solution. The equipment was set up as shown in the experiment schematic diagram (Fig. 2.1).

2.2.13 A watt hour meter, type PL 10053, was used to monitor the power consumption.

2.2.14 An infra red thermometer, model DP-88, DIGICON

2.2.15 A hot air oven, model UNB 400, MEMMERT

2.2.16 A household microwave was used to dry the samples

2.2.17 A raw material feed tank

2.2.18 An ethanol-acid mixture feed tank

2.3 Methodology

2.3.1 **Studies of batch acid catalyzed esterification of CPO with ethanol assisted by ultrasonic irradiation**

The batch esterification equipment was set up as showing in Figure 2.1. The esterification reactions were carried out in the glass reactor placed in a circulating

water bath. Chilled water was circulated from water chiller by a water pump. The sonotrode was submerged in the reaction solution to a depth of 20 mm. The reaction temperature was controlled by adjusting flow rate of the cooling water and monitored by using the digital thermometer. The temperature was periodically recorded throughout the experiments.

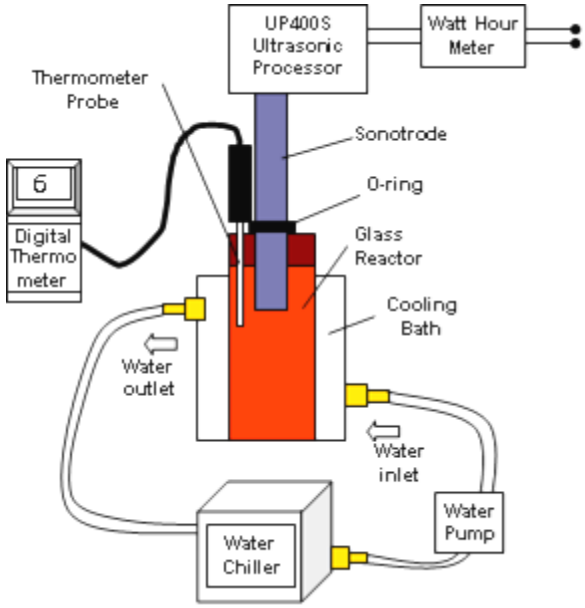

Figure 2.1 Schematic diagram of the batch esterification

Figure 2.2 Equipment setup of the batch esterification

Details of the experiments were stepwise described below.

2.3.1.1 Preliminary experiments. The experiments were designed by using Taguchi method (Peace, 1993) applying five randomly selected factors at four levels (Table 2.1). The preliminary experiments produced an $L_{16}(4^5)$ orthogonal array, corresponding to the 16 runs shown in Table 2.2.

Table 2.1 Factors and levels of the preliminary experiments

Factors	Description	Level 1	Level 2	Level 3	Level 4
Cat	: % H_2SO_4 by wt of FFA	1	2	5	20
Amp	: % Amplitude of acoustic power	35	55	75	100
MR	: Molar ratio of ethanol: FFA	5	10	20	40
Temp	: Reaction temperature in degree C	50	60	70	80
Time	: Reaction time in hour	0.5	1	2	4

Table 2.2 Orthogonal array of the preliminary experiments

Run No.	Cat	Amp	MR	Temp	Time
1	1	35	5	50	0.5
2	1	55	10	60	1
3	1	75	20	70	2
4	1	100	40	80	4
5	2	35	10	70	4
6	2	55	5	80	2
7	2	75	40	50	1
8	2	100	20	60	0.5
9	5	35	20	80	1
10	5	55	40	70	0.5
11	5	75	5	60	4
12	5	100	10	50	2
13	20	35	40	60	2
14	20	55	20	50	4
15	20	75	10	80	0.5
16	20	100	5	70	1

2.3.1.2 Secondary experiments exploiting the previous results. The secondary stage was finally defined by five re-ordered significant factors including two additional interaction factors i.e. CatxTemp and CatxMR (Table 2.3) that were needed after examining the interaction graphs obtained from the preliminary experiments. This experimental design produced a $L_8(2^7)$ orthogonal array, corresponding to the eight runs shown in Table 2.4. Both CPO and ethanol amount were fixed at 300 g per batch in order that every batch would have an equal volume optimized for the depth at which the sonotrode was submerged.

Table 2.3 Factors and levels of the secondary experiments

Factors	Descriptions	Level 1	Level 2
Cat	: % H_2SO_4 by wt of FFA	30	60
Time	: Reaction time in hour	1	2
Temp	: Reaction temperature in degree C	60	80
CatxTemp	: Catalyst interacts with temperature		
MR	: Molar ratio of ethanol: FFA	20	30
CatxMR	: Catalyst interacts with molar ratio		
Amp	: % Amplitude of acoustic power	35	75

Table 2.4 Orthogonal array of the secondary experiments

Run No.	Cat	Time	Temp	CatxTemp	MR	CatxMR	Amp
1	30	1	60	30x60	20	30x20	35
2	30	1	60	60x80	30	60x30	75
3	30	2	80	30x60	20	60x30	75
4	30	2	80	60x80	30	30x20	35
5	60	1	80	30x60	30	30x20	75
6	60	1	80	60x80	20	60x30	35
7	60	2	60	30x60	30	60x30	35
8	60	2	60	60x80	20	30x20	75

2.3.1.3 Further experiments based on the best conditions of the secondary experiments were conducted by using different reaction times.

2.3.1.4 Additional experiments were set up to investigate the effect of ester hydrolysis using two-stage esterification. The optimized conditions were based on those results from the further experiments which produced the least FFA to be used for conducting the first stage esterification. After finishing the first stage reaction, all reaction mixture was washed with warm water until obtained neutral washing water and then dried with a household microwave for 3 minutes (1.5 minute each) to insure that it had no water. Then the second esterification was conducted by using the same conditions as previously used.

2.3.1.5 The energy consumptions were recorded and compared with theoretical energy consumptions.

2.3.1.6 Phosphorus content analysis of some samples was conducted, as well as the final and initial phosphorus contents were compared. Determination of the phosphorus content was determined by the ASTM D 4951 standard method.

The batch experiment procedures were following;

1) Calculate CPO, ethanol and sulfuric acid used for each run according to their arrays. Both CPO and ethanol were fixed at 300 g per batch in order that every batch would have an equal volume optimized for the submerged depth of sonotrode.

2) Prepare ethanol-sulfuric acid solution by mixing them together.

3) Weigh CPO and put it into the reactor.

4) Pour the ethanol-sulfuric acid solution into CPO then close the reactor with its lid.

5) Put the reactor in a water bath which laid on an adjustable stand.

6) Submerge a sonotrode to the mixture until it attach closely to an o-ring over the lid.

7) Adjust the stand to ensure that there is no any gas leakage at any points.

8) Put the temperature probe to the reaction mixture through a small sealed puncture.

9) Turn on the temperature data logger and record initial temperature of the reaction mixture.

10) Connect the watt hour meter to a power line and connect an input line of the ultrasonic processor to the watt hour meter. Record initial watt hour.

11) Start irradiate ultrasound by switch on the power button of the ultrasonic processor, model UP400S and adjust amplitude (turn an amplitude knob) according the experiments.

12) Start the circulating pump to control the temperature as per the experimental design. Record the temperature periodically.

13) Stop irradiation when the reaction time is over.

14) Stop the cooling water circulation.

15) Record all parameters used and take sample to analyze FFA content.

2.3.2 **Studies of continuous acid catalyzed esterification of CPO with ethanol assisted by ultrasonic irradiation.**

2.3.2.1 Continuous acid catalyzed esterification at 80ºC (without controlling) with stainless steel reactor having volume of 4.6 L, inner diameter of 97 mm and length of 700 mm. The flow pattern used was vertical up flow.

2.3.2.2 Continuous acid catalyzed esterification at 80ºC (without controlling) with stainless steel reactor having volume of 1.47 L, inner diameter of 61 mm and length of 700 mm. The flow pattern used was vertical up flow.

2.3.2.3 Continuous acid catalyzed esterification at 80ºC (without controlling) with stainless steel reactor having volume of 1.47 L, inner diameter of 61 mm and length of 700 mm. The flow pattern used was vertical down.

2.3.2.4 Continuous acid catalyzed esterification at 60ºC with stainless steel reactor having volume of 1.47 L, inner diameter of 61 mm and length of 700 mm. The flow pattern used was horizontal flow. The reaction temperature is controlled at 60ºC.

2.3.2.5 The energy consumptions of each experiment were compared with the theoretical energy consumptions.

This continuous esterification experiments were concluded in Table 2.5.

Table 2.5 The continuous esterification experiments

Continuous experiments	Volume of reactors (L)	Inner diameter of reactors (mm)	Reactors' temperature (°C)	Flow patterns
1	4.6	97	80	Vertical up flow
2	1.47	61	80	Vertical up flow
3	1.47	61	80	Vertical down flow
4	1.47	61	60	Horizontal flow

For the continuous experiments, two sizes of reactors are shown in Figure 2.3 including the sonotrode used and the equipment setup is illustrated in Figure 2.4.

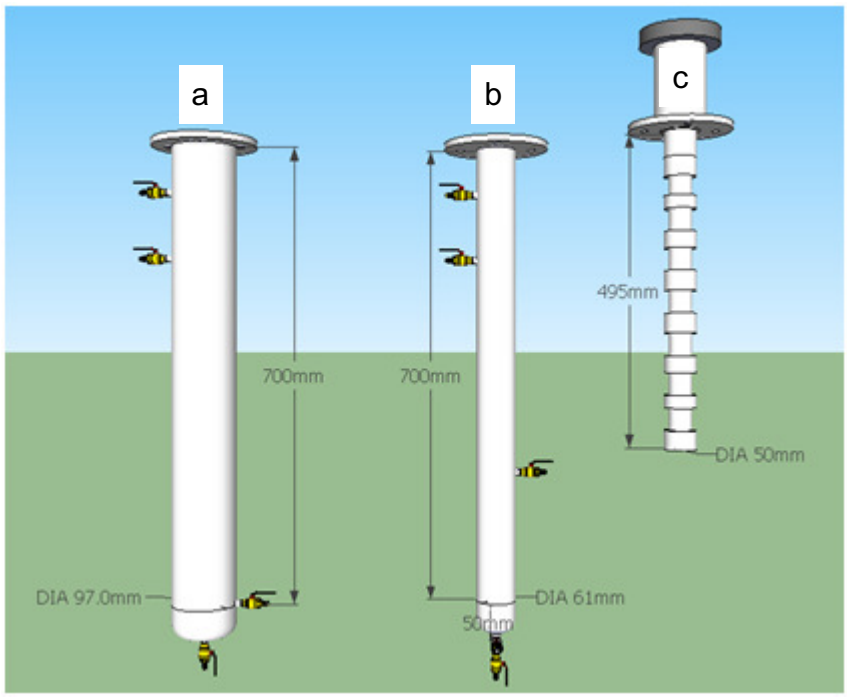

Figure 2.3 Continuous reactors (a: 4.60 L and b: 1.47 L) and a sonotrode (c)

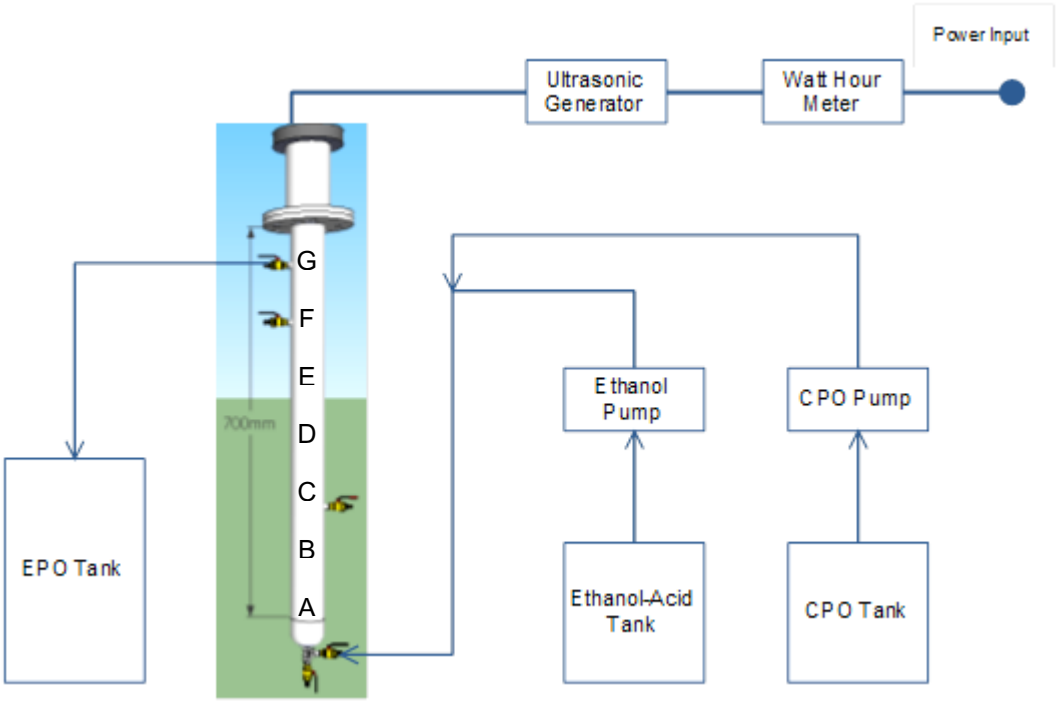

Figure 2.4 Schematic diagram of the continuous esterification (points of A, B, C, D, E, F and G are represented the temperature measuring points located 100 mm between each point)

(a) (b) (c)

Figure 2.5 A sonotrode (a), A continuous reactor (b) and an ultrasonic generator (c)

There were four experiments using different sizes of reactors and flow patterns, but all of them were performed under the same methodology as 3 factors and 2 levels shown in Table 2.6, consequently obtained the orthogonal array of $L_4(2^3)$ in Table 2.7.

Table 2.6 Factors and levels of the continuous experiments.

Factors	Descriptions	Level 1	Level 2
Cat	: % H_2SO_4 by wt of FFA	30	60
MR	: Molar ratio of ethanol: FFA	20	30
RT	: Retention time in hour	0.5	1

Table 2.7 Orthogonal array of the continuous experiments.

	Factors		
Run No.	Cat	MR	RT
1	30	20	0.5
2	30	30	1
3	60	20	1
4	60	30	0.5

The continuous experiment procedures were following;

1) Set up the equipment as per the schematic diagram in Figure 2.4.

2) Calculate CPO, ethanol and sulfuric acid used for each run according to their arrays.

3) Prepare ethanol-sulfuric acid solution by mixing them together.

4) Fill up CPO and ethanol-sulfuric acid solution into the reactor.

5) Connect the watt hour meter to a power line and connect an input line of the ultrasonic processor to the watt hour meter. Record initial watt hour.

6) Start pumping CPO and the ethanol-sulfuric acid solution to the reactor.

7) Start irradiating ultrasound by switch on the power button of the ultrasonic processor, model YPSH1020204.

8) Start the circulating (if needed) using tap water flowing through an absorbed media which fixed around the reactor to control the temperature as per the experiments. Periodically record the temperature at the reactor surface using an infra red thermometer.

9) Collect samples from an outlet valve as interval as desire.

10) Stop irradiation when the reaction time is over.

11) Stop CPO and the ethanol-sulfuric acid solution pumps.

12) Stop the circulating.
13) Record all parameters used.

2.3.3 **Studies of continuous acid catalyzed esterification of CPO with ethanol using continuous stirred-tank reactor (CSTR)**

This study aimed to compare with the continuous ultrasonic experiments, therefore the experimental design was performed in the same fashion of that mentioned in the continuous ultrasonic experiments. There were four experiments containing 3 factors and 2 levels shown in Table 2.8, consequently obtained the orthogonal array of $L_4(2^3)$ in Table 2.9. The reaction temperature was 60ºC, initial FFA was 6-8 wt% in range and the agitation was fixed at 700 rpm corresponding to N_{Re} of 20,249. The dimensions of this CSTR reactor are 310 mm ID and 1200 mm in length from input to output valves. It contains 87 L of volume. The schematic diagram of this experiment setup was illustrated in Figure 2.5 and details of the reactor were shown in appendix D.

Table 2.8 Factors and levels of the continuous experiments by CSTR.

Factors	Descriptions	Level 1	Level 2
Cat	: % H_2SO_4 by wt of FFA	30	60
MR	: Molar ratio of ethanol: FFA	20	30
RT	: Retention time in hour	0.5	1

Table 2.9 Orthogonal array of the continuous experiments by CSTR.

	Factors		
Run No.	Cat	MR	RT
1	30	20	0.5
2	30	30	1
3	60	20	1
4	60	30	0.5

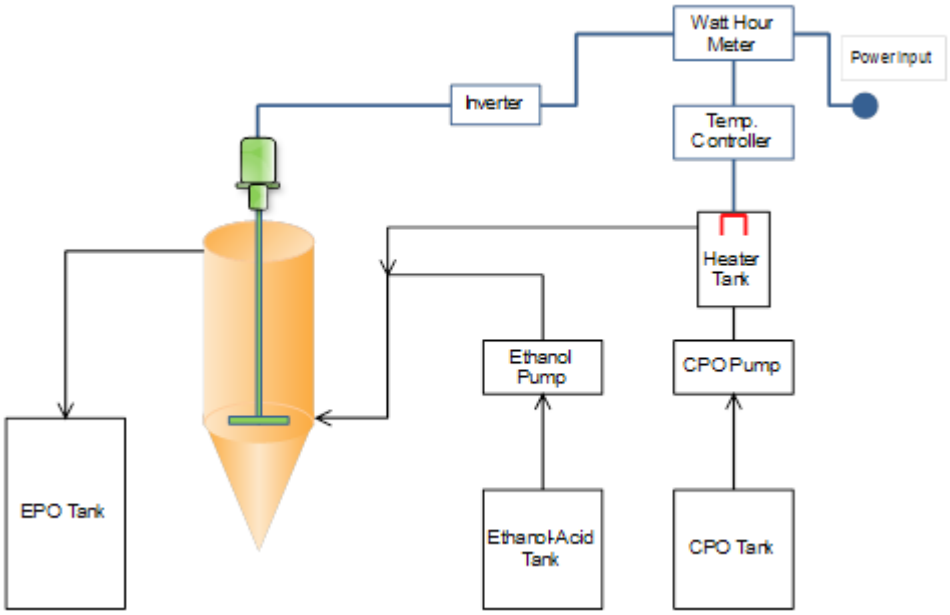

Figure 2.6 Schematic diagram of the CSTR esterification

The CSTR experiment procedures were following;

1) Set up the equipment as per the schematic diagram in Figure 2.6.

2) Calculate CPO, ethanol and sulfuric acid used for each run according to their arrays.

3) Prepare ethanol-sulfuric acid solution by mixing them together in an ethanol-acid tank.

4) Connect the watt hour meter to a power line and connect all electrical equipment from the watt hour meter. Record initial watt hour.

5) Start pumping CPO through a heater tank until it is full then stop pumping.

6) Start heating CPO till it has temperature about 75ºC.

7) Start pumping CPO and the ethanol-sulfuric acid solution to the reactor.

8) The agitation will be started after the mixture in the reactor is 1/3 in volume.

9) Record temperature at the reactor, periodically and record kWh after the experiment is finished.

10) Collect samples from an outlet valve as interval as desire.

11) Stop CPO and the ethanol-sulfuric acid solution pumps.
12) Stop the agitation.

2.4 Chemical analysis

2.4.1 For batch experiments, 30 mL samples were drawn from the final reaction mixture and immediately washed with warm water in a 250 mL separatory funnel, in order to stop the reaction and remove all contaminants such as ethanol, gum and sulfuric acid. The washing step was repeated until the washing water had a pH of 7. The clean samples containing saturated water were then dried at 60°C for 30 minutes in a hot air oven. The FFA content of the dried samples was then determined by the titration method (AOCS method Ca 5a-40).

2.4.2 For continuous experiments, 50 mL samples were periodically collected from the output valve of reactor to a 250 mL glass bottle and immediately washed twice with warm water to stop the reaction and remove most of contaminants such as ethanol, gum and sulfuric acid. The washing step was repeated in a separatory funnel until the washing water had a pH of 7, let water separated about 15 minutes and finally water was drained out. The clean samples containing saturated water were then dried with household microwave setting at 360 W for 1.5 minutes; the saturated water was separated at bottom of a porcelain container. Repeat microwave drying again and let the sample cool down. The FFA content of the dried samples was then determined by the titration method (AOCS method Ca 5a-40).

2.5 Data analysis

2.5.1 FFA results were analyzed by level average analysis and based on the smaller-the-better principle (Peace, 1993). The analysis were performed as following:

2.5.1.1 Determine the mean for each experimental run. If it has only one data point for each experimental run, the mean response is the single data. As for the continuous experiments, two data points of 3RT and 4RT are used to calculate a mean response characteristic (y).

2.5.1.2 Calculate the mean response of each factor for each level, such as Cat1 = ($\sum y_{Cat1}$)/n, when n is number of response characteristics in that level.

2.5.1.3 Calculate the overall experiment average (T); T = $\sum y_i/n$, when y_i is a response characteristic.

2.5.1.4 Develop the response table and graph using the mean response.

2.5.1.5 Determine the effect of each factor, Delta = Max-Min.

2.5.1.6 Re-ordered significance of each factor by considering the Delta.

2.5.1.7 Select target levels of the significant factors that they will be used for a confirmation run.

2.5.1.8 Check interactions by plotting the maximum and minimum of each pair of factors. Such as interaction between Cat and Amp (CatxAmp), finding the maximum and minimum response in the response table; example for the preliminary experiment Cat2 and Amp3 obtained the maximum response, Cat4 and Amp1 obtained the minimum response then select their response characteristics to plot an interaction graph. If an interaction is detected, the intersection is shown. Perform the same fashion for each pair of the interactions.

2.5.1.9 Define the predicted FFA, using the prediction equation (μ); when μ = T – (Catx-T) + (Ampx-T) + (MRx-T) +… when x is a minimum response level in the response table and Cat, Amp, MR,…are the significant factors.

2.5.1.10 Conduct the confirmation run using target levels of the significant factors.

2.5.2 Energy consumption was measured in kWh with a watt-hour meter to compare with a theoretical consumption. Energy efficiency is defined as the actual consumption in Wh/kg CPO divides by the theoretical consumption and reported in percentage.

CHAPTER 3

Results and Discussion

Results of all experiments were composed of three main parts i.e. batch ultrasonic, continuous ultrasonic and CSTR esterifications. They were stepwise demonstrated by using tabulated and graphical methods as following.

3.1 Studies of batch acid catalyzed esterification of CPO with ethanol assisted by ultrasonic irradiation

3.1.1 Preliminary experiments.

Results of the preliminary experiments are shown below.

Table 3.1 Factors of the preliminary experiments

Level	Factors				
	Cat	Amp	MR	Temp	Time
1	1	35	5	50	0.5
2	2	55	10	60	1
3	5	75	20	70	2
4	20	100	40	80	4

Table 3.2 Results of the preliminary experiments

Run No.	Factors					y
	Cat	Amp	MR	Temp	Time	(% FFA)
1	1	35	5	50	0.5	5.34
2	1	55	10	60	1	4.78
3	1	75	20	70	2	3.27
4	1	100	40	80	4	1.77
5	2	35	10	70	4	2.59
6	2	55	5	80	2	3.58
7	2	75	40	50	1	4.54
8	2	100	20	60	0.5	4.46

Table 3.2 Results of the preliminary experiments (Cont.)

Run No.	Factors					y
	Cat	Amp	MR	Temp	Time	(% FFA)
9	5	35	20	80	1	1.72
10	5	55	40	70	0.5	3.06
11	5	75	5	60	4	3.47
12	5	100	10	50	2	3.66
13	20	35	40	60	2	0.74
14	20	55	20	50	4	1.03
15	20	75	10	80	0.5	2.27
16	20	100	5	70	1	2.89
Average, T						**3.07**
Conf. run	20	35	40	80	2	**1.15**

Table 3.3 The response table of the preliminary experiments

Level	Cat	Amp	MR	Temp	Time
1	3.79	2.60	3.82	3.65	3.79
2	3.79	3.11	3.32	3.36	3.48
3	2.98	3.39	2.62	2.95	2.81
4	1.73	3.20	2.53	2.34	2.22
Delta	2.06	0.79	1.29	1.31	1.57
Order	1	5	4	3	2
Select	Cat4	Amp1	MR4	Temp4	Temp4

$\mu = T + (Cat4-T) + (Time4-T) + (Temp4-T) + (MR4-T) + (Amp1-T)$

$\mu = Cat4+Time4+Temp4+MR4+ Amp1-4T$

$\mu = 1.73+2.22+2.34+2.53+2.60-4(3.07) = -0.86$

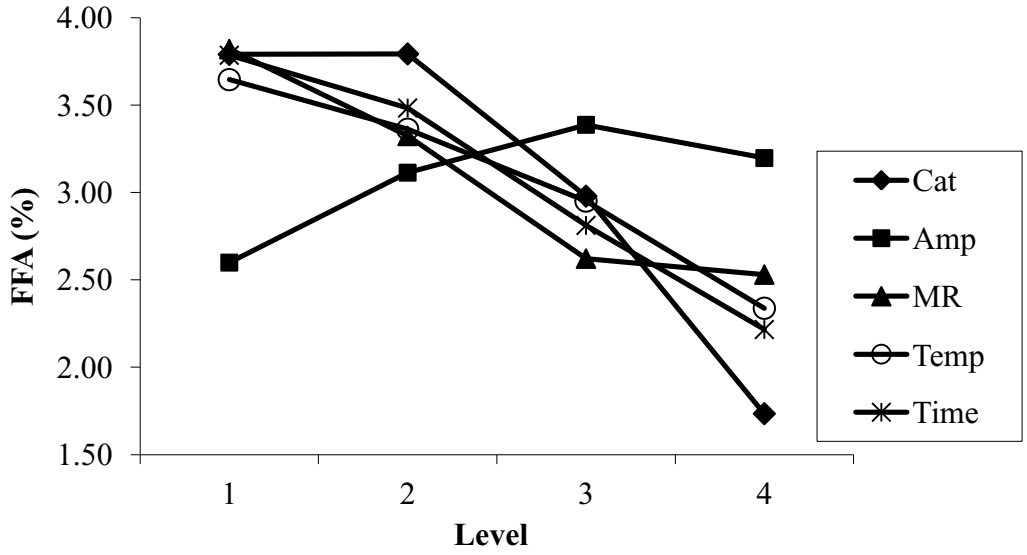

Figure 3.1 The response graph of the preliminary experiments

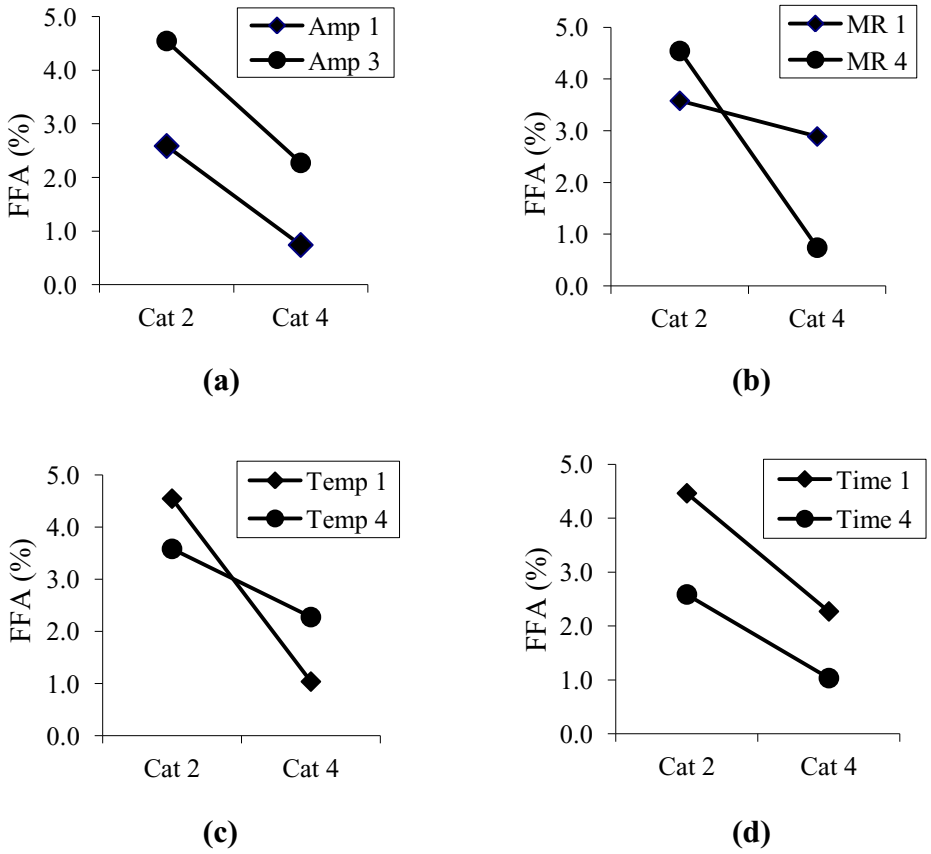

Figure 3.2 Interaction graphs between Cat-Amp (a), Cat-MR (b), Cat-Temp (c) and Cat-Time (d) of the preliminary experiments

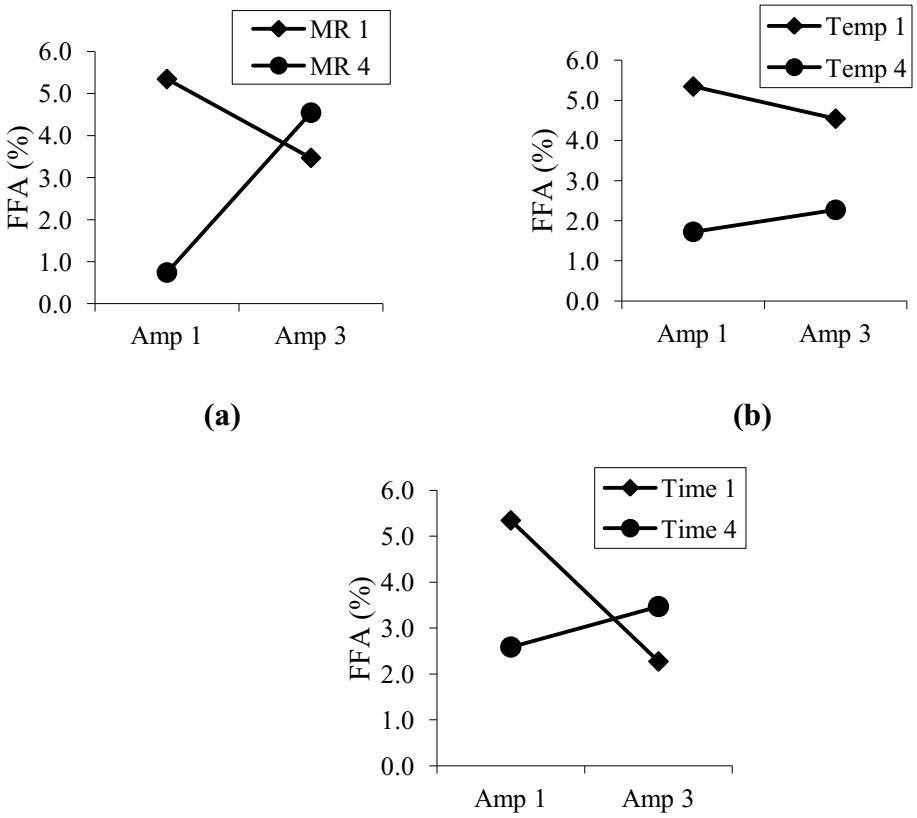

Figure 3.3 Interaction graphs between Amp-MR (a), Amp-Temp (b) and Amp-Time (c) of the preliminary experiments

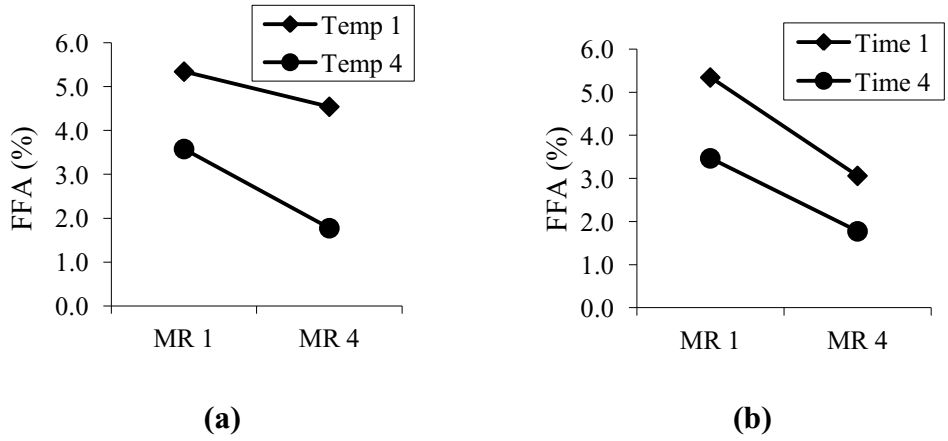

Figure 3.4 Interaction graphs between MR-Temp (a) and MR-Time (b) of the preliminary experiments

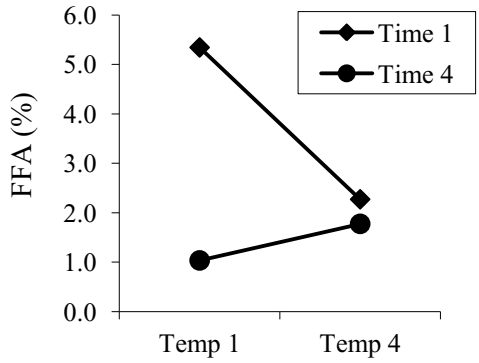

Figure 3.5 An interaction graph between Temp-Time of the preliminary experiments

The response table and graph of the preliminary experiments are shown by Table 3.3 and Figure 3.1, respectively. The analysis of the Delta values was been shown that the significant factors in descending order were amount of catalyst, reaction time, reaction temperature, molar ratio of ethanol to FFA and amplitude of acoustic power. All the factors were used to calculate the predicted FFA (μ value), but the calculation resulted in a negative value (-0.86). According selected target level of each factor using to conduct a confirmation run which obtained FFA content of 1.15 wt% that did not correspond with the predicted FFA. As regards the interactions from Figure 3.2-3.5, those CatxMR (catalyst interacted with molar ratio of ethanol) and CatxTemp (catalyst interacted with temperature) were significant, but amplitude was a less significant factor that AmpxMR and AmpxTime could be disregarded. Hence those significant interactions should be involved the experiments and they were taken into consideration in seeking to achieve the optimum result for the secondary experiments. The response graph illustrated that all the effective factors except the amplitude of acoustic power reduced the FFA content in the same way. Therefore, a second set of experiments was conducted based on the preliminary results by re-ordering the significant factors, taking into account the interactions and assigning new levels as shown in Table 3.4.

3.1.2 Secondary experiments

The secondary experiments exploited results of the previous one and its results are shown below.

Table 3.4 Factors of the secondary experiments

	Factors						
Level	Cat	Time	Temp	CatxTemp	MR	CatxMR	Amp
1	30	1	60	30x60	20	30x20	35
2	60	2	80	60x80	30	60x30	75

Table 3.5 Results of the secondary experiments

Run No.	Factors							y
	Cat	Time	Temp	CatxTemp	MR	CatxMR	Amp	(% FFA)
1	30	1	60	30x60	20	30x20	35	1.41
2	30	1	60	60x80	30	60x30	75	0.96
3	30	2	80	30x60	20	60x30	75	1.41
4	30	2	80	60x80	30	30x20	35	1.21
5	60	1	80	30x60	30	30x20	75	0.66
6	60	1	80	60x80	20	60x30	35	1.10
7	60	2	60	30x60	30	60x30	35	0.46
8	60	2	60	60x80	20	30x20	75	0.61
Average, T								**0.98**
Conf. run								**0.47**

Table 3.6 The response table of the secondary experiments

Level	Cat	Time	Temp	CatxTemp	MR	CatxMR	Amp
1	1.25	1.03	**0.86**	0.98	1.13	**0.97**	1.04
2	**0.70**	**0.92**	1.09	**0.97**	**0.82**	0.98	**0.91**
Delta	**0.54**	0.11	**0.23**	0.02	**0.31**	0.01	**0.13**
Order	**1**	5	**3**	6	**2**	7	**4**
Select	Cat2	Time2	Temp1		MR2		Amp2

μ = T+ (Cat2-T) + (MR2-T) + (Temp1-T)

μ = Cat2+ MR2+Temp1 -2T

μ = 0.70+0.82+0.86-2(0.98) = 0.42

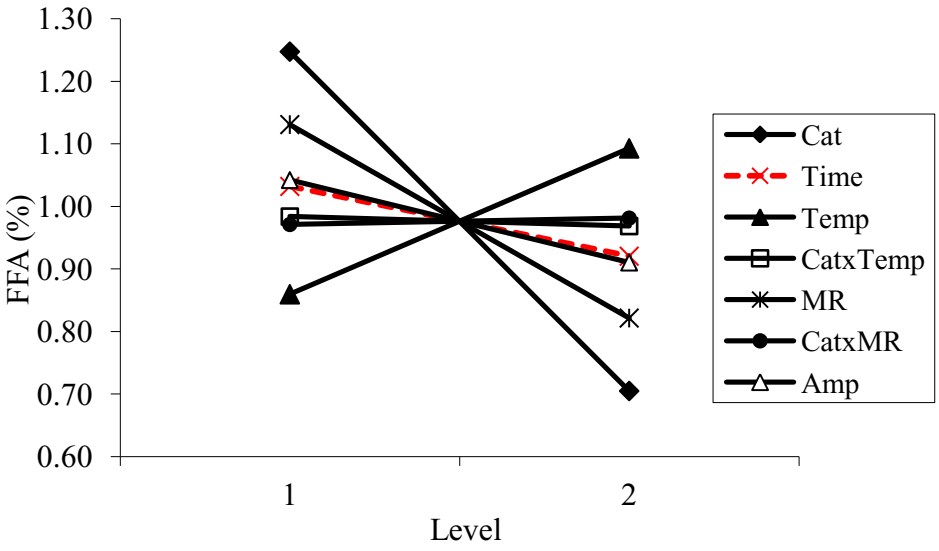

Figure 3.6 The response graph of the secondary experiments

The results of the secondary experiments are shown in Table 3.5. The response table and graph are shown in Table 3.6 and Figure 3.6, respectively. Data analysis was performed in the same fashion as for the preliminary results. The factors and interactions were considered by comparing each effect to the next strongest effect (Peace, 1993). The significant factors in descending order are amount of catalyst, molar ratio of ethanol: FFA and reaction temperature. Based on the Delta values, the amplitude of acoustic power, reaction time, and the CatxTemp and CatxMR interactions were disregarded in accordance with the one-half rule of thumb; that is, they were less than half of the next strongest effect. The predicted FFA was a positive value of 0.42 wt% corresponding to 0.47 wt% of the confirmation run result. Figure 3.6 shows the effect of the five factors: amount of catalyst, molar ratio of ethanol: FFA and amplitude had a positive effect at a higher level, but reaction temperature had a negative effect. The secondary experiments showed the optimum conditions to be: catalyst amount at 60 wt% of FFA, molar ratio of ethanol to FFA at 30:1, temperature at 60ºC, reaction time of two hours, and amplitude of acoustic power at 75%. It was apparent that reaction time was a less significant factor and the results obtained differed only slightly between different periods. Therefore further

experiments were conducted using the optimum conditions with different reaction times to fine-tune this parameter.

3.1.3 Further experiments

The further experiments were performed with the same fashion of the confirmation run of the secondary experiments with different reaction times. Results are showed in Table 3.7 and Figure 3.7. There were 3 repeatable runs compared with the confirmation run of the secondary experiments. The results showed that the FFA content was reduced over different reaction times between 30 and 120 minutes. All three runs of this part produced less than 0.5 wt% of FFA within one hour by using the optimum conditions (catalyst at 60 wt% of FFA, molar ratio of ethanol to FFA at 30:1, temperature at 60ºC, reaction time of one hour, and amplitude of acoustic power at 75%) Therefore new optimal conditions were derived from the repeated experiments and the results were not significantly varied by changing the reaction time between one and two hours suggesting that a point of reaction equilibrium was reached at one hour. By considering the esterification reaction shown in Eq 3.1 below, it can be seen that the reaction is reversible with undesired water being produced. In the presence of triglycerides and water especially under acidic condition, hydrolysis can easily take place producing FFA (Eq 3.2-3.4 below). However, if the water is removed, the reaction will shifts to the product side.

$$R_1COOH + CH_3CH_2OH \xleftrightarrow{H_2SO_4} R_1COCH_2CH_3 + H_2O \quad \text{(Eq 3.1)}$$

$$TG + H_2O \xleftrightarrow{H_2SO_4} DG + R_1COOH \quad \text{(Eq 3.2)}$$

$$DG + H_2O \xleftrightarrow{H_2SO_4} MG + R_1COOH \quad \text{(Eq 3.3)}$$

$$MG + H_2O \xleftrightarrow{H_2SO_4} C_3H_8O_3 + R_1COOH \quad \text{(Eq 3.4)}$$

3.1.4 Additional experiments

Results of the additional experiment are shown in Table 3.7 below.

Table 3.7 The FFA content obtained from further and additional experiments

Time	Secondary expt.	Further experiments			Additional expt.
(min)	Conf. run	Run #1	Run #2	Run #3	2 Steps
0	5.06	5.96	5.96	5.96	5.96
30	0.69	0.97			
60		0.5	0.45	0.48	0.475
120	0.47				0.22

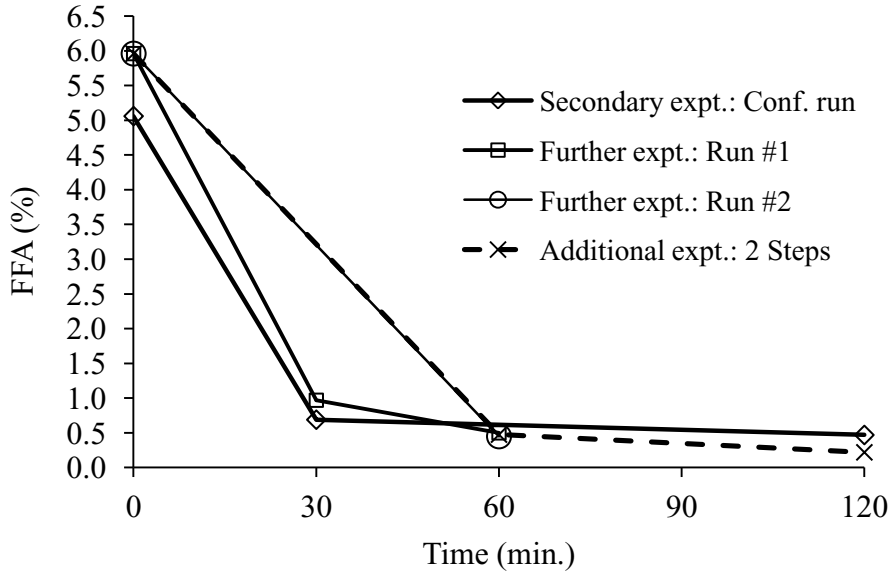

Figure 3.7 The FFA content obtained from further and additional experiments

The additional experiment involving two stages esterification was conducted and the result was detailed in Table 3.7 and Figure 3.7 (2 steps line). The conditions employed in both steps of the esterification were: catalyst at 60 wt% of FFA, molar ratio of ethanol to FFA at 30:1, temperature at 60ºC, reaction time of one hour, and amplitude of acoustic power at 75%. The result was revealed the FFA content was finally reduced to 0.22 wt%. Therefore it can be concluded that after one hour of reaction the equilibrium was attained due to a reversible of esterification reaction (Eq 3.1) including hydrolysis reactions (Eq 3.1-3.4). Therefore after water

abolishment and the performance of the second step esterification under the same conditions for a further hour, the FFA content was able to be reduced further indicating that a new equilibrium had been reached and the water had acted to interrupt the process of esterification.

3.1.5 The energy consumption of the batch experiments

Table 3.8 Theoretical and actual energy consumptions

No	CPO (g)	EtOH (g)	ΔT (ºC)	Q (kJ)	Q′ (Wh)	Consumed Power (Wh)
1	235.58	64.42	30.0	18.35	5.10	64
2	235.58	64.42	30.0	18.35	5.10	61
3	238.36	61.64	30.0	18.31	5.08	61
4	255.88	44.12	30.0	18.04	5.01	61
5	238.36	61.64	30.0	18.31	5.08	59
6	255.88	44.12	30.0	18.04	5.01	59
7	238.36	61.64	30.0	18.31	5.08	70
8	238.36	61.64	30.0	18.31	5.08	58
9	255.88	44.12	30.0	18.04	5.01	62
10	238.36	61.64	30.0	18.31	5.08	62
11	255.88	44.12	30.0	18.04	5.01	59
Average	244.23				5.06	61.45
	1 kg				21	252

Remark: Cp of CPO and ethanol are 1.929 and 2.440 kJ/(kg C), respectively.

The experimental and theoretical energy consumption was 252 and 21 Wh/kg of CPO, respectively. The energy efficiency was 8.23%, it was quite low. However this experimental consumption was corresponding to 250 Wh/kg oil for the transesterification of soybean oil using the ultrasonic method (Ji, 2006). The most advantage of the ultrasonic esterification method is no requiring an external heating source of which saving a heating unit.

3.1.6 Phosphorus content analysis of some samples

The initial and final (after conducting the reaction) phosphorus contents of CPO were 11.24 and 1.46 mg/kg, respectively. This values shows that a lower phosphorus content can be achieved concomitantly under the acid catalyzed esterification assisted by ultrasonic irradiation and the final phosphorus content meets the methyl ester standard (EN 14214: 2008 in Appendix A). Thus, the esterification process can reduces the phosphorus content to an acceptant level without performing a separated degumming step.

3.2 Studies of continuous acid catalyzed esterification of CPO with ethanol assisted by ultrasonic irradiation

3.2.1 The 1st continuous experiments; continuous acid catalyzed esterification at 80ºC with stainless steel reactor having volume of 4.6 L, inner diameter of 97 mm and height of 700 mm. The flow pattern was a vertical up flow.

Table 3.9 Factors of the 1st continuous experiments

Level	Factors		
	Cat	MR	RT
1	30	20	0.5
2	60	30	1

Table 3.10 Orthogonal array of the 1st continuous experiments

Run No.	Factors		
	Cat	MR	RT
1	30	20	0.5
2	30	30	1
3	60	20	1
4	60	30	0.5

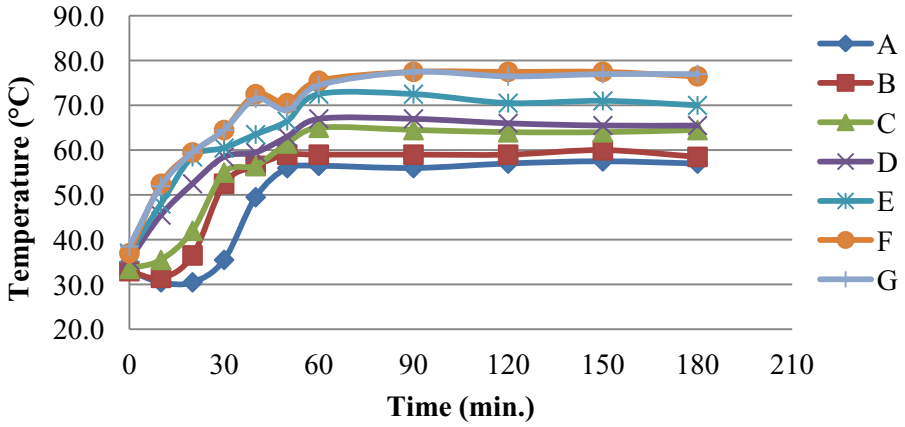

Figure 3.8 Reactor temperature profile: Run # 1 of the 1st continuous experiments

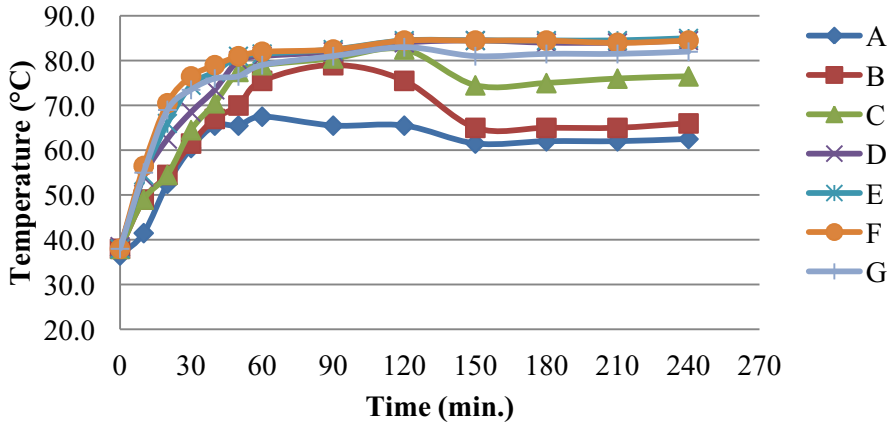

Figure 3.9 Reactor temperature profile: Run # 2 of the 1st continuous experiments

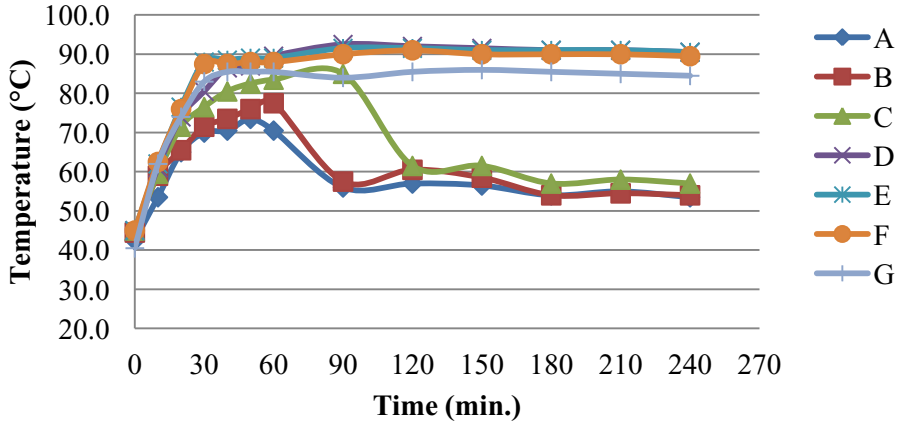

Figure 3.10 Reactor temperature profile: Run # 3 of the 1st continuous experiments

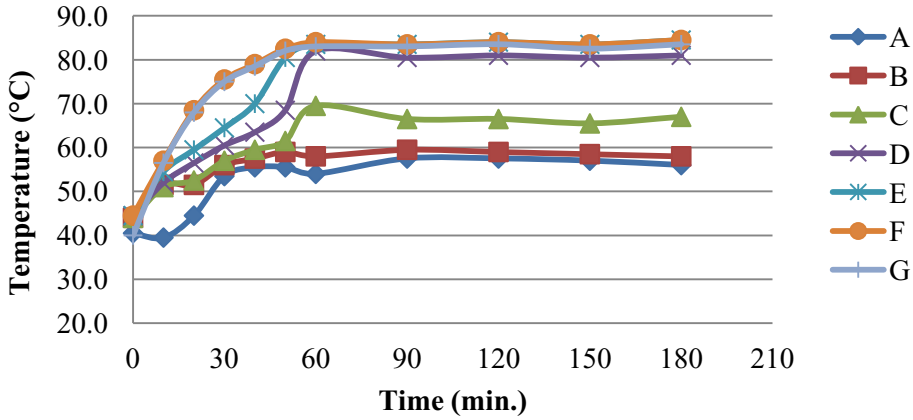

Figure 3.11 Reactor temperature profile: Run # 4 of the 1st continuous experiments

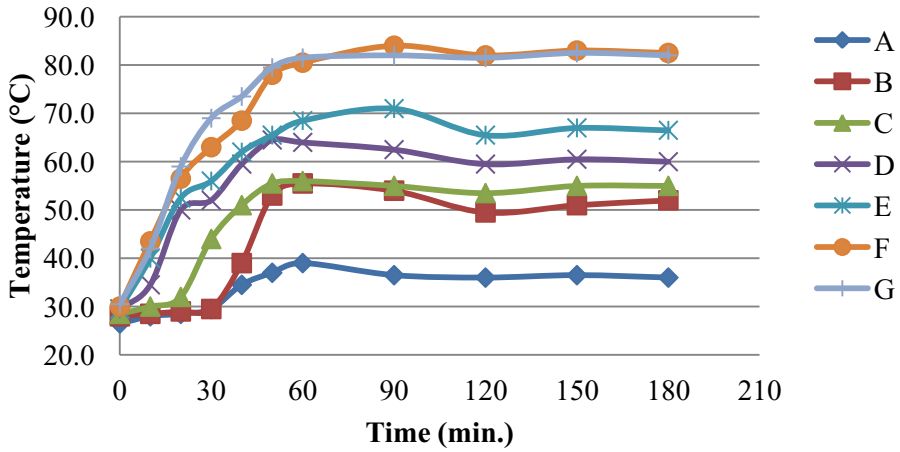

Figure 3.12 Reactor temperature profile: Run # 5 of the 1st continuous experiments

Table 3.11 Results of FFA analysis of the 1st continuous experiments

Time	Average FFA (%)				
(min)	Run # 1	Run # 2	Run # 3	Run # 4	Run # 5
0	4.88	4.88	4.88	4.88	5.76
30	3.72			1.59	2.99
60	2.56	1.44	1.81	1.46	2.18
90	**2.06**	1.47	2.21	**1.39**	**1.84**
120	**1.89**	1.54	2.33	**1.51**	**2.02**
150	1.84	1.67	2.19	1.43	1.98
180	1.90	**1.63**	**2.22**	1.56	1.90
210		1.90	2.00		
240		**2.06**	**2.09**		
Average					**1.93**
Cal FFA					**1.50**

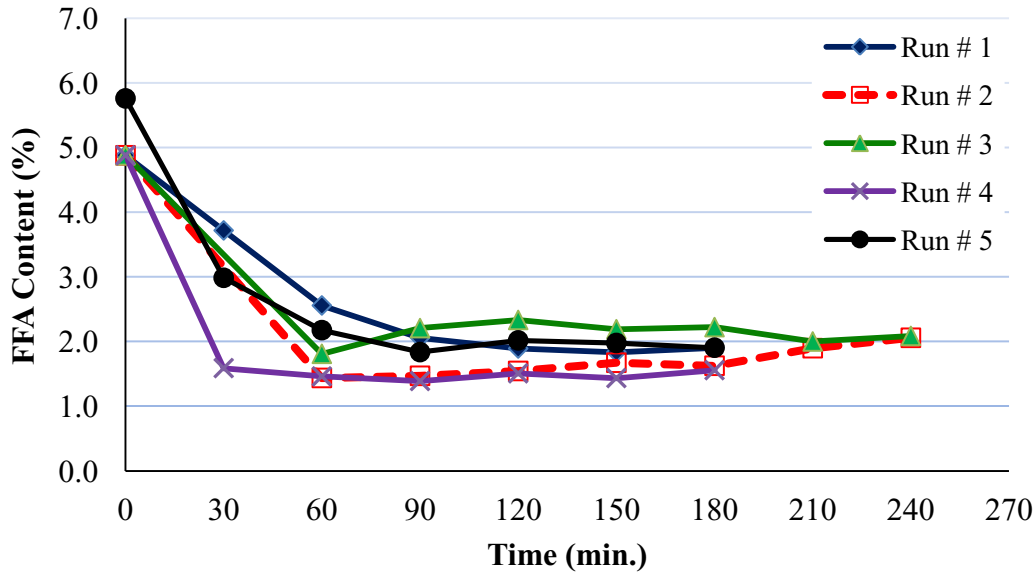

Figure 3.13 The FFA reduction of the 1st continuous experiments

Table 3.12 Response characteristics of the 1st continuous experiments

Run No.	Factors					Response Characteristic (y)
	Cat	MR	RT	y1	y2	
1	30	20	0.5	2.06	1.89	**1.97**
2	30	30	1	1.63	2.06	**1.84**
3	60	20	1	2.22	2.09	**2.15**
4	60	30	0.5	1.39	1.51	**1.45**
T						**1.85**

Table 3.13 The response table of the 1st continuous experiments

Level	Cat	MR	RT
1	1.91	2.06	**1.71**
2	**1.80**	**1.64**	2.00
Delta	0.11	0.42	0.29
Order		1	2
Select	Cat2	MR2	RT1
μ	= T+(MR2-T)+(RT1-T)		
μ	= 1.50		

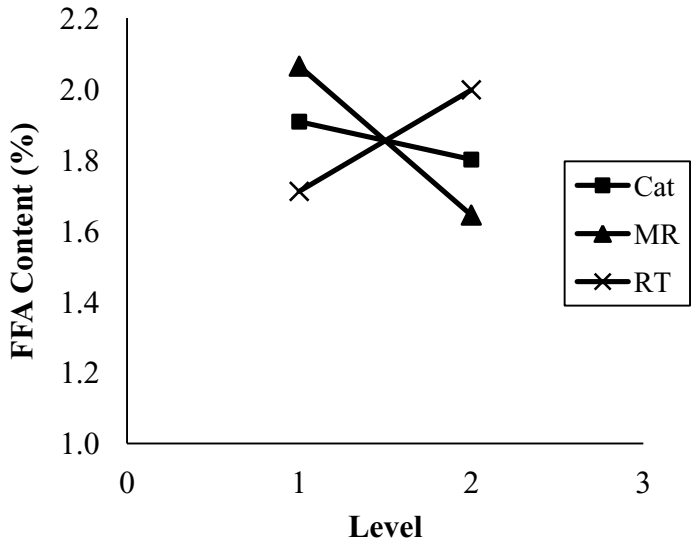

Figure 3.14 The response graph of the 1st continuous experiments

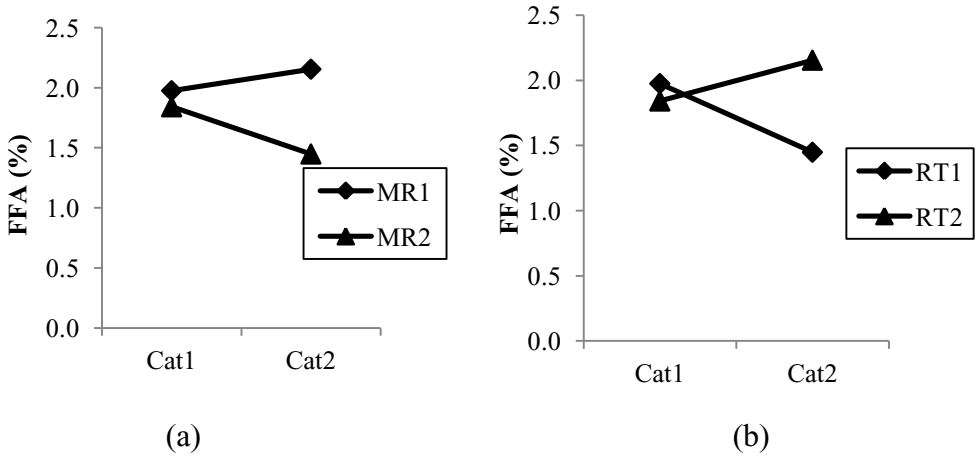

Figure 3.15 The interaction graphs between Cat-MR (a) and Cat-RT (b) of the 1st continuous experiments

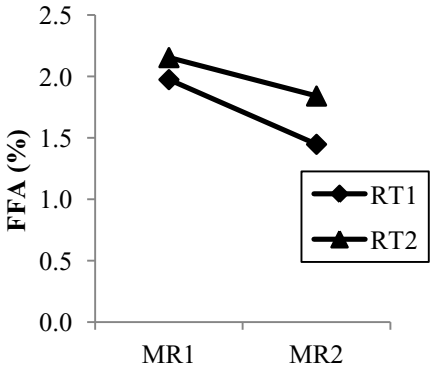

Figure 3.16 The interaction graph between MR-RT of the 1st continuous experiments

Temperature profiles of 5 runs obtaining from the 1st continuous experiments showed steady state after 1 hour running (Figure 3.8-3.12). At steady state, run number 1-4 had temperature between 60 to 80ºC because the reaction temperature had no controlling and at the input side had lower temperature than the output side. Run number 5 had more distribution in temperature over the height of reactor (Figure 3.12). According the FFA reduction graph (Figure 3.13), it is found that FFA was reduced when reaction time increased and it was ongoing to steady state after 90 minutes (3RT for the shortest retention time). It was suitable to select the results at 3RT and 4RT for data analysis. The response table showed that the most significant factor was a molar ratio followed by retention time, but catalyst content

could be neglect corresponding to the response graph showing less steepness. Selected factors for a confirmation run were Cat2, MR2 and RT1, consequently obtained average FFA content of 1.93 wt% but the predicted FFA was 1.5 wt%. There was no interaction between MR and RT.

3.2.2 The 2nd continuous experiments; continuous acid catalyzed esterification at 80ºC with stainless steel reactor having volume of 1.47 L, inner diameter of 61 mm and height of 700 mm. The flow pattern was a vertical up flow.

Table 3.14 Factors of the 2nd continuous experiments

Level	Factors		
	Cat	MR	RT
1	30	20	0.5
2	60	30	1

Table 3.15 Results of FFA analysis of the 2nd continuous experiments

Time	Average FFA (%)				
(min)	Run # 1	Run # 2	Run # 3	Run # 4	Run # 5
0	5.49	5.49	5.49	5.49	5.49
60	1.92			1.70	1.53
90	**2.15**			**1.30**	**1.44**
120	**2.18**	2.24	1.75	**1.37**	**1.52**
150	2.15	2.21	1.64	1.65	1.44
180	2.19	**2.20**	**1.66**	1.57	1.46
210		1.98	1.45		
240		**1.90**	**1.52**		
Average					**1.48**
Cal FFA					**1.37**

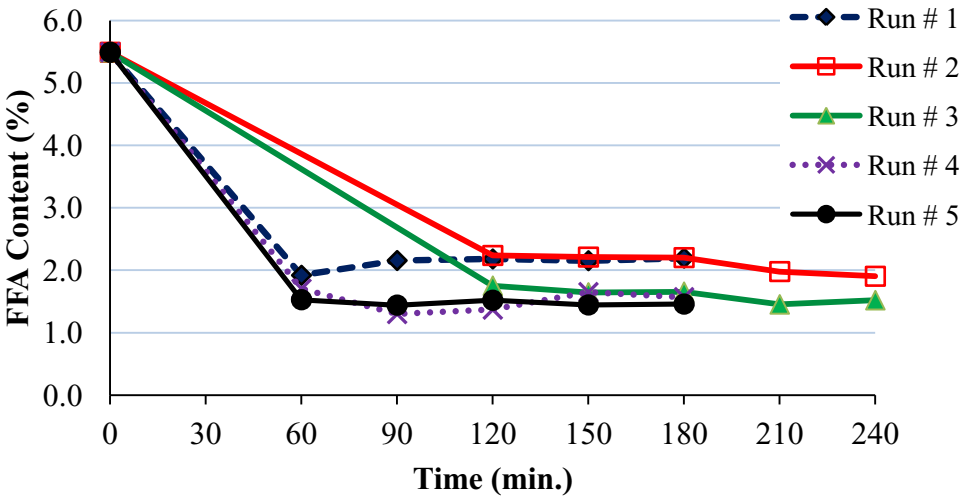

Figure 3.17 The FFA reduction of the 2nd continuous experiments

Table 3.16 Response characteristics of the 2nd continuous experiments

Run No.	Factors					Response Characteristic (y)
	Cat	MR	RT	y1	y2	
1	30	20	0.5	2.15	2.18	2.17
2	30	30	1	2.20	1.90	2.05
3	60	20	1	1.66	1.52	1.59
4	60	30	0.5	1.30	1.37	1.33
T						**1.79**

Table 3.17 The response table of the 2nd continuous experiments

Level	Cat	MR	RT
1	2.11	1.88	**1.75**
2	**1.46**	**1.69**	1.82
Delta	0.65	0.18	0.07
Order	1	2	
Select	Cat 2	MR 2	RT 1

μ = T+(Cat2-T)+(MR2-T)

μ = 1.37

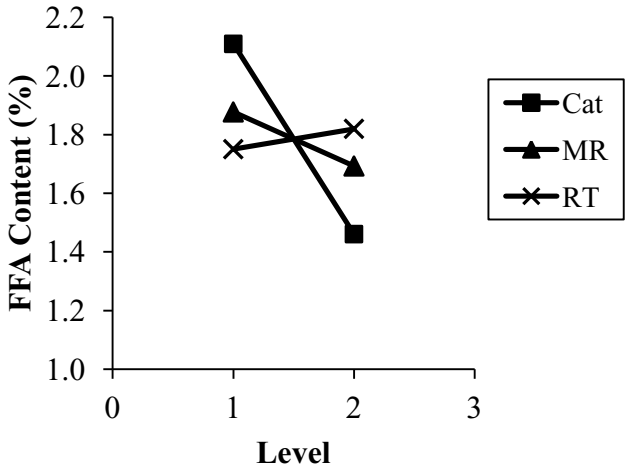

Figure 3.18 The response graph of the 2nd continuous experiments

Temperature profiles of 5 runs obtaining from the 2nd continuous experiments showed steady state after 0.5 hour running (Figure C11-C15, Appendix C). At steady state, all points except feed point (point A) of all runs had temperature nearly 80ºC. Clearly, temperature distribution of a narrow reactor was better than a wide one, it meant that cavitation took place thoroughly in a suitable narrow reactor which corresponding to the sonotrode diameter. According the FFA reduction graph (Figure 3.17), it was found that FFA was reduced when reaction time increased and it was ongoing to steady state after 60 and 120 minutes for the runs of RT 0.5 and 1 hour, respectively. Therefore, results at 3RT and 4RT were suitable for data analysis. The response table showed that the most significant factor was a catalyst content followed by molar ratio, but retention time could be neglect corresponding to its steepness and negative effect in the response graph in which showing positive effect of catalyst content and molar ratio. Selected factors for a confirmation run are Cat2, MR2 and RT1; consequently obtained average FFA content of 1.48 wt% corresponding to the predicted FFA of 1.37 wt%. There was no interaction of the both significant factors.

3.2.3 The 3rd continuous experiments; continuous acid catalyzed esterification at 80ºC with stainless steel reactor having volume of 1.47 L, inner diameter of 61 mm and height of 700 mm. The flow pattern was a vertical down flow.

Table 3.18 Factors of the 3rd continuous experiments

Level	Factors		
	Cat	MR	RT
1	30	20	0.5
2	60	30	1

Table 3.19 Results of FFA analysis of the 3rd continuous experiments

Time	Average FFA (%)				
(min)	Run # 1	Run # 2	Run # 3	Run # 4	Run # 5
0	5.49	5.49	5.49	5.49	5.49
60	1.75			0.94	
90	**1.68**			**1.10**	
120	**1.65**	1.10	1.35	**1.09**	1.11
150	1.59	1.06	1.29	1.09	0.99
180	1.62	**1.17**	**1.39**	1.12	**1.11**
210		1.09	1.32		1.12
240		**1.21**	**1.35**		**1.10**
Average					**1.11**
Cal FFA					**1.04**

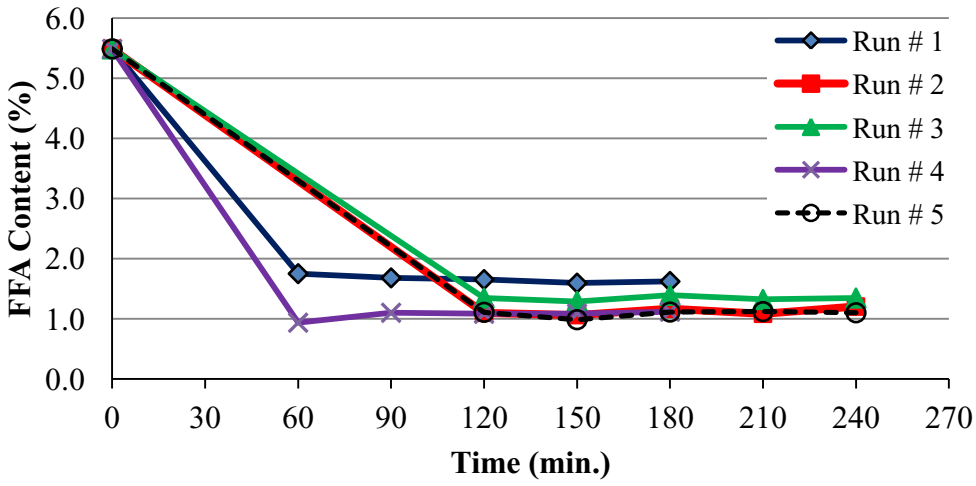

Figure 3.19 The FFA reduction of the 3rd continuous experiments

Table 3.20 Response characteristics of the 3rd continuous experiments

Run No.	Factors					Response Characteristic (y)
	Cat	MR	RT	y1	y2	
1	30	20	0.5	1.68	1.65	1.67
2	30	30	1	1.17	1.21	1.19
3	60	20	1	1.39	1.35	1.37
4	60	30	0.5	1.10	1.09	1.09
T						**1.33**

Table 3.21 The response table of the 3rd continuous experiments

Level	Cat	MR	RT
1	1.43	1.52	1.38
2	**1.23**	**1.14**	**1.28**
Delta	0.20	0.38	0.10
Order	2	1	3
Select	Cat2	MR2	RT2

μ = T+(Cat2-T)+(MR2-T)+(RT2-T)

μ = 1.04

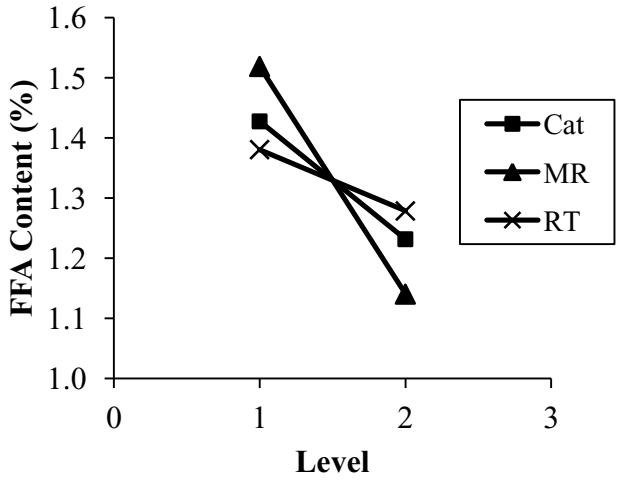

Figure 3.20 The response graph of the 3rd continuous experiments

Temperature profiles of 5 runs obtaining from the 3rd continuous experiments showed steady state after 0.5 hour running (Figure C16-C20, Appendix C). At steady state, all runs had average temperature nearly 80ºC. It was shown that temperature distribution was better than the up flow experiments (the 2nd experiments) According the FFA reduction graph (Figure 3.19), it was found that FFA was reduced when reaction time increased and it was ongoing to steady state after 60 and 120 minutes for the runs of RT 0.5 and 1 hour, respectively. The response table showed that the most significant factor was a molar ratio followed by catalyst content, but retention time can be neglect corresponding to its steepness in the response graph in which showing positive effect of all three factors. Selected factors for a confirmation run are Cat2, MR2 and RT2; consequently obtained average FFA content of 1.11 wt% corresponding to the predicted FFA of 1.04 wt%. There is no interaction of the both significant factors.

3.2.4 The 4th continuous experiments; continuous acid catalyzed esterification at 60ºC with stainless steel reactor having volume of 1.47 L, inner diameter of 61 mm and height of 700 mm. The flow pattern was a horizontal flow.

Table 3.22 Factors of the 4th continuous experiments

	Factors		
Level	Cat	MR	RT
1	30	20	0.5
2	60	30	1

Table 3.23 Results of FFA analysis of the 4th continuous experiments

Time	Average FFA (%)				
(min)	Run # 1	Run # 2	Run # 3	Run # 4	Run # 5
0	6.26	6.26	6.26	6.26	6.26
60	2.08			1.02	
90	**2.13**			**0.96**	
120	**2.15**	0.97	0.96	0.91	0.32
150	2.16	1.00	0.91	**0.94**	0.37
180	2.14	**0.97**	**0.96**	0.96	**0.35**
210		0.97	0.90		0.37
240		**0.98**	**0.92**		**0.36**
Average					**0.35**
Cal FFA					**0.36**

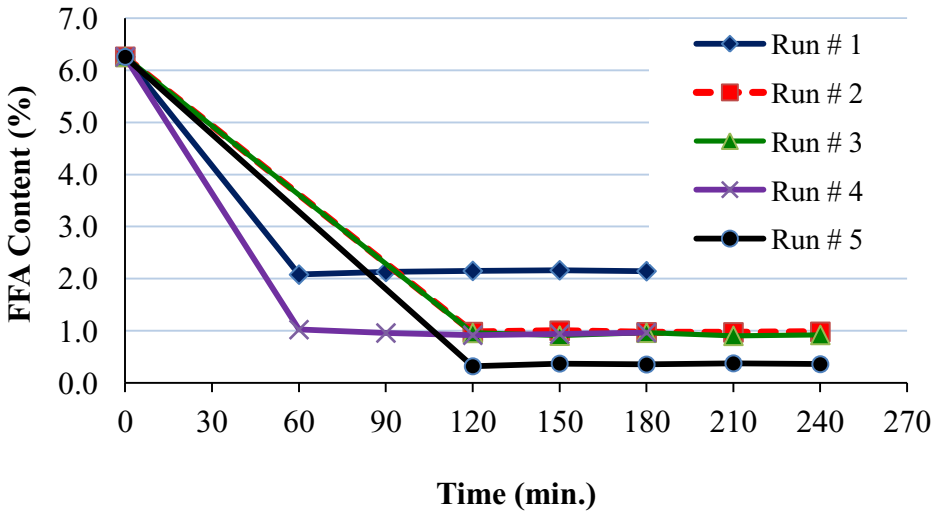

Figure 3.21 The FFA reduction of the 4th continuous experiments

Table 3.24 Response characteristics of the 4th continuous experiments

Run No.	Factors					Response Characteristic (y)
	Cat	MR	RT	y1	y2	
1	30	20	0.5	2.13	2.15	2.14
2	30	30	1	0.97	0.98	0.97
3	60	20	1	0.96	0.92	0.94
4	60	30	0.5	0.96	0.94	0.95
T						**1.25**

Table 3.25 The response table of the 4th continuous experiments

Level	Cat	MR	RT
1	1.56	1.54	1.54
2	**0.94**	**0.96**	**0.96**
Delta	0.61	0.58	0.58
Order	1	2	3
Select	Cat2	MR2	RT2
μ	= T+(Cat2-T)+(MR2-T)+(RT2-T)		
μ	= 0.36		

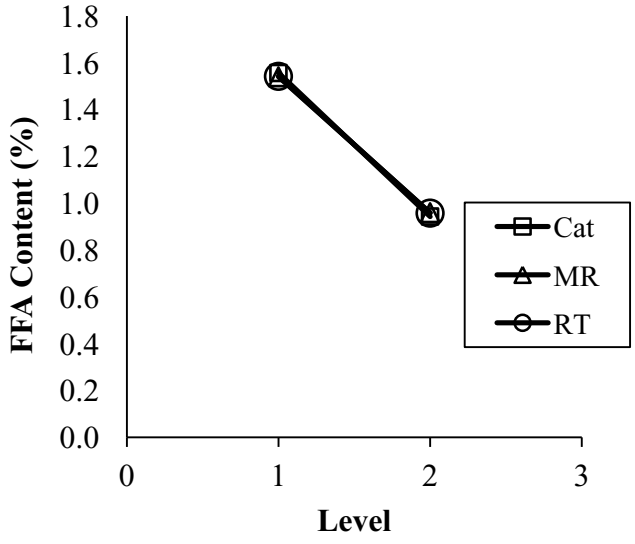

Figure 3.22 The response graph of the 4th continuous experiments

Temperature profiles of 5 runs obtaining from the 4th continuous experiments showed steady state after 0.5 to 1 hour running (Figure C21-C25, Appendix C). At steady state, all points of all runs had temperature nearly 60ºC because of temperature controlling. According the FFA reduction graph (Figure 3.21), it was found that FFA was reduced when reaction time increased and it was ongoing to steady state after 60 and 120 minutes for the runs of RT 0.5 and 1 hour, respectively. The response table showed that all three factors were the same level significant factors, in descending order as catalyst content, molar ratio and retention time corresponding to the response graph showing positive effect of them. Selected factors for a confirmation run were Cat2, MR2 and RT2; consequently obtained average FFA content of 0.35 wt% corresponding to the predicted FFA of 0.36 wt%. There was no interaction of the significant factors.

3.2.5 The energy efficiency of continuous experiments

Table 3.26 Energy efficiency of the continuous experiments

Experiments	Run # 1	Run # 2	Run # 3	Run # 4	Run # 5
1st	32.09%	25.46%	30.34%	39.94%	37.89%
2nd	20.47%	11.12%	12.21%	20.42%	21.39%
3rd	24.25%	15.74%	15.65%	22.48%	16.04%
4th	12.17%	7.03%	6.77%	14.66%	6.85%

When considering each run of each experiment, it is found that run number 1 and 4 had closely efficiency of energy consumption and run number 2 and 3 had closely of those. That might be caused by a retention time; the longer RT had lower energy efficiency. Possibly, input electrical power was excessively high in order to generate ultrasound, too much if comparing with heating by a conventional method, and also because of heat loss at surface of the reactors without insulation. All four experiments showed the energy efficiency in same fashion. The horizontal flow represents the least energy efficiency that caused by more heat loss with cooling water used for controlling temperature.

3.2.6 Comparing between reactor sizes

In the continuous experiment, there were two sizes of reactors, 97 and 61 mm of inner diameter corresponding to 4.60 and 1.47 L belonging to the 1st and 2nd continuous experiments (item 3.2.1 and 3.2.2), respectively. The sonotrode diameter is 50 mm. The average FFA obtained from the 1st and 2nd continuous experiments were 1.85 and 1.79 wt%, respectively, but the response of factors of the 2nd continuous experiments is more obvious than those the 1st one and the order of significant factors are different. This may be caused by mismatching between diameter of sonotrode and reactor. In the narrow diameter reactor matching to the sonotrode diameter, ultrasound can irradiate more thoroughly that make better mixing and cavitation corresponding to a lower FFA content and a higher temperature profile. Therefore, the matching of reactor and sonotrode in size should be considered when the ultrasonic method is preceded. Consequently, the 61 mm ID reactor was be used for the next experiments.

3.2.7 Comparing between flow patterns

In the continuous experiment, there were two flow patterns, up and down flow in the 2nd and 3rd experiments, respectively. The up flow was a bottom feeding and product flowed out at the top valve, the feed stream was a counter current to ultrasound irradiation. The down flow was opposite to the up flow. The results are found that the average FFA content of down flow (1.33 wt%) is significantly better than that of up flow pattern (1.79 wt%) and also the confirmation run of the down flow experiment obtained the better result of 1.11 wt% FFA compared to 1.48 wt% of the up flow experiment. Moreover the energy efficiency of the down flow is apparently higher than the up flow (see Table 3.26). This may be in sense of generated heat is naturally dissipated upward and concurrent with the up flow pattern of the mixture so it is easy to take the heat off. This phenomenon is happened opposite to the down flow pattern which uses the heat with more efficiency.

3.2.8 Comparing between reactor configurations

The first three continuous experiments are all vertical flow and the reaction took place at 80ºC, but their results cannot obtain 0.5 wt% FFA, this might be

affected by hydrolysis of CPO which highly occur with high temperature under acid condition as same as results of the batch experiments. Thus the author performed the additional continuous experiments using 61 mm inner diameter reactor under the confirmation run condition of the 3rd ultrasonic experiment at 60ºC and also did the same of batch experiment to prove the influence of the hydrolysis, the results were shown in Figure 3.48.

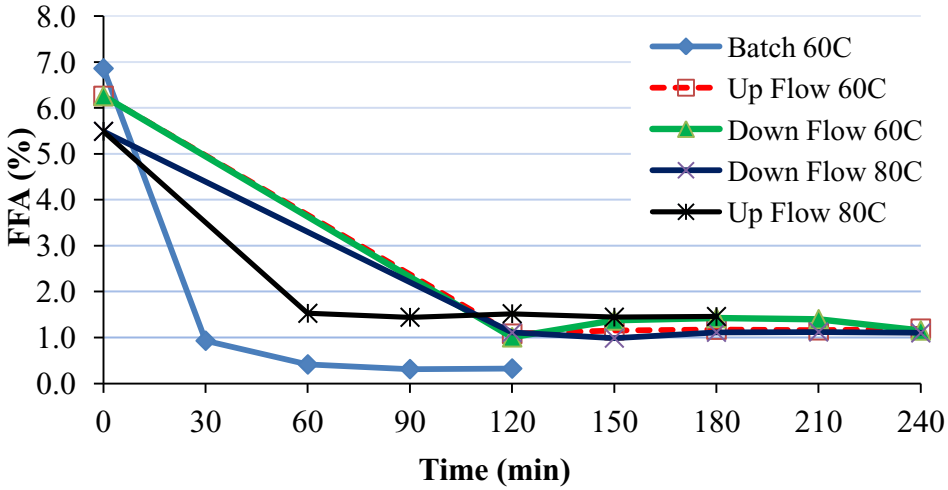

Figure 3.23 Additional experiments of the continuous experiments

The results were shown that the batch experiment (60ºC) could extremely reduce FFA content to 0.4 wt% after 60 minutes compared to other experiments especially performing at 80ºC. For up flow experiments with the different reaction temperatures, at 60ºC obtained a lower FFA content at 1.18 wt% compared to 1.48 wt% of performing at 80ºC. For the down flow experiments, they are no significant of FFA content. Anyhow it can be concluded that the reaction temperature at 60ºC is obviously optimized than at 80ºC because of hydrolysis effect, but why the batch experiment obtained better results than continuous one at the same 60ºC. The hypothesis for this reason is mixing effect. Normally, the dissolution of ethanol in CPO at 60°C looks well when it has a good agitation in the batch, but in the vertical ultrasonic reactor, the mixing takes place with micro jet generated after implosion of cavities and it does not provide an appropriate mixing condition because the ethanol in feed stream tends to flow upward in a shorter time (short cut flowing) including high viscosity of the mixture, especially at a lower temperature. Therefore the good

mixing in the reactor is probably difficult. The reaction system likes a quasi-homogeneous more that an ideal homogeneous system. At a lower reaction temperature, the quasi-homogeneous of ethanol-CPO solution is much in evidence but it is necessary to react at a lower temperature by reason of avoiding the hydrolysis reactions. The possible way to obtain a good mixing at 60ºC under ultrasound is to arrange the reactor in a horizontal configuration due to keep ethanol as long as the specific retention time. Hence, the 4th continuous experiments were conducted to prove the mixing assumption and the results were proved in 3.2.4. The FFA content obtained by a confirmation run of the experiments was 0.35 lower than 1.11 wt% of a vertical down flow. Consequently, it can be summarized that the mixing has more influence for the viscous esterification of CPO with ethanol assisted by ultrasound irradiation. The best conditions for continuous esterification of CPO with ethanol assisted by ultrasound irradiation are catalyst content of 60 wt% of FFA, molar ratio of ethanol: CPO at 30: 1, retention time at 1 hour and horizontal reactor configuration.

3.3 Studies of acid catalyzed esterification of CPO with ethanol using continuous stirred-tank reactor

The factors and orthogonal array of the experiments were same as the continuous ultrasonic experiments shown in Table 3.9 and 3.10, respectively. This CSTR experiments were conducted at 60ºC under turbulence mixing condition, N_{Re} > 20,000. Results of the CSTR were followed.

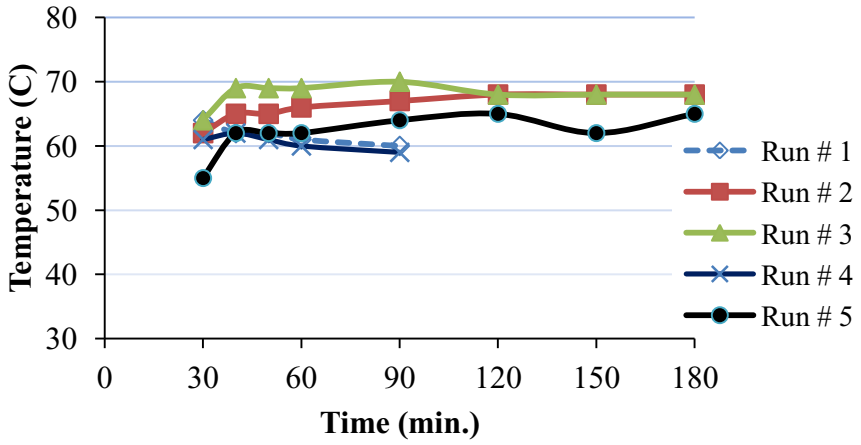

Figure 3.24 Reactor temperature profiles of the CSTR experiments

Table 3.27 Results of FFA analysis of the CSTR experiments

Time	Average FFA (%)				
(min)	Run # 1	Run # 2	Run # 3	Run # 4	Run # 5
0	7.07	8.32	6.11	6.24	7.50
30	2.01			1.69	
45	2.07			1.63	
60	2.37	1.00	1.36	1.60	0.85
75	2.51			1.72	
90	2.52	0.95	1.27	1.74	0.81
120		0.99	1.33		0.74
150		0.99	1.47		0.80
180		0.98	1.53		0.88
Average					**0.81**
Cal FFA					**0.90**

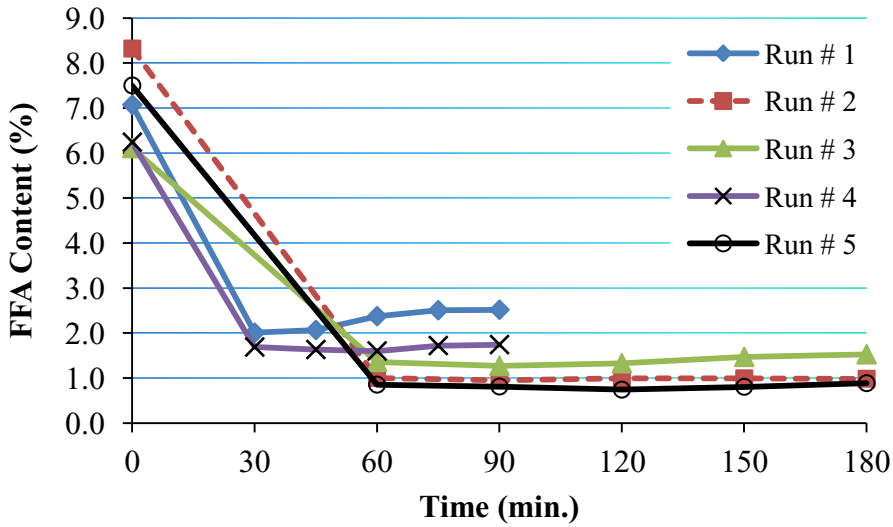

Figure 3.25 The FFA reduction of the CSTR experiments

Table 3.28 Response characteristics of the CSTR experiments

Run No.	Factors					Response Characteristic (y)
	Cat	MR	Time	y1	y2	
1	1	1	1	2.37	2.52	2.44
2	1	2	2	0.99	0.98	0.99
3	2	1	2	1.33	1.53	1.43
4	2	2	1	1.60	1.74	1.67
T						**1.63**

Table 3.29 The response table of the CSTR experiments

Level	Cat	MR	Time
1	1.72	1.94	2.06
2	**1.55**	**1.33**	**1.21**
Delta	0.17	0.61	0.85
Order		2	1
Select	Cat 2	MR 2	Time 2
μ	= T+(MR2-T)+(Time2-T)		
μ	= 0.90		

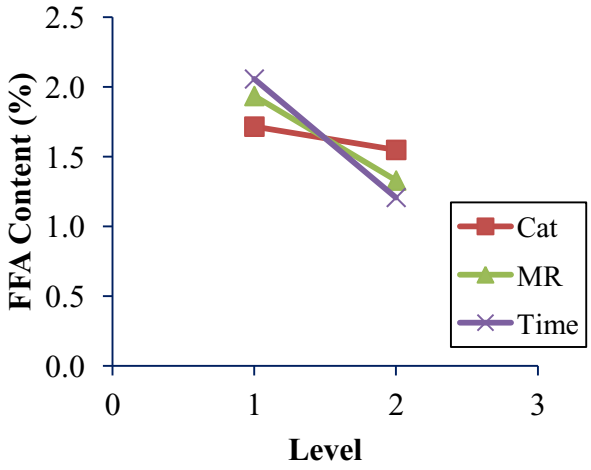

Figure 3.26 The response graph of the CSTR experiments

The interaction graphs of the CSTR experiments were shown in Figure C11 and C12 in an appendix C.

Table 3.30 Energy efficiency of the CSTR experiments

	Energy (Wh/kg CPO)				
	Run # 1	Run # 2	Run # 3	Run # 4	Run # 5
CSTR	28.24	41.28	34.92	29.44	33.94
Theory	21.67	31.31	25.72	22.56	27.05
Efficiency	76.74%	75.86%	73.67%	76.62%	79.70%

The CSTR experiments were run at 60ºC for 3 RT long and their temperature profiles were shown in figure 3.24. Their results were shown in Table 3.27 and Figure 3.25. The response characteristics showed the average FFA at 1.63 wt%. After analysis by response table in Table 3.29, it showed the significant factors in descending order as retention time, molar ratio and catalyst content corresponding to the response graph in Figure 3.26 and calculated FFA was 0.90 wt% closing to 0.81 wt% of the confirmation run. Therefore, the optimum conditions for esterification of CPO with ethanol using CSTR were retention time at 1 hour, molar ratio of ethanol: FFA is 30: 1 and catalyst content is 60 wt% of FFA, it could reduce the FFA content from 7.50 to 0.81 wt%.

However the final FFA content still higher than 0.5 wt% that means the effectiveness of CSTR method is lower than the ultrasonic irradiation method. The researcher had ever run this reactor as a batch type and found that it could reduce FFA to 0.5 wt%, but why a continuous run could not be. It may describe by considering the study of Leevijit et al. (2006) on transesterification of palm oil in series of continuous stirred tank reactors. Leevijit et al. (2006) performed 6 stages CSTRs that it could obtain the same results of the batch or plug flow reactors. The author described that single CSTR could not show the ideal mixing performance as the plug flow reactor because it probably has short cut flow and stagnant zone. So if fully mixing performance is needed, it has to use more than one CSTR. His study used six CSTRs to obtain fully mixing performance as same as a plug flow reactor showing in the Figure 3.27.

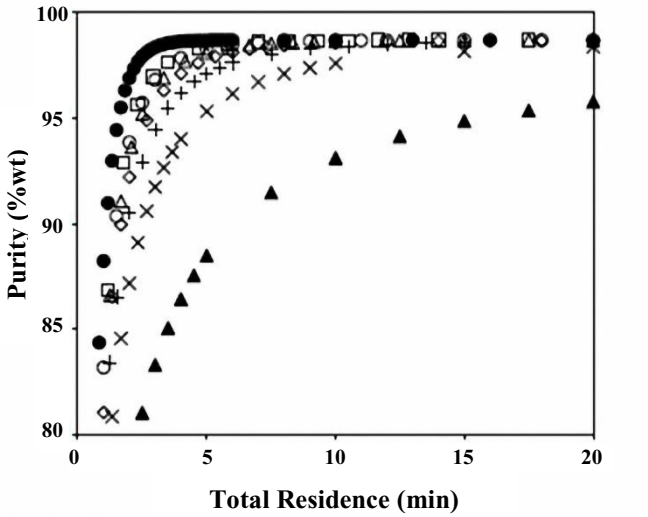

Figure 3.27 Predicted purity for the transesterification of palm oil in series of CSTRs at molar ratio 6:1, temperature 60°C, NaOH concentration 1 wt % of oil; (▲) 1-CSTR; (×) 2-CSTRs; (+) 3-CSTRs; (◊) 4-CSTRs; (Δ) 5-CSTRs; (o) 6-CSTRs; (□) 7-CSTRs; (●) PFR. (Leevijit et al., 2006)

For the CSTR experiments of this research, the reactor contains 3 stages of blades (N_{Re} = 20,249) that can be imagined to 3 series of CSTRs, so mixing condition of the viscous mixture of CPO and ethanol is hardly to be homogeneous mixture. If the complete mixing is needed, it should have many stages of blade. It can be concluded that FFA reduction capacity of ultrasonic esterification of CPO with ethanol is superior to that of esterification by CSTR system. Therefore, to reduce FFA content lower than 0.5 wt% in CSTR should be study further.

For the energy efficiency of the CSTR experiments are 72-78% in range which enormously better than the ultrasonic ones, it is probably caused by a large size of the reactor and good insulation system which can efficiently consume energy.

CHAPTER 4

Conclusion

4.1 Batch ultrasonic experiments

The optimum conditions for batch acid catalyzed esterification of CPO with ethanol assisted by ultrasonic irradiation in descending order are catalyst amount of 60 wt% of FFA, molar ratio of ethanol to FFA at 30:1, temperature at 60ºC, reaction time of one hour and amplitude of acoustic power at 75%, consequently reduce FFA content from 6.0 to 0.5 wt% in the batch size of 300 g (mixture of CPO and ethanol) irradiated by the ultrasonic generator model UP400S, 24 kHz, 400 W, Hielscher, Germany. The final FFA content of 0.5 wt% shows equilibrium of this reaction system which pertaining to hydrolysis of ester. If this water content can be abolished, the equilibrium will shift to the product side that showing FFA reduction to 0.22 wt% in 2 steps esterification. The water seems to play the role as a reaction inhibitor. The hydrolysis under strong acid condition can happen in a high degree, especially at a higher temperature at 80ºC. Therefore to avoid this hydrolysis, the esterification should be conducted at a lower temperature of 60ºC which is optimized temperature because CPO is melted between 45-50ºC. However, it is hardly to get homogeneity of the reaction under a lower temperature unless having a good mixing condition.

4.2 Continuous ultrasonic experiments

The optimum conditions for continuous acid catalyzed esterification of CPO with ethanol assisted by ultrasonic irradiation in descending order are catalyst content of 60 wt% of FFA, molar ratio of ethanol to CPO at 30: 1, retention time of one hour, reaction temperature at 60ºC and horizontal reactor configuration, consequently reduce FFA content from 6.2 to 0.35 wt% in the 1.47 L reactor irradiated by the ultrasonic generator model YPSH1020204, 20 kHz, 1000 W, Hangzhou Success Ultrasonic Equipment Co., Ltd., China. There are no doubts for catalyst content, molar ratio and retention time, but for horizontal arrangement is to provide the best

mixing condition of ethanol with CPO which ethanol inclines to flow upward by its low density under a lower mixing condition by micro jet of cavities' implosion.

4.3 CSTR experiments

The optimum conditions for continuous acid catalyzed esterification of CPO with ethanol conducted by CSTR at 60ºC in descending order are retention time of one hour, molar ratio of ethanol to CPO at 30: 1 and catalyst content of 60 wt% of FFA in the 87 L reactor, obtaining FFA content of 0.81 wt% from the initial FFA of 7.5 wt%. The FFA reduction capacity of the CSTR is inferior to ultrasonic method probably caused by mixing effect under a viscous mixture. It seems to be a quasi-homogeneous system with viscous mixture of CPO-ethanol. To increase the mixing effect, it needs more CSTR series or more blades. However this CSTR esterification requires further study to reduce a lower FFA content.

4.4 The energy consumption

As for comparing the energy consumption shows that batch ultrasonic, continuous ultrasonic and CSTR experiments have an energy efficiency of 8.23, 6.85 and 79.70%, respectively. The CSTR esterification has the highest energy efficiency probably because of a large size of the reactor and good insulation system. The ultrasonic method is suitable for a shorter reaction time to compensate the inferior energy efficiency or both of them can be processed together. By starting with CSTR followed by ultrasonic irradiation is probably suitable by mean of FFA reduction and energy efficacy.

The continuous acid catalyzed esterification of CPO with ethanol assisted by ultrasonic irradiation is suitable for CPO pretreatment before the base catalyzed transesterification. It can reduce FFA and phosphorus content to 0.35 wt% and 1.46 mg/kg, respectively. This phosphorus content also meets the new version of EN 14214: 2008. The obviously advantage of ultrasonic irradiation over the conventional method are that no external heating source is required for the reaction, resulting in saving the heating unit and a shorter time to achieve a lower FFA content.

4.5 Suggestions

4.5.1 Ultrasonic method

The acid catalyzed esterification of CPO with ethanol assisted by ultrasound is not an easy process because the reaction take place with roughly 5 wt% of FFA dissolved in the whole matrix. Apparently, the difficulties of the process still consist of its high viscosity matrix, limited under 60ºC according the hydrolysis reaction and mixing effect as well. However, its capability on FFA reduction is superior to other methods. Disadvantages of this method are low energy efficiency and capacity involved retention time about an hour. To increase its energy efficiency it may redesign the sonotrode to a longer one followed by reactor expansion in order to increase the flow rate of reactants which can efficiently consume the radiated energy, it is consequently increased the capability. Although the ultrasonic method can insure the final FFA content, but it is probably to be appropriate for the shorter time processes such as transesterification etc.

4.5.2 CSTR method

The acid catalyzed esterification of CPO with ethanol using CSTR is conventional process which widely used in various industries, especially transesterification for biodiesel production. But for the esterification of CPO under the optimized conditions at 60ºC, still has a critical limitation on mixing effect due to low reaction temperature and high viscosity, as well. Therefore, the reactor should be redesign to have more CSTR systems by putting more blades with a separation plate in between to create each CSTR system. That should be an ideal homogeneous mixing under the CSTR system, subsequently it should have a higher capability to reduce FFA content, as well.

References

Addison, K. Oil yields and characteristics; Available online: http://www.journeytoforever.org /biodiesel_ yeild.html (01/02/2009)

Bradshaw, G.B. and Meuly, W.C. 1944. Preparation of detergents. US Patent 2: 360-844.

Chongkhong, S. 2007. Production of Methyl Ester by Esterification of Palm Fatty Acid Distillate. Thesis Report, Department of Chemical Engineering, Prince of Songkla University, Thailand.

Clark, J. The mechanism for esterification reaction; Available online: http://www.chemguide.co.uk/physical/catalysis/esterify.html (11/02/2009)

Crabbe, E., Hipolito, C.N., Kobayashi G. and Sonomoto, K. 2001. Biodiesel production from crude palm oil and evaluation of butanol extraction and fuel properties. Process Biochemistry; 37: 65-71.

Cum, G., Gallo, R. and Spadaro, A. 1988. Effect of static pressure on the ultrasonic activation of chemical reaction. Selective oxidation at benzylic carbon in the liquid phase. J. Chem. Soc., Perkin Trans II; 375-383.

Feuge, R.O., Grose, T. 1949. Modification of vegetable oils. VII. Alkali catalyzed interesterification of peanut oil with ethanol. JAOCS; 26: 97-102.

Freedman, B., Pryde, E.H. and Mounts, T.L. 1984. Variables affecting the yields of fatty esters from transesterified vegetable oils. JAOCS; 61: 1638-1643.

Hanh, H.D., Dong, N.T., Okitsu, K., Nishimura, R. and Maeda, Y. 2009a. Biodiesel production by esterification of oleic acid with short-chain alcohols under ultrasonic irradiation condition. Renewable Energy; 34: 780-783.

Hanh, H.D., Dong, N.T., Okitsu, K., Nishimura, R. and Maeda, Y. 2009b. Biodiesel production through transesterification of triolein with various alcohols in an ultrasonic field. Renewable Energy; 34: 766-768.

Ji, J., Wang, J., Li, Y., Yu, Y. and Xu Z. 2006. Preparation of biodiesel with the help of ultrasonic and hydrodynamic cavitation, Ultrasonics; 44: e411-e414.

Kelkar, M.A., Gogate, P.R. and Pandit, A.B. 2008. Intensification of esterification of acids for synthesis of biodiesel using acoustic and hydrodynamic cavitation. Ultrasonics Sonochemistry; 15: 188-194.

Koc, A.B. 2009. Ultrasonic monitoring of glycerol settling during transesterification of soybean oil. Bioresource Technol.; 100: 19-24.

Kulavanich, P., Klinpikul, S. Kulavanich, S. and Chiramanee, S. 1988. Transformed Products and Marketing Development Project of Small Palm Oil Milling Regarding HM The King's Patronage. Prince of Songklanakarin University, Songkla. 127 p. (in Thai).

Kusdiana, D. and Saka, S. 2003. Effects of water on biodiesel fuel production by supercritical methanol treatment. Bioresource Technology; 91: 289-295.

Leevijit, T., Wisutmethangoon, W., Prateepchaikul, G., Tongurai, T. and Allen, M. 2006. Trans-esterification of Palm Oil in Series of Continuous Stirred Tank Reactors. As. J. Energy Env; 7(03): 336-346.

Ma, F. and Hanna, M.A. 1998. The effects of catalyst, free fatty acids and water on transesterification of beef tallow. Trans. ASAE; 41: 1261-1264.

Marchetti, J.M. and Errazu, A.F. 2008. Esterification of free fatty acids using sulfuric acid as catalyst in the presence of triglycerides. Biomass and Bioenergy. Article in press.

Margulis, M.A. 1992. Fundamental aspects of sonochemistry. Ultrasonics; 30(3): 152-155.

Margulis, M.A. 1994. Fundamental problems of sonochemistry and cavitation. Ultrason. Sonochem.; 1(2): S87-S90.

May, C.Y. 1994. Palm oil carotinoids. Food and nutrition bulletin; vol. 15 (1993/1994), No.2, June 1994.

Morad, N.A., Abd Aziz, M.K. and Zin, R.M. 2006. Process design in degumming and bleaching of palm oil. Research Report No. 74198. Centre of Lipids Engineering and Applied Research (CLEAR). Universiti Teknologi Malaysia.

Moulton, K.J., Koritala, S. and Frankel, E.N. 1983. Ultrasonic hydrogenation of soybean oil. J. Am. Oil Chem. Soc.; 60(7): 1257-1258.

Moulton, K.J., Koritala, S., Warner, K. and Frankel, E.N. 1987. Continuous ultrasonic hydrogenation of soybean oil. II. Operating condition and oil quality. J. Am. Oil Chem. Soc.; 64(4): 542-547.

Peace, G.S. 1993. Taguchi methods: a hands-on approach. 2nd ed. Addison-Wesley Publishing Company, USA.

Rokhina, E.V., Lens, P. and Virkutyte, J. 2009. Low-frequency ultrasound in biotechnology: state of the art. Trends in Biotechnology; 27 (5): 298-306.

Sambanthamurthi, R., Sundram, K. and Tan, Y.A. 2000. Chemistry and biochemistry of palm oil. Progress in Lipid Research; 39: 507-558.

Srivastava, A. and Prasad, R. 2000. Triglycerides-based diesel fuels. Renewable and Sustainable Energy Reviews; 4: 111-133.

Stavarache, C., Vinatoru, M., Nishimura, R. and Maeda, Y. 2005. Fatty acids methyl esters from vegetable oil by means of ultrasonic energy. Ultrasonics Sonochemistry; 12: 367-372.

Stavarache, C., Vinatoru M. and Maeda Y. 2007.Aspects of ultrasonically assisted transesterification of various vegetable oils with methanol. Ultrasonics Sonochemistry; 14: 380-386.

Suslick, K.S. 1989. The chemical effects of ultrasound. Scientific American; February: 80-86.

Thompson, L.H. and Doraiswamy, L.K. 1999. Sonochemistry: Science and Engineering (Reviews). Ind. Eng. Chem. Res.; 38: 1215-1249.

University of Strathclyde. What is biodiesel?; Available online: http://www.esru.strath.ac.uk /EandE/Web_sites/02-03/biofuels/what_ biodiesel.htm (09/12/2008)

Vanichseni, T., Intaravichai, S., Saitthiti, B. and Kiatiwat, T. 2002. Potential Biodiesel Production from Palm Oil for Thailand. Kasetsart Journal; Vol. 36: 1, January.

Wikipedia. Esterification; Available online: http://en.wikipedia.org/wiki/Esterification (10/02/2009)

Wright, H.J., Segur, J.B., Clark, H.V., Coburn, S.K., Langdon, E.E. and DuPuis, R.N. 1944. A report on ester interchange. Oil and Soap; 21: 145-148.

Appendices

Appendix A

Biodiesel Standards

Table A1 Comparison of different national standards for biodiesel

		Europe	**Austria**	**Germany**	**USA**	**Thailand**
Standard	Unit	EN	ON	DIN V	ASTM D-	Thai
Date		Sep	July	Sep 1997	Jan 2002	2006
Application		FAME	FAME	FAME	FAMAE	FAME
Density at 15°C	g/cm	0.86 -	0.85 -	0.875 -	-	860 to
Viscosity at 40°C	mm^2/s	3.5-5.0	3.5-5.0	3.5-5.0	1.9-6.0	3.5-5.0
Distillat. 95%	°C	-	-	-	90% @	<360
Flashpoint	°C	>101	>100	>110	>130	>120
CFPP (cold filter	°C	*country	0/-15	0/-10/-20	-	-
Sulfur	% mass	<10	<0.02	<0.01	<0.05	<0.0010
CCR 100%	% mass	-	<0.05	<0.05	-	-
10% dist. resid.	% mass	<0.3	-	-	-	<0.3
Sulfated ash	% mass	<0.02	<0.02	<0.03	<0.02	<0.02
Water	mg/kg	<500	-	<300	<0.05%	<500
Total contaminate	mg/kg	<24	-	<20	-	<24
Cu-Corros.	Number	1	-		<No.3	1
Oxidation	Hours	>6	-	-	-	>6
Cetane Number	Number	>51	>49	>49	>47	>51
Acid value	mgKOH/g	<0.5	<0.8	<0.5	<0.8	<0.5
Methanol	% mass	<0.20	<0.20	<0.3	-	<0.20
Ester content	% mass	>96.5	-	-	-	>96.5
Monoglyceride.	% mass	<0.8	-	<0.8	-	<0.80
Diglyceride	% mass	<0.2	-	<0.4	-	<0.20

		Europe	Austria	Germany	USA	Thailand
Triglyceride	% mass	<0.2	-	<0.4	-	<0.20
Free glycerol	% mass	<0.02	<0.02	<0.02	<0.02	<0.02
Total glycerol	% mass	<0.25	<0.24	<0.25	<0.24	<0.25
Iodine value	g	<120	<120	<115	-	<120
Linolenic acid	% mass	<12	-	-	-	<12
C18:3 and high.	% mass	-	<15	-	-	-
C(x:4) & greater	% mass	<1	-	-	-	-
Phosphor	mg/kg	<4	<20	<10	<0.001%	<10
Ramsbottom	% mass	-	-	-	0.1	-
Carbon residue	% mass	-	-	-	<0.050	
Gp I metals	mg/kg	<5	-	-	-	<5.0
Gp II metals	mg/kg	<5	-	-	-	<5.0
Alkalinity	mg/kg	-	-	<5	-	-

(www.journeytoforever.org)

Remark:

RME: Rapeseed oil methyl ester

FAME: Fatty acid methyl ester

VOME: Vegetable oil methyl ester

FAMAE: Fatty acid mono alkyl ester

Appendix B

Taguchi Methods

All contents in this appendix B are referred to (Peace, 1993).

1. Background

Dr. Genichi Taguchi's methods are a product of the Japanese post-World War II era. When resources were scarce and financial support was at best minimal, the demands for reconstruction of Japanese industry were enormous. Dr. Taguchi was born on January 1, 1924. His advanced formal training was directed toward textile engineering at Kiryu Technical Colledge, but he devoted extensive personal study to statistics. From an engineering background, Dr. Taguchi converted his study of statistics and advanced mathematics into a system merging statistical techniques and engineering expertise. The realities of deadlines and production limitations helped to shape his approach to apply experimental technique to actual design and production situations. This fostered a growing appreciation for taking assumptions for engineering knowledge to reduce the size of experiments and thereby speed up the experimentation process. He adapted the use of orthogonal array as an effective experimental design tool for greatly reducing the size of experiments while still achieving new insights and improving product designs and process productivity.

2. Determining the objectives

Developing a meaningful objective may require research on the part of the experimentation team. Retrieval of historical data, special tests or extra production runs may be needed. To determine the objectives, it needs many ways to achieve such as brainstorming, Pareto chart, process flow diagram, cause-and effect diagram, fault tree analysis, and failure made and effect analysis (FMEA) etc. By forming a foundation for understanding the process through the use of various techniques, the team can make an agreement on the objectives of the study and determine a relevant and meaningful quality characteristic for measuring success. The basic rules are:

2.1 Clearly define the objectives in terms that everyone on the team can understand.

2.2 Insure that all team members agree on and can support the objectives selected by majority of the team.

2.3 Attain mutual agreement on the criteria for measuring the ability to achieve the objectives.

2.4 Put into place communication safeguards to insure that all affected personnel become aware of any changes in the objectives or quality characteristic.

2.5 Provide the opportunity to respond to any changes so as to assure continued agreement and support by all team members.

2.6 Measurable characteristics are those end results that can be measured on a continuous scale such as dimensions, weight, pressure and clearance etc. Within the framework of measurable characteristics, it can be classified into nominal-the-best, smaller-the-better and larger-the-better characteristics. Nominal-the-best refers to a characteristic with a specific numerical goal or target value. A smaller-the-better characteristics is one in which the desire goal is to obtain a measure of zero such as machine wear, residue, percent contamination etc. A larger-the-better characteristics is opposite of a smaller-the-better characteristics is to achieve the highest value possible. Infinity is the ultimate objective. The examples of this characteristic are strength, shelf life, flash point and corrosion resistance etc.

3. Selecting the independent variables

After determining the team objectives and defining the quality characteristic, we will measure the ability to achieve our objective; we need to select the independent variables that have significant impact on this measurement. We can think of the quality characteristic as the dependent variable and each of the influences that affect it as an independent variable. The term factor is typically used instead of an independent variable. Normally, the tasks of selecting process variables (factors) and assigning appropriate factor level settings are the most time consuming and mentally exhausting part of the experiment planning. However, performing a thorough investigation of the potential factors affecting the selected quality characteristic will pay off in the long run. Careful selection of the process and product factors will help to uncover those effects that have significant influence on the end result. In generating

the list of potentially strong factors, the use of brainstorming is extremely valuable. In developing a list of factors, several approaches utilizing these tools may be considered. For example, the cause-and-effect diagram may be selected because it provides a systematic structure for creating the list of factors and it is easy to use and understand. Once the list of factors developed, the next step is to review each suggested factor and determine which factors should be incorporated into the study and which should be left for later consideration. The significant factors should be selected by discussion of the team members and set the agreement on those. This procedure is a screening the list of variables. Then factors classifying is needed by grouping into control and noise factors. The next step is to decide on the number of level of each factor and to specify the setting or value for each level. In defining appropriate levels for a particular control factor, you may learn that these values cannot in fact be controlled. Therefore, the factor needs to be redefined as a noise factor. The value or setting for another factor is held constant. In this case, the factor could be eliminated from further consideration in the particular study. Therefore, the process of screening the factors, classifies them as either control or noise factors and assigning value is actually an iterative process.

4. Experiment strategy

The majority of reasons to perform an experiment can be categorized into five major classifications.

4.1 Single experiment: to obtain a better understanding of how the process works, to know the important factors in a process. What causes changes in the end product?

4.2 Continuous experiment: to strive for continuous improvement, to reduce the variation by specific amount or down to a predetermined level.

4.3 Screening experiment: this process may have just been installed or may still be in the stages of being built. The process is sophisticated or very complex with many variables of potential importance. You are interested in refining the list of process factors down to a more manageable number in order to perform further experimentation to determine optimal settings for the most significant factors.

4.4 Focusing experiment: the experiment objective is specially targeted toward solving a problem. The purpose of the study is to determine the culprit or culprits by

studying simultaneous changes in the process and product variables. The advantage of this technique over other cause-and-effect tools occurs when the problem is sporadic and frequency of occurrence suggests that the problem is more likely to occur under a yet undetermined unique combination of process factor values.

4.5 Sequential experiment: this experiment is applicable where the process consists of many steps with numerous factors at each stage. The incorporation of all factors of interest into one experiment would result in a study too large to conduct practically. But by segmenting the process, a study of the first section can be performed first, followed by a second study involving the final portion of the process.

By determining which strategy best applies to our particular situation, we will be more capable properly planning the experiment and reducing the time needed to do so. Most important, the appropriate strategy will make the road smoother and easier and insure that we are able to achieve the objective.

5. Orthogonal arrays

The foundation for designing an experiment using Taguchi methodology is the orthogonal array. The orthogonal array is so efficient in obtaining only a relatively small amount of data and being able to translate it into meaningful and verifiable conclusion. Furthermore, the designs of experiments utilizing orthogonal arrays are basically simple to understand and the guidelines are easy to follow. Orthogonal means being balanced and not mixed. In the context of experimental matrices, orthogonal means statistically independent. If we examine a typical orthogonal array (Table B1), we will note that each level has an equal number of occurrences within each column.

Table B1 L_8 orthogonal array

$L_8(2^7)$							
No.	**1**	**2**	**3**	**4**	**5**	**6**	**7**
1	1	1	1	1	1	1	1
2	1	1	1	2	2	2	2
3	1	2	2	1	1	2	2
4	1	2	2	2	2	1	1
5	2	1	2	1	2	1	2
6	2	1	2	2	1	2	1
7	2	2	1	1	2	2	1
8	2	2	1	2	1	1	2

Therefore, orthogonal arrays are much more cost effective and can provide more timely information.

5.1 Terminology

To facilitate the understanding of orthogonal arrays, it is essential to understand the standard nomenclature for describing each orthogonal array. Each array can be identified by the form $L_A(B^C)$. The subscript of L, which is designated by A, represents the number of experimental runs or combination of factors which can be conducted in the experiment. B denotes the number of levels within each column. The letter C, the exponential of letter B, identifies the number of columns available within the orthogonal array. orthogonal arrays are available with a variety of levels.

Analysis is based on combining the data associated with each level for each factor or interaction (column). The difference in the average results for each level is the measure of the effect of that factor. Those factors with the greatest effect or difference are the ones that can be used to improve the process and/or product.

6. Linear graphs

Assigning interactions at random to any available column within the orthogonal array can lead to incorrect analysis and faulty conclusions. To prevent the occurrence of these experimental design errors, Dr. Taguchi has developed a system for mapping interactions to the appropriate columns of the array. By setting up a graphical representation of the relationships among factors and the interactions between them, the experimenter can systematically assign factors (main effects) and interactions to the column within the orthogonal array without fear of confounding the effects of factors and their interactions. These graphical representations are called linear graphs.

Linear graphs are constructed of interconnecting dots or circles. Each dot or circle within a linear graph represents a column within the orthogonal array in which a factor can be assigned. The connecting line represents the interaction between the two factors represented by the dots at each end of line segment.

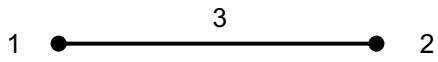

6.1 Assigning factors to linear graphs

The designing of the experiment can be easily accomplished in the following sequential steps.

6.1.1 Select the orthogonal array. This step requires first calculating the total degrees of freedom needed foe studying the factors and interactions of interest. The degrees of freedom required are then matched against the degrees of freedom of the orthogonal arrays within the appropriate array series. The smallest array with at least as many degrees of freedom as required is selected.

6.1.2 Draw the required linear graph. Based on the factors and interactions identified for study in the planning phase, construct a linear graph. Use dots or circles to represent factors, and connect the dots with straight lines where interactions have been planned into the experiment.

6.1.3 Match the required graph to a standard linear graph. Using Appendix B (Peace, 1993), compare the graph drawn in step 2 to the alternate shapes available for the orthogonal array selected. Select the standard linear graph that most closely resembles the graph drawn earlier.

Example of standard linear graphs for

$L_4(2^3)$

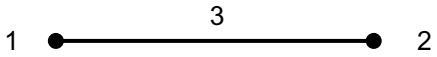

$L_8(2^7)$

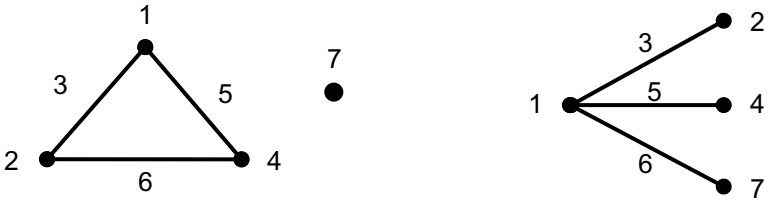

$L_{16}(4^5)$

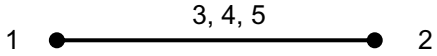

6.1.4 Redraw the required linear graph. Based on the standard linear graph selected in step 3, modify the required graph to resemble the preferred graph from the appendix.

6.1.5 Assign factors and interactions. Mark each factor and interaction beside the appropriate dot or line segment. If a line segment of the linear graph will not be required to represent an interaction, that line may be used for assigning a factor.

6.1.6 Compare alternative mapping for the standard linear graph (if appropriate). If the orthogonal array selected has available more than one linear graph with the same identical shape, you can compare the potential column assignments from each of the graphs for your more expensive and hard to change factors. If the linear graph which appears more efficient is different from the one that you had previously selected, copy your modified linear graph, and renumber the dots and line segments as shown in the preferred linear graph pattern.

7. Preparing and conducting the experiments

7.1 Preparing the experiment.

Appropriate material and equipment must be used when conducting the experiment. Otherwise, the integrity of the experiment may be jeopardized and perhaps even violated. Therefore, it is important that required material and proper equipment are selected for completing each of the experimental runs.

If the purpose of the experiment is to make the process robust against differences in the incoming material, it is most essential that the material selected represent the full spectrum of material variability. For insuring robustness, only two levels, the opposing extremes, are typical required. The equipment to be used in conducting the experiment must be appropriate for the intent. Measuring something just to be obtaining data is like traveling without a destination and hoping that the road will take you somewhere meaningful. The primary factor in equipment selection is to provide a quantifiable measure tied directly to the objective of the experiment. That is the apparatus must be able effectively to obtain readings or measurements of the quality characteristic of interest. The precision of the instrument must be as good as or better than that desired for insuring a desired level of quality or variability.

7.2 Conducting the experiment

A valuable tool for coordinator is the experimental run sheet. This is a printout of the experimental run sequence with the corresponding setting or values for each factor in the experiment. The sheet can assist the coordinator in monitoring the progress of the experimental runs. The printout can serve as a checklist by which the operators mark off the setting change for each control factor as they go from the setup for one experimental run to the next.

8. Level average analysis

The type of analysis to be performed on the experiment data will be dictated by the design of the experiment. We can categorize the different designs in terms of the type of quality characteristic and the involvement of noise factors. When the quality characteristic has been defined in terms of a continuously measurable variable and no noise factors have been designed into the experiment, level average analysis may be the most appropriate technique for interpreting the data.

Level average analysis gets its name from determining the average response for factor and interaction levels and analyzing the importance of factors and interactions based on these computed values. The goal behind level average analysis is to identify the strongest effects and determine the combination of factors and interactions investigated that can produce the most desired result. The first step is to calculate the average experiment result for each level, factor and interaction (if defined in the experiment). The relative impact of each factor can be determined using either response table or graph. It is recommended that the analysis be performed both ways.

Using tabular method for analysis, a response table should be constructed displaying the average experiment result for each factor level under study. For each factor, the range in average response values should then be computed. In an experiment involving two level factors, this is merely the difference between the average values of two settings. However for three levels or more, you must identify the highest average response and the lowest average response. Be careful in identifying the proper levels for computing the range. The extreme values may not necessarily obtain from the highest and lowest factor settings. Once the differences have been ascertained, the next step is to separate the strong effects from the mild and weak effects. A sound and consistent approach is to rank the factors in order from the largest difference to the smallest. Then you will want to move from the largest to the smallest delta looking for a logical breaking point between the strong effects and the mild and weak effects. A rule of thumb is to identify approximately half of the effects as having a significant impact on the quality characteristic.

The strongest factors can also be identified graphically by plotting the average response value for each factor level; we can make relative comparisons of the slope between points plotted. Again, the factors can be ranked based on the relative steepness of the slopes. The rule of selecting approximately half of the factors investigated still applies. Once the strong effects and desired levels have been ascertained, a calculation of the predicted results is made based on the impact of the significant effects on the experiment results. Then the confirmation run is performed using the optimal factor level identified in the analysis. The results of the

confirmation run are compared against the predicted results to verify the analysis and confirm the assumptions made in designing the experiment.

If the interactions have been incorporated into the design of the experiment, analysis may become more detailed. Using the tabular method of analysis, the range for any interaction understudy is similarly compared to the ranges for each of the factors under study. If the interaction is not determined to be important based on the relative comparisons and logical breaking point, analysis of the interaction does not need to go any further. If on the other hand the interaction is deemed important, a matrix of the various combinations of the two factors comprising the interaction should be constructed. The levels of the associated factors can be selected on the basis of the factor level combination resulting in the most desired experiment result.

Graphical analysis also can be even more helpful in determining the best combination of interacting factors. The slope of the interaction is compared to the slope of each of the factors or main effects. As in tabular analysis, if the interaction is not considered important, we do not need to go any further. If the interaction is determined to have a strong effect, we will then need to construct an additional graph comprised of points representing the average response for each combination of interacting factors. The recommended factor levels are then selected based on the preferred point on the graph. The advantage of developing an interaction graph is that not only can you determine the most desired point, but the strength of the interaction is often clearer when shown graphically.

The analysis strategy will change depending on the type of quality characteristic. If the output of interest is a larger-the-better characteristic, the emphasis will be on determining which levels result in the highest response. For a smaller-the-better characteristic, the goal is to identify those factor levels that will achieve the lowest expected results. For nominal-the-best quality characteristics, the analysis is more complicated. Moving the average process results closer to the desired or target value is hardly desirable if the variation from one unit or batch to the next increases. Therefore, regular analysis is not recommended for handling nominal-the-best quality characteristics. A preferred approach is to run repetitions for each experimental run and to treat the repetitions as noise factor setting combinations.

Once the confirmation run has been performed, the actual and predicted results can be compared against each other. If the results are similar, then the experiment can be deemed a success, and preferred settings should be instituted. If the confirmation run results are disappointing, the team will need to return to the planning phase to reevaluate the elements that went into the experiment. A possible cause is the omission of a key factor from the experiment. Perhaps a powerful interaction was not considered. Another common cause is the setting of factor levels too close together for the experiment. In these situations, the factor is found insignificant during the analysis and is not accounted for in the validation. During the confirmation run, this factor operates at a value beyond the experimental values. Although the factor is not a strong effect within the experiment range, moving outside the region cause a significant change in the output of interest. Therefore, the results are different from what was predicted. Another potential problem occurs when randomization is used to conduct the experiment. After performing the experiment with the order of experimental run scrambled, the team fails to reorder the sequence of the runs for the analysis. If the confirmation run results are not as good as the predicted results, but better than the current production results, you may want to consider implementing the recommended settings temporarily while returning the planning phase. This at least gives you some improvement until better understanding of the process or product can lead to a better confirmation run and more desirable results.

Appendix C

Interaction Graphs and Temperature Profiles

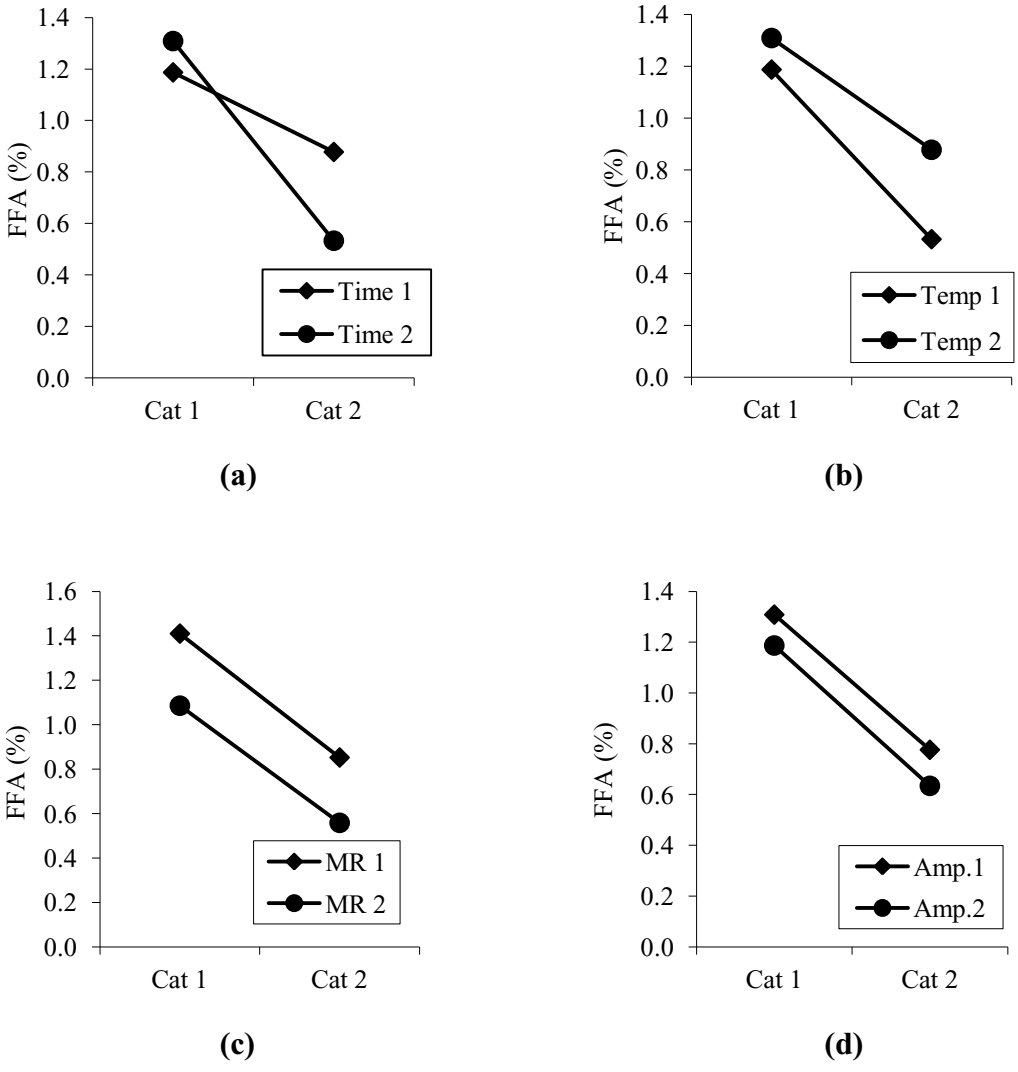

Figure C1 Interaction graphs between Cat-Time (a), Cat-Temp (b), Cat-MR (c) and Cat-Amp (d) of the secondary experiments

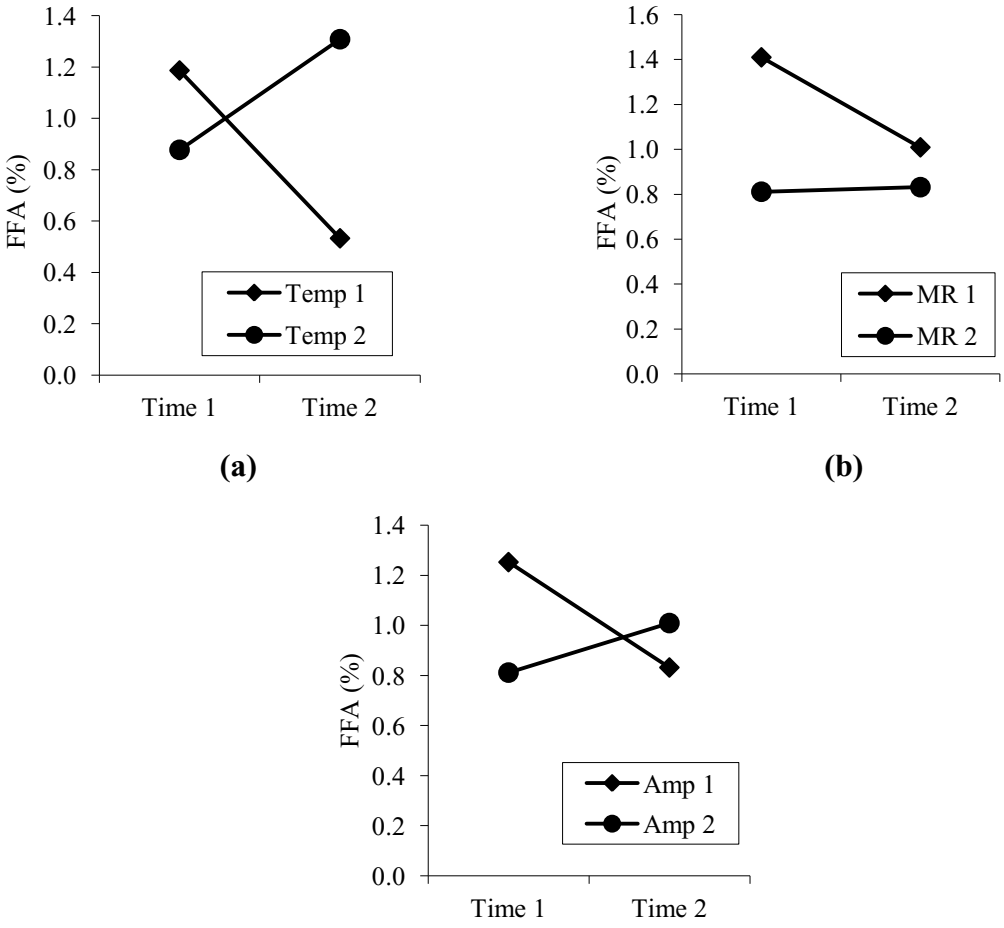

Figure C2 Interaction graphs between Time-Temp (a), Time-MR (b) and Time-Amp (c) of the secondary experiments

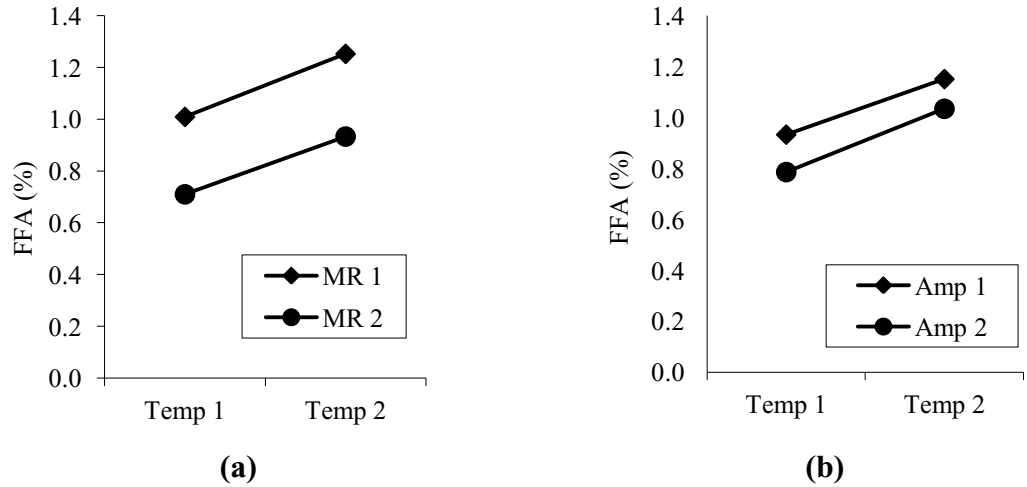

Figure C3 Interaction graphs of between Temp-MR (a) and Temp-Amp (b) of the secondary experiments

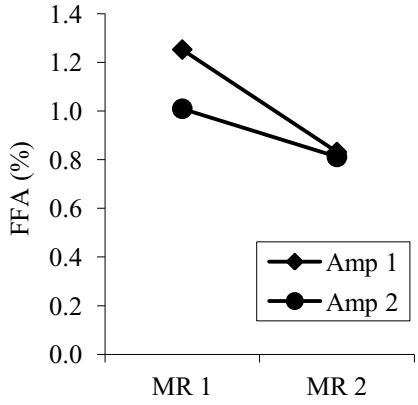

Figure C4 The interaction graph between MR-Amp of the secondary experiments

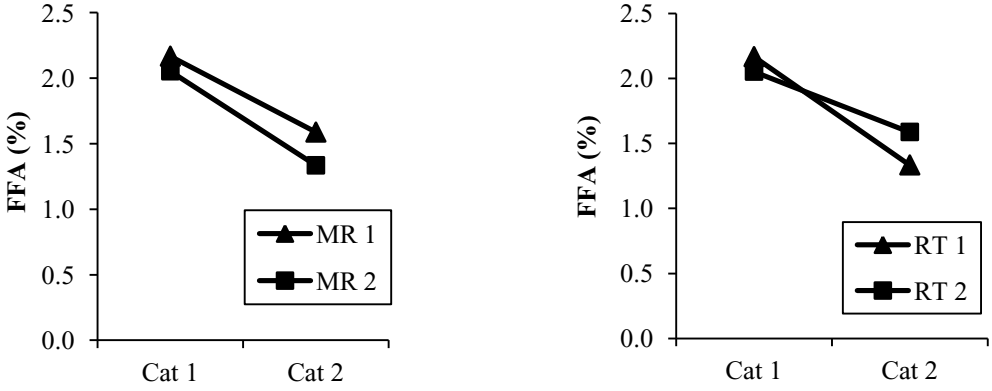

(a) (b)

Figure C5 Interaction graphs between Cat-MR (a) and Cat-RT (b) of the 2nd continuous experiments

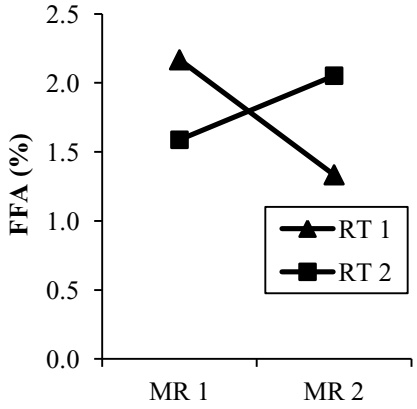

Figure C6 The interaction graph between MR-RT of the 2nd continuous experiments

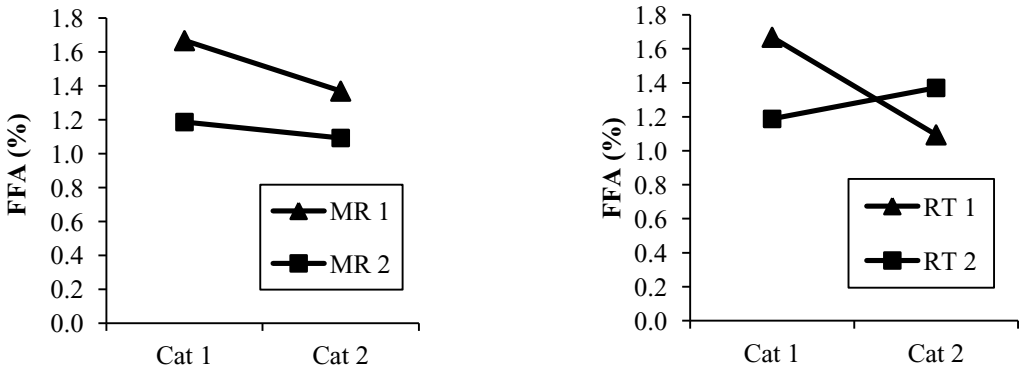

(a) (b)

Figure C7 Interaction graphs between Cat-MR (a) and Cat-RT (b) of the 3rd continuous experiments

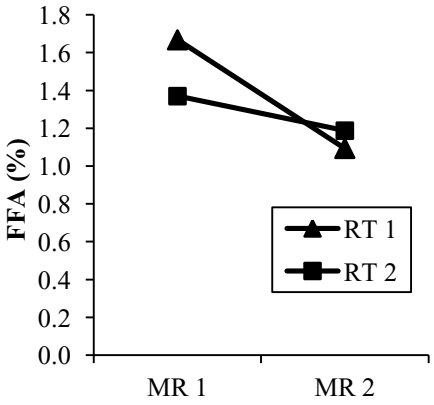

Figure C8 The interaction graph between MR-RT of the 3rd continuous experiments

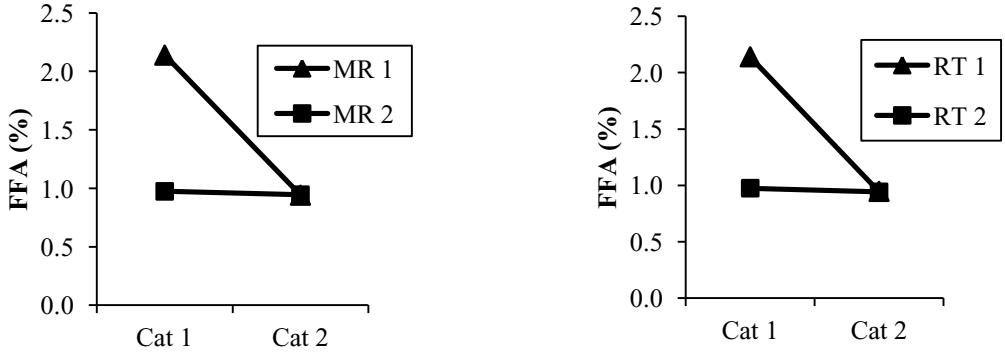

(a) (b)

Figure C9 Interaction graphs between Cat-MR (a) and Cat-RT (b) of the 4th continuous experiments

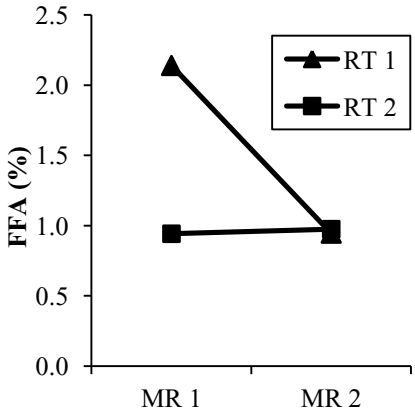

Figure C10 The interaction graph between MR-RT of the 4th continuous experiments

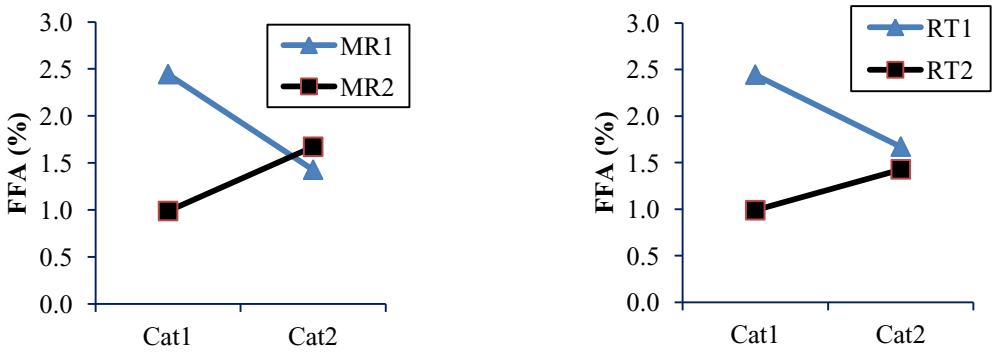

Figure C11 Interaction graphs between Cat-MR (a) and Cat-RT (b) of the CSTR experiments

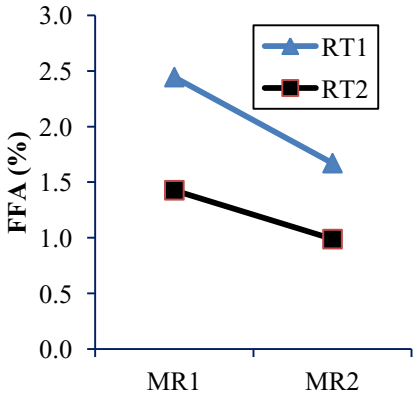

Figure C12 The interaction graph between MR-RT of the CSTR experiments

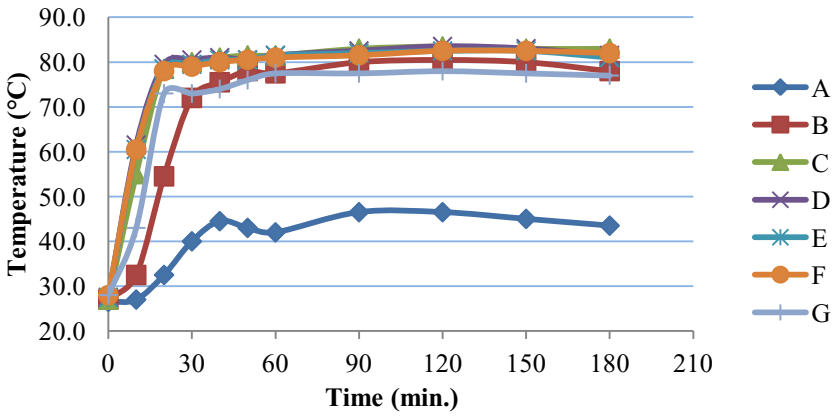

Figure C13 Reactor temperature profile: Run # 1 of the 2nd continuous experiments

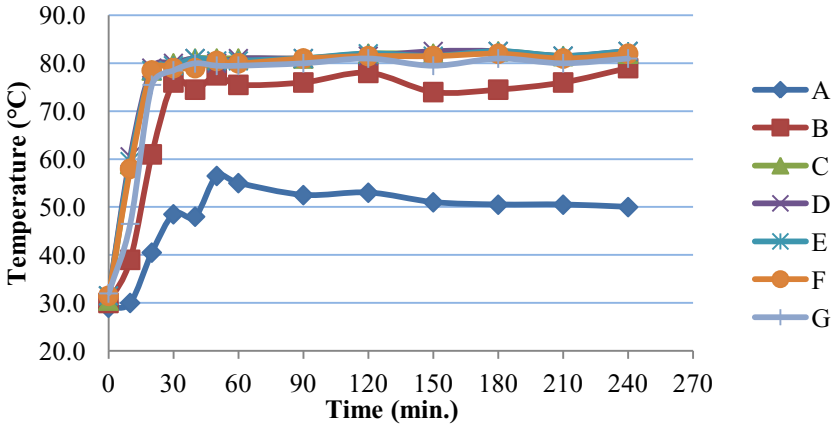

Figure C14 Reactor temperature profile: Run # 2 of the 2nd continuous experiments

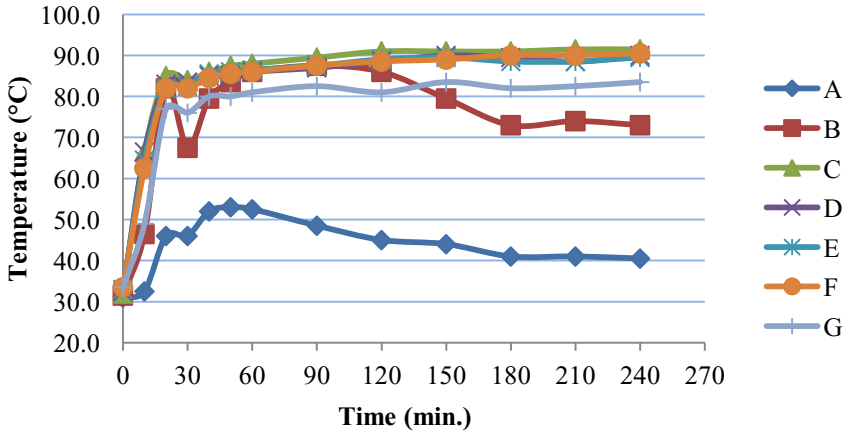

Figure C15 Reactor temperature profile: Run # 3 of the 2nd continuous experiments

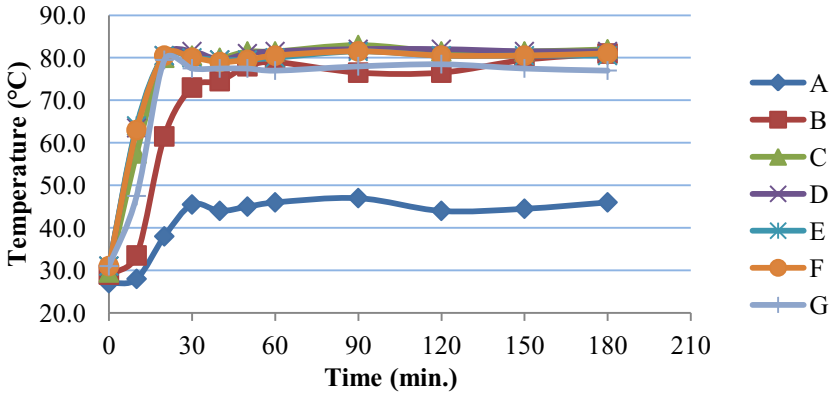

Figure C16 Reactor temperature profile: Run # 4 of the 2nd continuous experiments

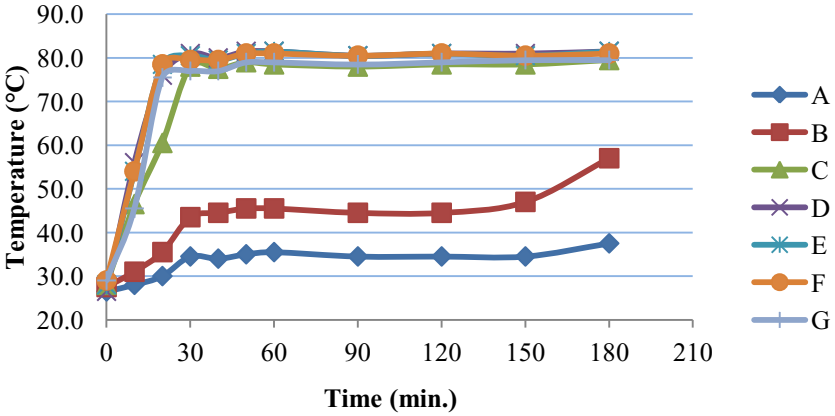

Figure C17 Reactor temperature profile: Run # 5 of the 2nd continuous experiments

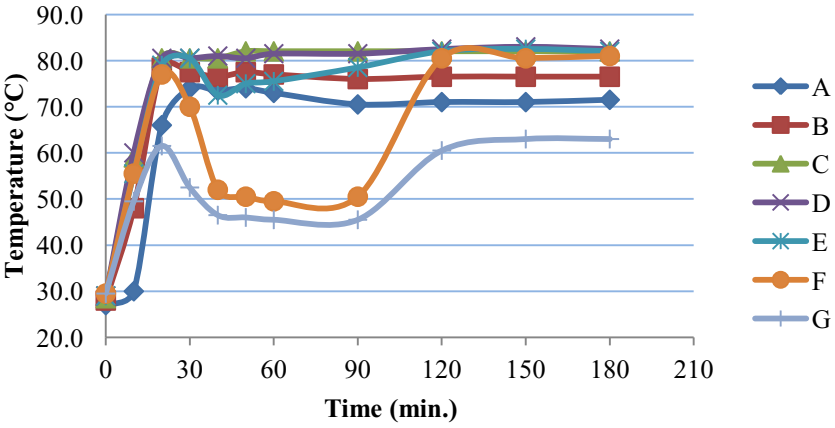

Figure C18 Reactor temperature profile: Run # 1 of the 3rd continuous experiments

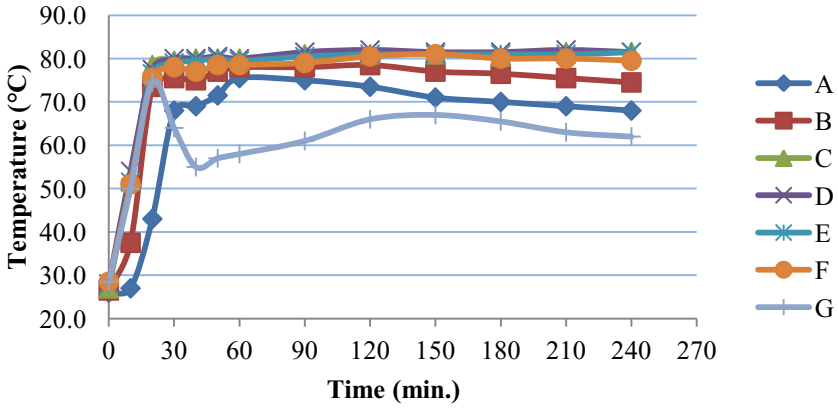

Figure C19 Reactor temperature profile: Run # 2 of the 3rd continuous experiments

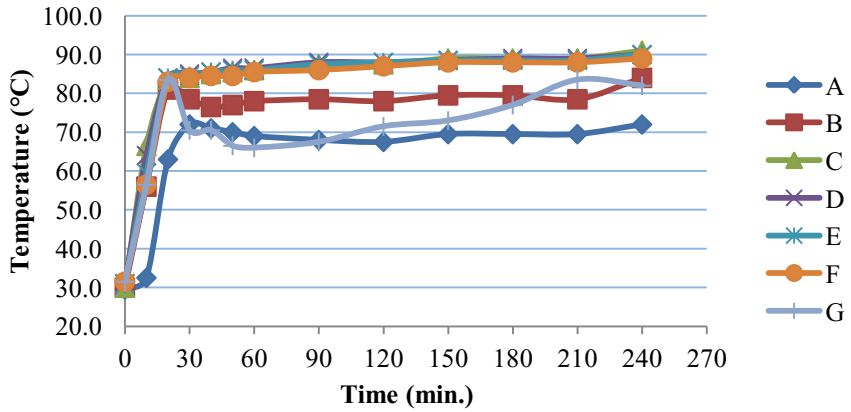

Figure C20 Reactor temperature profile: Run # 3 of the 3rd continuous experiments

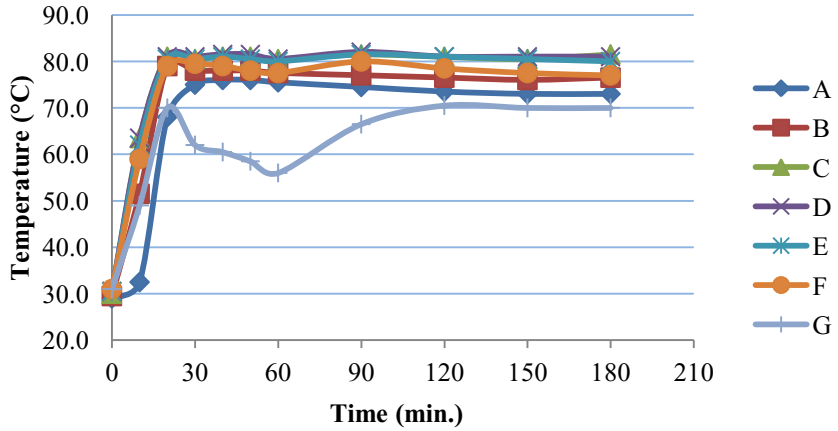

Figure C21 Reactor temperature profile: Run # 4 of the 3rd continuous experiments

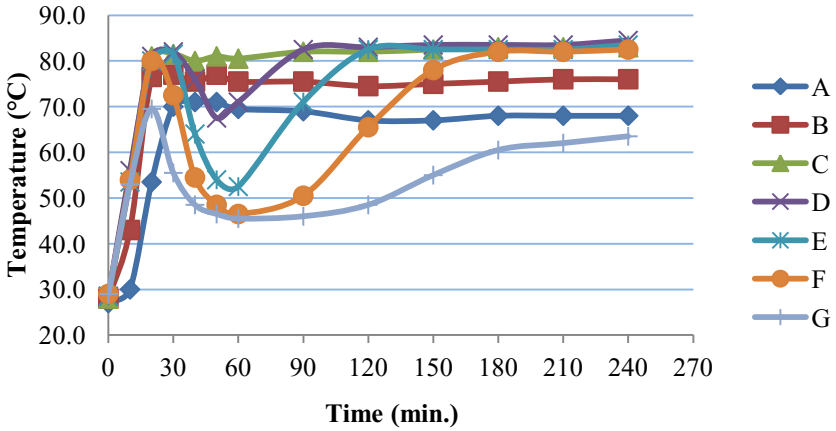

Figure C22 Reactor temperature profile: Run # 5 of the 3rd continuous experiments

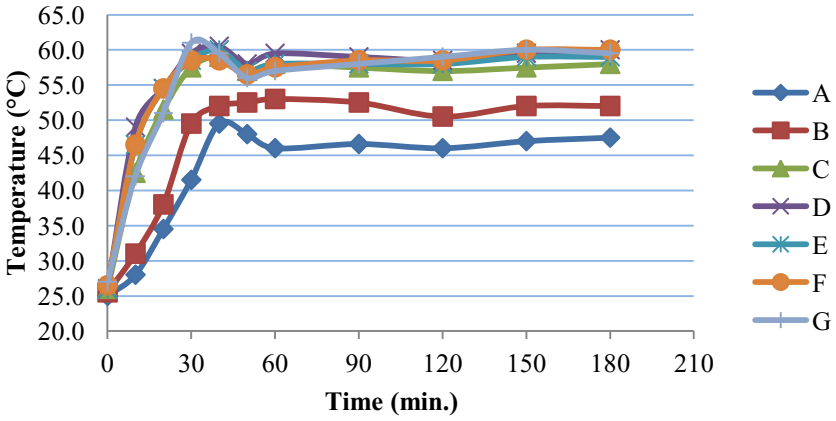

Figure C23 Reactor temperature profile: Run # 1 of the 4th continuous experiments

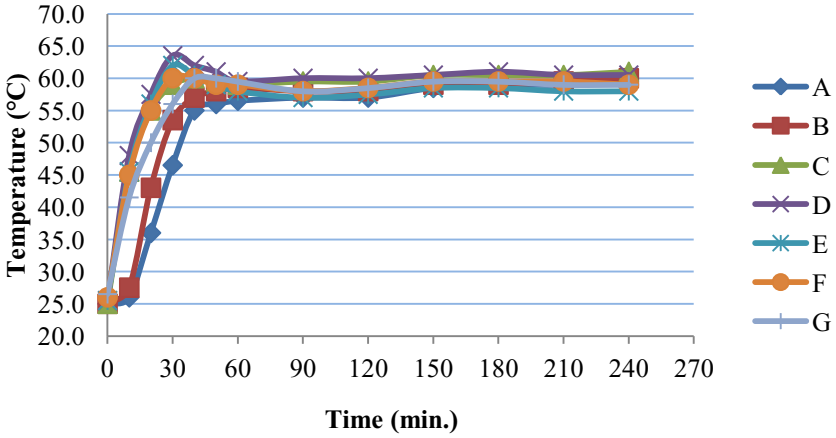

Figure C24 Reactor temperature profile: Run # 2 of the 4th continuous experiments

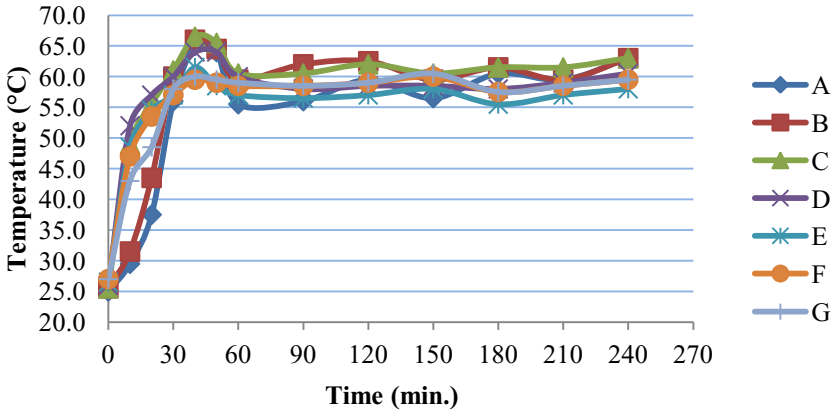

Figure C25 Reactor temperature profile: Run # 3 of the 4th continuous experiments

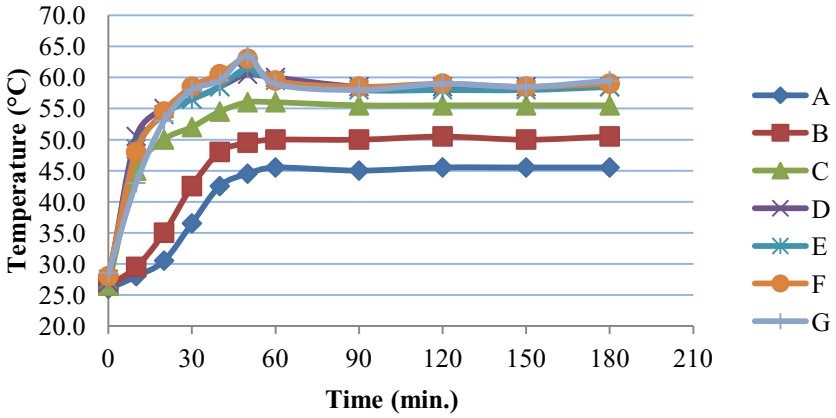

Figure C26 Reactor temperature profile: Run # 4 of the 4th continuous experiments

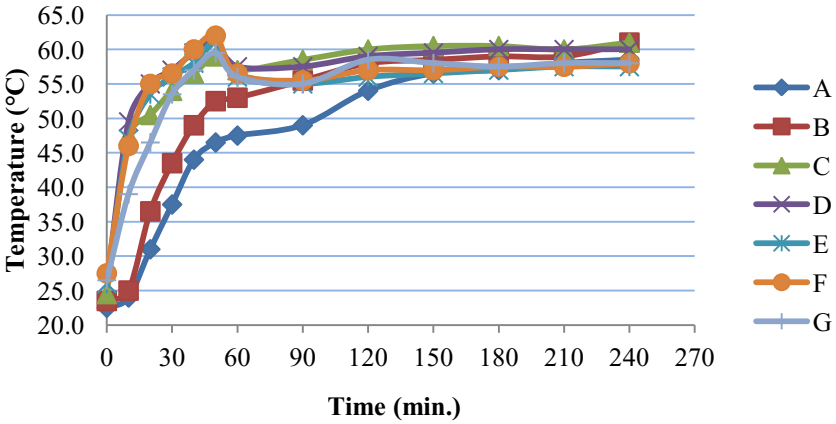

Figure C27 Reactor temperature profile: Run # 5 of the 4th continuous experiments

Appendix D

CSTR Drawing

A continuous stirred-tank reactor drawings are illustrated.

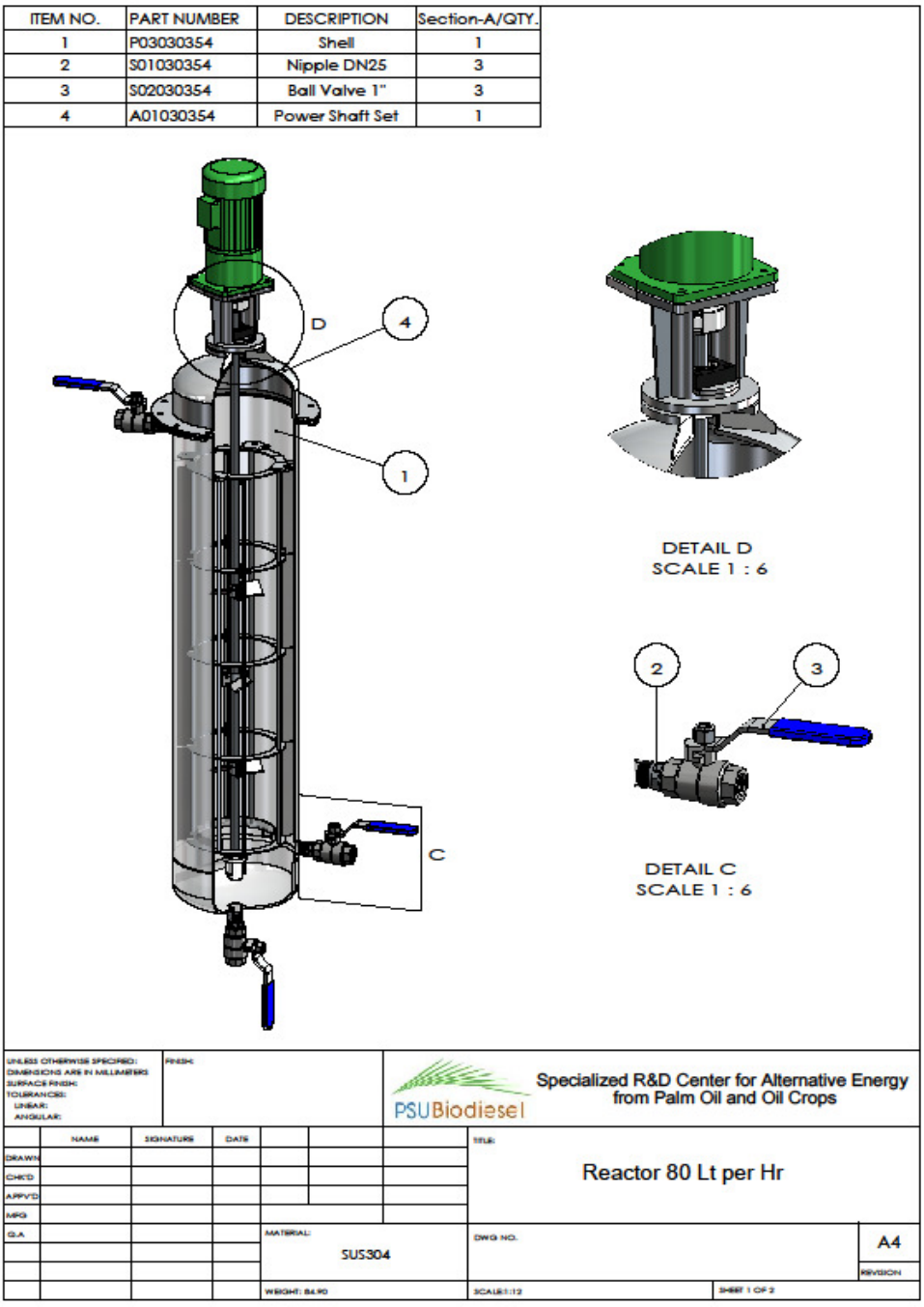

Figure D1 The overview of a CSTR for continuous esterification.

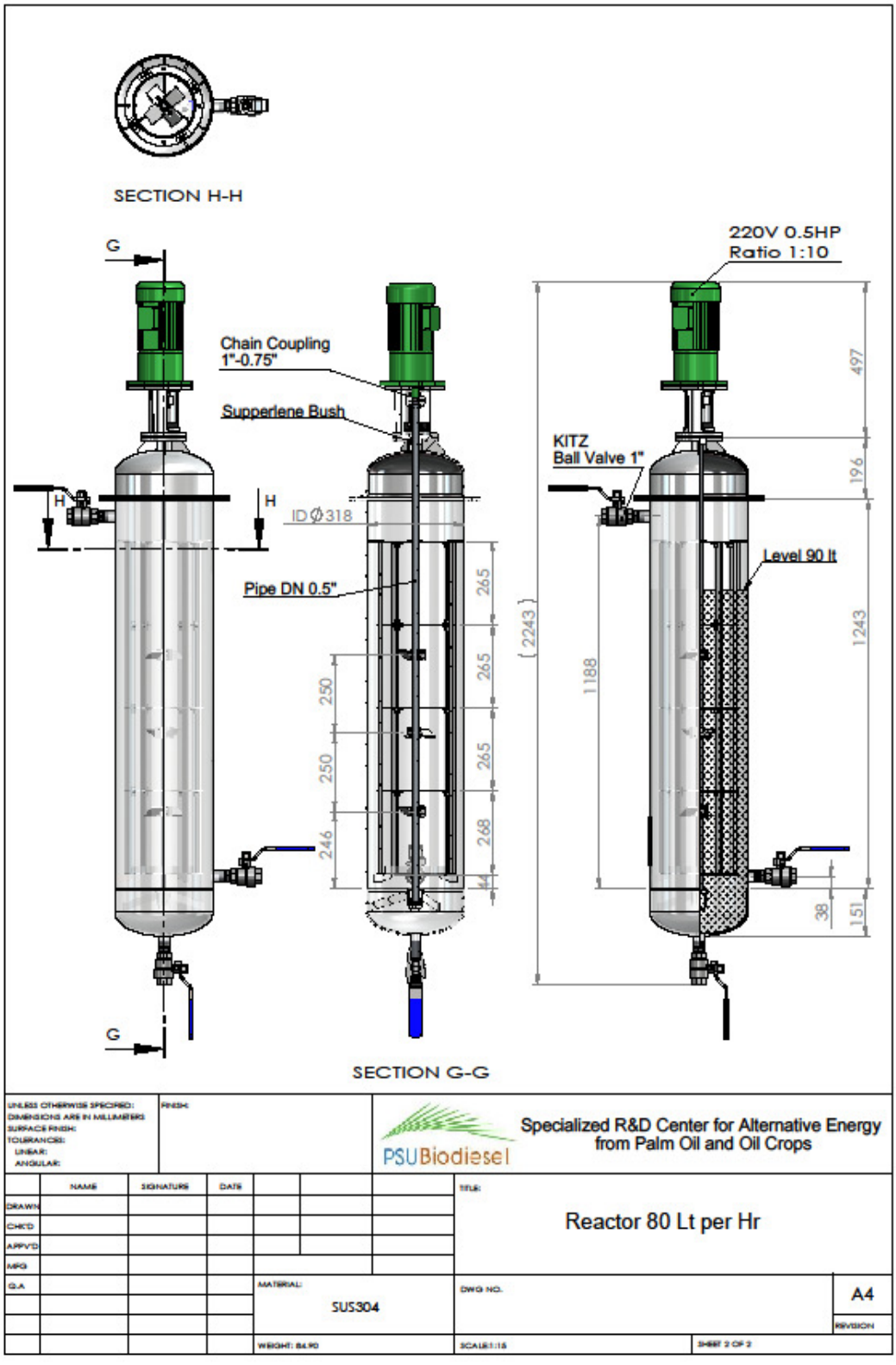

Figure D2 The details of a CSTR for continuous esterification.

VITAE

Name Mr.Thanet Waisuwan

Student ID 5110130003

Educational Attainment

Degree	Name of Institution	Year of Graduation
B.Sc. (Chemistry)	Prince of Songkla University	1988
M.Eng. (Chemical)	Prince of Songkla University	1996

Scholarship Awards during Enrolment

1. The National Research Council of Thailand (NRCT)
2. Prince of Songkla University Graduate Studies Grant Contract (2010 Academic Year)

Work-Position and Address

Senior Engineer, Specialized R&D Center for Alternative Energy from Palm Oil and Crops, Faculty of Engineering, PSU Hatyai, Songkhla.

Patent Pending

Petty patent: Chakrit Tongurai and Thanet Waisuwan. 2012 Continuous Palm Fruit Frying for Palm Oil Mill. No.1203000082. Thailand Patent Office.

List of Publication and Proceedings

Thanet Waisuwan, Sutham Sukmanee and Chakrit Tongurai. 2011. Batch Process Esterification of Crude Palm Oil with Ethanol Assisted under Ultrasonic Irradiation. The 2011 International Conference on Alternative Energy in Developing Countries and Emerging Econimies (2011 AEDCEE), 25-28 May 2011, J.B. Hotel Hatyai, Thailand.